1-1-2002

Evaluation of fiber composite and stainless steel as alternative dowel bar material

Jeffrey G. Hoffman
Iowa State University

Evaluation of fiber composite and stainless steel as alternative dowel bar material

by

Jeffrey G. Hoffman

A thesis submitted to the graduate faculty

in partial fulfillment of the requirements for the degree of

MASTER OF SCIENCE

Major: Civil Engineering (Geotechnical Engineering)

Program of Study Committee:
James K. Cable, Co-major Professor
John M. Pitt, Co-major Professor
Carl W. Roberts
Kejin Wang

Iowa State University

Ames, Iowa

2002

Graduate College
Iowa State University

This is to certify that the master's thesis of

Jeffrey G. Hoffman

has met the thesis requirements of Iowa State University

Signatures have been redacted for privacy

TABLE OF CONTENTS

LIST OF FIGURES

LIST OF TABLES

ABSTRACT

Dowel bars are used to transfer loads between adjacent pavement sections within a jointed concrete pavement. Epoxy coated steel is the most common material used for dowel bars, but steel dowel bars have been found to be susceptible to corrosion. The objectives of this research is to investigate fiber reinforced plastic (FRP) and stainless steel as alternative dowel bar materials, and to study the effects of FRP and stainless steel dowels size and spacing on load transfer behavior of concrete pavements.

The load transfer behavior of the pavement was evaluated biannually by utilizing a falling weight deflectometer (FWD), measuring joint faulting and joint opening, and conducting a visual distress survey. The analyses indicate the epoxy coated steel outperformed the alternative materials. The average research lifetime load transfer for the epoxy coated steel is 91 percent, while the best performance of the alternative material at the same 12 inch on center spacing is approximately 87 percent for the stainless steel. The data also indicate the decrease in spacing, from 12 to 8 inches, increases the load transfer for stainless steel and 1.5 inch diameter FRP dowels. Although the FRP dowels with decreased spacing were outperformed by the epoxy coated steel dowels, they performed adequately.

It is recommended that the current dowel bar standard continue to be implemented for concrete pavements requiring dowels as load transfer devices. However, if the pavement is to be constructed in a corrosive environment or a longer design life is desired, stainless steel spaced at 12 inches and 1.5 inch diameter FRP dowels spaced at 8 inches should be considered.

1 INTRODUCTION

1.1 Background

Jointed portland cement concrete pavement has been utilized throughout the country with relative success. The utilization of transverse joints in the jointed concrete pavement is a method to prevent the development of random cracks due to stresses induced by moisture and thermal gradients, and restrained slab movement due to friction between the pavement and subbase. Although random cracking is prevented, the transverse joints create planes of weakness within the pavement that should be strengthened through the use of load transfer devices. The purpose of load transfer devices is simply to transmit load from the loaded pavement slab to the adjacent unloaded slab, distributing the load over a larger area. The two most common methods of load transfer are aggregate interlock of the concrete and dowel bars placed at the joint.

Aggregate interlock utilizes the shear resistance between the concrete slabs to transfer the load. As the tire load approaches the joint, the loaded pavement begins to deflect and initial contact is made with the opposing slab, with any further deflection resisted by the bearing capacity and friction of the aggregate. Studies have shown the performance of aggregate interlock is dependent on joint opening width and concrete texture [1,2,3,4]. Pavements relying on aggregate interlock for load transfer are more susceptible to pumping, faulting, and reduced load transfer efficiency due to weakened subgrade soils from moisture fluctuations. Tayabji and Colley [5] report aggregate interlock pavements experienced significant distress in wet climates, and are generally used only in the dry climate of western United States. Aggregate interlock may also be adequate for low traffic volume roads.

In areas with wet climates or experience wet seasons, the typical load transfer device is steel dowel bars. Use of steel dowels as load transfer devices was first reported on a concrete pavement project near Newport News, Virginia, in 1917 [6]. Steel's shear strength and stiffness allow the dowel to transfer loads. However, an important detrimental property of steel is its susceptibility to corrosion. The steel dowel bars are exposed to corrosive agents such as salts and deicers that can attack the dowels through paths created sawing pavement joints. Corrosion can result in severe pavement problems directly related to the volumetric increase of corroded steel. The expanded dowel may prevent horizontal slab movement and cause joint spalling and cracking. The dowel area that can effectively carry loads is also reduced, resulting in reduced load transfer efficiency. McDaniel [7] estimates that it would cost approximately $212 billion to repair damage of U.S. highways associated with corrosion.

A typical method of corrosion inhibition is the use of a coating material to cover steel dowel bars. Darter and Barenberg recommend utilizing dowel bars with a full length suitable coating such as asphaltic cement [8], however further research and experience has yielded epoxy resin as the typical coating material. Although generally effective, the coatings may accelerate the corrosion rate of steel dowels if uncoated areas are present. Uncoated areas may occur due to flaws in the coating process or scratches from careless storing, handling or placement of dowels during construction.

The corrosion of steel is a chemical reaction termed an oxidation-reduction process in which one metal will give up electrons (oxidized) and one metal gains electrons (reduced). The locations of the oxidation and reduction processes are termed the anode and cathode, respectively. Corrosion of a single, steel dowel bar can occur due to the presence of both

anodes and cathodes, along with water to act as an electrolyte to carry the electrons. When a dowel is scraped, uncoated areas can corrode in the shape of a semi-circle (pit) in which the area exposed will become the anode and the adjacent steel still protected is a cathodic areas. The corrosion will occur more rapidly due to the relative short distance between the anode and cathode that the electrons must flow. The pitted corrosion will reduce the area capable of carrying a load, thus reducing the load transfer efficiency.

Joint sealants have also been utilized to reduce steel corrosion. The transverse joint sealants are typically composed of elastic material to allow for pavement slab movements associated to temperature gradients [9]. Typical sealants are asphalt based sealant, silicone, and rubber. The inhibition of steel corrosion is accomplished by reducing the exposure to corrosive agents carried by surface water. Minimizing water infiltration also has the added benefit of reducing the potential for pumping and faulting due to subgrade or subbase softening, resulting in loss of structural support. In addition to reducing water infiltration, joint sealants also prevent incompressible material from becoming lodged between joints, preventing slab movements. The incompressibles can contribute to spalling and possibly blow-ups due to excessive pressure along the joint faces.

Along with the corrosive nature of steel dowels, jointed concrete pavement reinforced with dowel bars may develop dowel looseness, or hollowing. The hollowing of concrete is generally associated with the repetitive loading of the pavement; however, they also may be present due to improper consolidation during construction and concrete shrinkage. Repetitive loading can create the hollowing effect due to stress concentrations at the contacts between the dowel and concrete. If the stress concentrations are large enough, the concrete will gradually be crushed. The resulting looseness prevents the dowel from resisting

movement, with shear forces generated only after the vertical displacement allowed by the existing looseness occurs. The looseness may also contribute to corrosion problems of coated dowel bars due to the impact and rubbing of dowel bar on the rough textured concrete, thus scratching the protective coating.

The implications of the looseness are discussed by Davids, who utilized a finite element model to analyze the effects. It was determined that as the gap between the dowel and concrete increased, the shear stress of the dowel decreased [10]. The stress applied to the concrete remained the same, so it would be expected that the stress be transferred to another portion of the pavement system such as the subbase. Davids' model suggests subbase material experienced a maximum vertical stress increase of 68% due to a gap increase from 0.00 to 0.12 mm. As expected, a decrease in dowel shear corresponded with a decrease in the load transfer efficiency and joint effectiveness.

1.2 Research Needs

The problems and continuing questions associated with steel dowel bars and protective coatings, proves the need for continued research. Currently, testing and research is being focused on the use of alternative materials for load transfer, specifically the use of fiber composite and stainless steel due to their durability and resistance to corrosion, along with strong tensile strength.

Stainless steel materials have been used in the commercial industry since the 1920's and fiber composite materials have been utilized in the aerospace and aeronautic industries. Stainless steel is manufactured by melting steel scrap metal with various other metals, with the type of metals and proportions dependent on the desired qualities. Stainless steel dowels

can be manufactured as solid stainless steel bars, mild steel or other material with a bonded stainless steel coating, hollow pipes, or pipes filled with concrete.

The fabrication of fiber composite dowels includes a matrix of polymeric material that is reinforced by fibers or other reinforcing material. Included within the matrix are resins (polymers), fiber reinforcements, fillers and additives. Fibers are typically composed of glass, but may also be aramid or carbon. The fibers are generally produced by a pultrusion method in which the glass fibers are bundled together and drawn through a resin bath so that the fibers are oriented parallel to the longitudinal axis of the dowel bar. The bar is then heated to allow the resin to cross-link and harden. The dowels can then be cut to the desired length.

Although these materials have been used in other industries, the construction industry has been reluctant to utilize these materials. The biggest barrier for stainless steel and fiber composite dowel bars appears to be the initial increased material cost and limited amount of knowledge of fiber composite properties. Current research is being devoted to providing material property information and determining the affects of the negative aspects of fiber composite dowels, including a lower modulus of elasticity and reduced shear strength capacity [11]. The research is also geared to determine if increased initial costs of both fiber composite and stainless steel can be offset by an improved and longer lasting pavement.

Research is currently underway in several field projects throughout the country. Several research projects investigating alternative dowel bars are currently being funded by the Federal Highway Administration (FHWA) under the Test and Evaluation Project 30 (TE-30), High Performance Concrete Pavement (HPCP), established to explore innovative pavement design and construction concepts. The projects underway are located in several

areas throughout the country. There are four projects in Illinois, one in Kansas, two in Minnesota, one in Ohio, and two in Wisconsin. Along with the field tests, Iowa State University has conducted laboratory testing of fiber composite dowel bars to provide material properties to use in design.

1.3 Research Objectives

The research consists of evaluating fiber composite and stainless steel dowel bars in a highway pavement. The goal of this research is to evaluate field performance and provide recommendations on design, materials, construction practices and performance characteristics of stainless steel and fiber composite dowel bars. The project includes monitoring the installation of the dowel bars during construction, conducting visual distress surveys after construction, and evaluating pavement performance. The performance of 12 inch and 8 inch-on-center dowel spacing and fiber composite dowel bar diameter are also built-in variables of the experiment. The evaluation period will allow a comparison of the performance of highway joints reinforced with fiber composite and stainless steel dowel bars to the performance of conventional epoxy-coated steel dowel bars, under the same design criteria and field conditions.

2 LITERATURE REVIEW

2.1 Fiber Reinforced Polymer (FRP) Composites

A composite material can be defined as any material composed of more than one component, with each component contributing its strengths as a material to the overall performance of the composite. Common composites found in the construction industry are asphaltic and Portland cement concrete, which utilize the strength of the aggregate with the binding nature of the cements. FRP composites are composed of some combination of fibers and resin, with the fibers providing strength and stiffness and the resin providing a matrix to hold and protect the fibers.

Fibers within FRP composites are typically made of glass, aramid, or carbon. The glass fibers are primarily composed of silica, typical for any glass product. However, in addition to the silica, the fibers also contain oxides of calcium, boron, sodium, iron, and aluminum [12]. By varying the amount of each, different glass fibers can be produced, with the main types classified as E-glass, C-glass, and S-glass. E-glass is the most economical of the three and most widely used. The downside to the glass fibers are their susceptibility of corrosion in a high alkaline environment. [13,14,15]. However, the resin matrix surrounding the fibers provides a protective coating resisting the alkali corrosion [16].

Carbon fibers, typically called graphite and commonly used for golf club shafts, are more resistant to chemicals and corrosion [17], however have low toughness and impact resistance [18]. The graphite is made from a series of heat treatments of polyacrylintrile. The manufacturing process to create the graphite results in the most expensive of the three fibers.

Aramid fibers in comparison are tough and impact resistant, but are not as stiff as the carbon fibers. The aramid fibers consist of organic polymers which are highly oriented in the axial direction, resulting in a high tensile strength. The aramid fibers have been shown to be resistant to water, seawater, alkali, and chlorides [18,19]

The resin matrix surrounding the fiber reinforcement is a polymer, which is a molecule made of repeating units termed monomers. The molecule chains are classified as either thermoplastic or thermoset. Thermoplastic resins can be remolded if reheated, while thermoset resins become a rigid solid and cannot be reformed. The behavioral difference between the two resins can be explained by the chemical bonding. The thermoplastic resins are a linear repeating unit while thermoset resins form cross-linked molecules. A schematic of the two resins are shown in Figure 1. FRP composites generally utilize thermoset resins which are typically composed of vinyl ester, polyester, and epoxy.

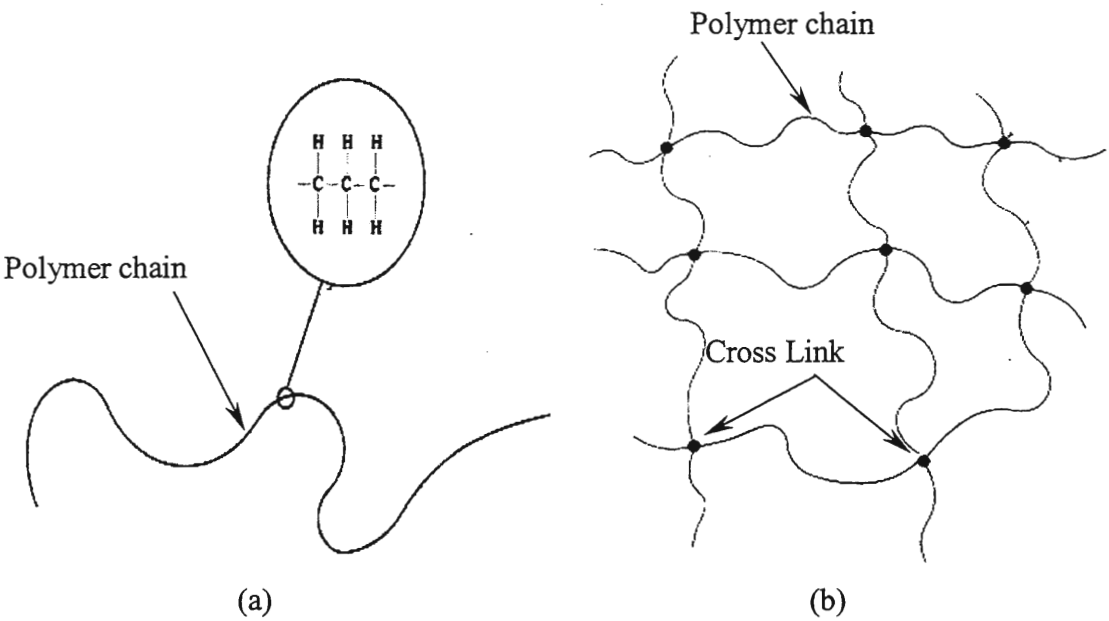

Figure 1. Structural shape of resins, (a) thermoplastic, (b) thermoset. [20]

2.2 Stainless Steel

Stainless steel is an iron based alloy that must contain a minimum of 10.5 percent chromium and less than 1 percent carbon. The chromium creates a surface film that resists oxidation and creates a corrosion resistant material. The manufacturing process consists of melting scrap metal with various alloys of chromium, nickel, and molybdenmum, depending on the stainless steel type. The material is melted by passing an electric current through the carbon electrodes of an electric arc furnace. The molten material is then transferred into a decarbonization vessel (AOD, Argon Oxygen Decarbonization) which reduces the carbon levels. At this same time, the final alloy additions are made to make the exact chemistry desired for the stainless type.

There are five types of stainless steel, in which, further modifications can be made by altering the chemical composition. Modifications may be desired for different corrosion conditions, temperature ranges, strength requirements, improve weldability, machinability, work hardening, and formability. The classifications are based on the crystalline structure of the alloy and are:

- Martensitic
- Ferritic
- Austenitic
- Duplex
- Super Austenitics and Duplex

Martensitic stainless steel consists of 12 to 18 percent chromium and less than 1 percent carbon. It is magnetic, can be hardened if heat treated, and has poor welding characteristics. Typical uses include knife blades, surgical instruments, shafts, and springs.

The Ferritic stainless steel contains the same amount of chromium but less than 0.2 percent carbon. The resulting difference is the alloy cannot be hardened by heat treatment. Typical uses of Ferritic stainless steel include automotive exhaust and fuel lines, cooking utensils, and bank vaults.

The third stainless steel category is Austenitic and is the stainless steel type utilized for this experiment. In comparison to Ferritic stainless steel, Austenitic consists of slightly more chromium, and in addition has 8 to 14 percent nickel. The resulting alloy is nonmagnetic, cannot be hardened by heat but can by cold treatment, is the most corrosion resistant, easily welded, high and low temperature resistant, and has excellent cleanablity. The typical uses include kitchen sinks, food processing equipment, chemical vessels, and ovens. The limitations of this stainless steel is that it undergoes oxidation at extreme temperatures (925 degrees Celsius), should be used in low concentrations of reducing acid, and very high levels of halide ions, such as chloride, can breakdown the corrosion resistant surface.

Duplex stainless steels contain 18 to 26 percent chromium and 4 to 7 percent nickel. In addition, most Duplex stainless steels contain 2 to 3 percent molybdenum. The resulting alloy structure is a combination of both Ferritic and Austenitic, thus the name Duplex. Characteristics of the alloy include high resistance to stress corrosion cracking, increased resistance to chloride attack, very weldable, and higher tensile and yield strengths. Currents applications of Duplex stainless steel include sea water environments, heat exchangers, and food pickling plants.

The last category is the Super Austenitics and Duplex stainless steels. These alloys are specially designed to withstand the conditions that the normal alloys cannot. These

conditions include an acidic environment and areas in which insufficient oxygen is available to maintain the oxide film.

The chemical composition and typical mechanical properties of stainless steel by different grades are presented in Tables 1 and 2. Information presented on stainless steel was obtained from the Stainless Steel Information Center of the Specialty Steel Industry of North America [21].

Table 1. Chemical Composition of Stainless Steel. [21]

Chemical Compositon, %									
Maximum values unless noted.									
Stainless Grade	**C**	**Mn**	**P**	**S**	**Si**	**Cr**	**Ni**	**Mo**	**N**
410 (Martensitic)	0.15	1.00	0.040	0.030	0.50	11.50-13.00			
430 (Ferritic)	0.15	1.00	0.040	0.030	1.00	16.00-18.00	0.75		
304 (Austenitic)	0.08	2.00	0.045	0.030	1.00	18.00-20.00	8.00-10.50		
316 (Austenitic)	0.08	2.00	0.045	0.030	1.00	16.00-18.00	10.00-14.00	2.00-3.00	
2205 (Duplex)	0.02	2.00	0.045	0.030	1.00	22.00-23.00	5.50-6.00	3.00-3.50	0.17

Table 2. Stainless Steel Mechanical Properties. [21]

Stainless Grade[a]	**Tensile Strength**		**Yield Strength**		**Elongation**[b]	**Hardness**[c]
	ksi	MPa	ksi	MPa		
410 (Martensitic)	70	483	45	310	25	B80
430 (Ferritic)	75	517	50	345	35	B85
304 (Austenitic)	84	579	42	290	55	B80
316 (Austenitic)	84	579	42	290	50	B79

[a] Steel in annealed condition
[b] Elongation in 2" (50.08 mm)
[c] Hardness in Rockwell B

2.3 Iowa State University Laboratory Investigations

A significant amount of research has been conducted on fiber composite and stainless steel in the laboratories of Iowa State University. Most of the research has focused on the engineering properties of the material with limited information regarding the field performance. Properties that were investigated include tensile strength, modulus of elasticity, and durability within a simulated field environment.

In 1992, Kent Fish [11] began the investigations by looking at the feasibility of fiber composites as reinforcement within concrete structures. During the investigations, Fish tested 127 beams for tensile strength both directly and flexurally, and determined the modulus of elasticity through the same testing. The average direct tensile strengths for the one-half inch FRP bars was 120 kips per square inch (ksi), with a modulus of elasticity of 4.91×10^6 pounds per square inch (psi). The results also indicate that FRP bars experienced larger deflections than beams reinforced with steel, primarily due to the lower modulus of elasticity. Fish also summarized the advantages and disadvantages of FRP compared to standard steel reinforcement and is summarized below in Table 3.

Table 3. Advantages and Disadvantages of FRP for use in Construction.

Advantages	Disadvantages
High tensile strength	Low Modulus of Elasticity
High corrosion resistance	Long development length
Lightweight	Brittle tensile failure
Fewer concrete splitting problems	Low compressive strength
No magnetic fields	Low dowel shear strength

At approximately the same time Fish was conducting his work, Albertson [22] was performing a study of the overall capacity and load deflection characteristics of FRP and steel dowel systems. Albertson utilized 1.25 inch diameter FRP dowels and 1.5 inch diameter steel dowels to test for shear strength, tension, and deflections. The average deflection at the face of the joint from a 10,000 pound load for the steel and FRP dowels was 0.0075 and 0.113 inches, respectively. The larger FRP dowel deflection verifies Fish's results.

Hughes [23] investigated the static, fatigue, and dynamic behavior of FRP dowels and compared the results to steel dowels when used as in transverse joints of highway pavements. Hughes constructed a full scale laboratory test with a 6 foot wide by 12 foot long by 12 inch thick concrete slab. It was loaded repeatedly with 9,000 pounds, for a minimum of 2 million cycles. The joints were reinforced with either 1.5 inch diameter steel dowels spaced at 12 inches or 1.75 inch diameter FRP dowels spaced at 8 inches on center. The slabs were tested for both relative deflection and load transfer efficiency. Load transfer for Hughes' research was defined as the load transferred to the unloaded slab divided by the total load applied, with an ideal load transfer of 50%. The research determined that the load transfer for FRP dowels stayed nearly constant over the 2 million loading cycles, at 44.5% with a maximum of 50% load transfer as defined by Hughes. The 1.5 inch diameter steel dowels experienced a decrease in load transfer from 43.5% to 41.0%. Hughes also noted that both dowel systems incurred a gradual increase in relative displacements over the loading cycles.

As part of his research, Hughes also installed FRP dowels in two transverse joints on a new concrete pavement on U.S. Highway 30 east of Ames, IA. The FRP dowels were 1.75 inches in diameter and spaced at 8 inches on center, in place of the standard 1.5 inch diameter steel dowels spaced at 12 inches. At the time of his report the test site was still

being monitored, but it was reported that the FRP dowels were performing equivalent to the steel dowels during non-destructive testing and visual inspections.

While Hughes was investigating fatigue, Lorenz [24] was conducting research on potential aging effects of FRP dowels when exposed to a wet, salt, or lime environment. This research was conducted to investigate the effectiveness of the resin matrix to protect the glass fibers. Earlier aging studies determined that degradation of glass fibers in an alkaline environment should be expected. However, the glass fibers did not have the vinyl ester resin coating. The FRP dowel bars were surrounded by concrete similar to that used in paving operations and the aging process was accelerated by placing the specimen into the appropriate environment at a temperature of 140 degrees Fahrenheit for 63.3 days. The desired effect of the aging process was to produce a specimen equivalent to one that spent 50 years in each environment. The aged specimen were tested for shear strength and pullout capacity, and compared to unaged specimen. Lorenz concluded that the glass fibers encapsulated in the vinyl ester resin were very resistant to the accelerated aging. He also noted that the shear and pullout capacity of the aged specimen compared well with the unaged specimen, with little to no affect on the dowel characteristics.

Mehus [25] continued the work began by Lorenz by investigating the long term durability of commercially available FRP products for reinforcement of structural concrete. Mehus conducted his research by aging the FRP dowels in an alkaline environment with an approximate pH of 12, and aged for 81 days at 140 degrees Fahrenheit to simulate a 50 year old specimen. Unlike Lorenz, the environment was established to simulate the pore water within a concrete pavement. Thus, the FRP dowels were placed directly in the aqueous solution, without being cast in concrete. The study also tested unaged dowels for comparison.

Mehus concluded that aging in a highly alkaline environment significantly reduces the ultimate tensile strength and maximum strain capacity in comparison to the unaged specimen. He also noted that the reductions do not occur linearly, but rather a rapid reduction is seen during the initial aging, after which the strength and strain reductions occur slowly. After 19 days of aging, or 5.4 simulated years, the ultimate tensile strength of the aged specimen was lower by 29 to 60 percent, depending on the FRP manufacturer. The ultimate tensile strengths at the end of the aging process (50 years) decreased by 48 to 66 percent of the unaged ultimate tensile strength. The maximum strain capacity was reduced by 53 to 68 percent, but the modulus of elasticity was not affected. An unexpected aspect of this research occurred when the unaged FRP dowels exhibited approximately 50 percent lower ultimate tensile strengths than were expected as specified by the manufacturers. The Iowa State University results were verified by University of Wyoming (UW), which utilized a different testing technique developed at UW.

Research conducted by Porter et al. [16] is of significant importance because the glass fiber reinforced polymer (GFRP) dowel bars investigated were identical to those utilized in the research conducted by the author. Porter's objectives for the research were stated as:

1. Determine the material properties of all the GFRP dowel bars,
2. Investigate the behavioral parameters of aged and unaged GRFP dowel bars under elemental static testing,
3. Investigate the behavior of aged and unaged GFRP dowel bars under elemental fatigue loading (0.5 to 1 million cycles),
4. Investigate the fatigue behavior of GFRP dowel bars under an accelerated partial design life number of cycles (3 to 5 million cycles),
5. Determine the bond characteristics of both aged and unaged GFRP dowel bars,

6. Evaluate the condition of dowel bars placed in actual highway joints,
7. Investigate the failure modes and adequacy of alternative dowel bar parameters,
8. To develop a finite element model of jointed concrete highway pavement.

As stated, part of the research objective was to determine the material properties of the GFRP dowel bars. Two manufacturers supplied GFRP dowel bars for the project, one 1.5 inches in diameter and one at 1.88 inches. The proportions of Type-E glass fibers and isophthalic polyester resin determined for the dowel bars and are presented below in Table 4. Porter et al. also presented mechanical properties of various dowel bars which are shown in Table 5. The testing regime of the dowel bars included direct shear tests, fatigue testing, pullout tests, and simulated 50 year aging in an alkaline environment for specimen cast in concrete.

Table 4. GFRP Dowel Composition. [16]

Specimen	Weight Fraction	Volume Fraction
1.5" Dia., Glass Fiber	0.6997	0.5179
1.5" Dia., Resin	0.3003	0.4821
1.88" Dia., Glass Fiber	0.7378	0.5746
1.88" Dia., Resin	0.2622	0.4254

Table 5. Dowel Material and Mechanical Properties. [16]

Material	Diameter, in.	Modulus of Elasticity, E (10^6) psi	EI, (10^6) lb-in^2	Pullout Tests (lb/0.5")
Epoxy-coated Steel	1.5	29.0	7.206	11,490
Stainless Steel	1.5	28.0	6.958	940
GFRP	1.5	4.93	1.255	1430
GFRP	1.88	6.51	3.950	1660

The conclusions from the testing indicate GFRP dowels with a 1.5 inch diameter spaced at 12 inches were not adequate for load transfer for the anticipated design life of the pavement. The 1.5 inch diameter GFRP dowels spaced at 6 inches on center were effective in transferring load. Porter et al. recommended that for pavements less than 10 inches thick, GFRP dowels should be ¼-inch larger in diameter than that recommended by the American Association of State Highway and Transportation Officials (AASHTO), and spaced at the standard 12 inches on center. For pavement thickness greater than 10 inches, it is recommended that 1.5 inch diameter GFRP dowels be used, but spaced at 6 inches on center. Table 6 illustrates the GFRP recommendations compared to the current AASHTO recommendations for steel dowels.

Table 6. Design guides for Steel and GFRP.

Pavement Thickness, in.	AASHTO[a]		GFRP[b]	
	Diameter, in.	Spacing, in.	Diameter, in.	Spacing, in.
14	1.75	12	1.50	6
12	1.50	12	1.50	6
10	1.25	12	1.50	12
8	1.00	12	1.25	12
6	0.75	12	1.00	12

[a] Source: Reference [26]
[b] Source: Reference [16]

2.4 Field Studies

Field projects presented are part of an overall research program funded by the Federal Highway Administration (FHWA), TE-30, High Performance Rigid Pavements (HPRP). The research was initiated by the Highway Innovative Technology Evaluation Center (HITEC), whose purpose is "to expedite the introduction of new innovative technologies to the highway prgram particularly from the private sector and the entrpreneur who might not

otherwise seek to penetrate the diverse and difficult highway market [27, p.1]." Suggested innovation areas for the program include [28, p.1]:

- Increasing the service life.
- Decreasing construction time.
- Lowering life-cycle costs.
- Lowering maintenance costs.
- Constructing ultra-smooth ride quality pavements.
- Incorporating recycled or waste products while maintaining quality.
- Utilizing innovative construction equipment and procedures.
- Utilizing innovative quality initiatives.

HITEC presented an evaluation plan for alternative dowel bar materials. The plan consisted of a literature review of previous studies, field installations, and laboratory investigations. The field studies were required to be monitored by the highway agencies directly after construction completion and every six months for the first eighteen months of service life. The test site must then be monitored once a year for five years. Test site monitoring included visual survey in accordance to the Strategic Highway Research Program Manual (Distress Identification Manual for the Long-Term Pavement Performance Program, SHRP-P-338), load transfer testing using falling weight deflectometer (FWD), core sampling, and dowel bar location using non-destructive testing methods.

TE-30 project sites are currently in Illinois, Iowa, Kansas, Maryland, Michigan, Minnesota, Mississippi, New Hampshire, Ohio, Virginia, and Wisconsin, although not all project test sites are investigating FRP composite and stainless steel dowel bars. The project

summaries discussed below are presented in a report submitted to the Federal Highway Administration by Applied Pavement Technology Incorporated of Champaign, Illinois [28].

2.4.1 Illinois

Williamsville, IL: I-55 Southbound, 1996

The I-55 project is not officially a TE-30 project but was the first project in Illinois in which FRP dowels were investigated as a possible solution to the corrosion of standard steel reinforcement. The project design consisted of an 11.25 inch thick pavement with 45 foot transverse spacing, with intermediate "hinge" joints containing tie bars placed at 15 foot intervals. A total of four transverse joints contained 1.5 inch diameter FRP dowels were compared to three joints containing standard 1.5 inch diameter epoxy-coated steel dowel bars, both with 12 inch on center spacing. The FWD testing determined a gradual decrease in overall load transfer efficiency over three years, with the conventional steel dowel bars consistently showing higher levels of load transfer then the FRP dowels. The Illinois Department of Transportation has reported that no joints are exhibiting signs of distress.

Naperville, IL: Route 59, 1997

This project consisted of a 10 inch thick pavement utilizing the same transverse and "hinge" joint spacings as the I-55 project. Several different dowel bars were investigated, including different size and different FRP dowel manufacturers. Three manufacturers supplied 1.5 inch diameter FRP dowels, with one company also supplying a 1.75 inch diameter dowel. The FRP dowel sections were compared with pavement sections containing 1.5 inch diameter epoxy-coated steel dowel bars. After three years of monitoring, the pavement is performing well with no signs of distress. The conventional steel dowels have maintained the best load transfer efficiency at approximately 85%. The FRP dowels ranged

from 70% to 85%. It was also noted that the maximum joint deflections exhibited a trend of increasing deflection with time.

Jacksonville, IL: U.S. Route 67, 1999

U.S. Route 67 pavement design consisted of a 10 inch thick slab with transverse joints spaced at 15 foot intervals, Illinois Department of Transportation's (IDOT) new standard. This project continued the investigation of alternative dowel bars by placing FRP dowel bars from three manufacturers, an FRP tube dowel filled with hydraulic cement, carbon steel rods covered in stainless steel, and the standard epoxy-coated steel dowel bars. All dowels were 1.5 inches in diameter and spaced at 12 inches on center. At the time of the distribution of the status report, only one testing period had been analyzed with all dowels performing equally well.

Dixon, IL: Route 2, 2000

The Route 2 project is not an official TE-30 project, but it is a continuation of the previous projects conducted by the IDOT. The project was designed for an unspecified pavement thickness with transverse joints at 15 foot intervals. Preliminary results or findings are not available because the project was still in the construction phase at the time of the status report publication. The alternative dowel bars investigated for this project were:

- Fiber-Con™ dowel bar, manufactured by Concrete Systems, Inc., consisting of FRP tube filled with hydraulic cement.
- One and a half inch and 1.75 inch diameter, 0.109 inch thick grade 316 stainless steel tubes filled with cement grout.
- One and a half inch and 1.75 inch diameter carbon steel rods clad with grade 316 stainless steel, manufactured by Stelax Industries Inc.

2.4.2 Kansas

The Kansas Department of Transportation constructed an experimental project on Highway K-96 in Haven, Kansas. The projected focused on a wide variety of experimental features, with just one being alternative dowel bars. The basic pavement design was a 10 inch thick slab, with transverse joints at 15 foot intervals, and 1.25 diameter inch epoxy coated steel dowels spaced on 12 inch centers. One experimental section consisted of 2 inch diameter FRP tube dowels filled with high strength cement grout. The other alternative load transfer device was the X-Flex™ developed at Kansas State University. This device is constructed of 0.5 inch diameter epoxy-coated steel formed into a figure-eight shape, and placed on its side so that the joint is centered at the intersection of the two loops. KDOT has reported that the FRP dowel section has experienced one transverse crack and eight corner cracks, compared to the no cracking of the control section. Also, the joint faulting of the FRP dowel section is significantly larger at 0.08 and 0.25 millimeters in 1998 and 1999, respectively, compared to the control's 0.02 millimeters during both testing periods.

2.4.3 Minnesota

Richfield, MN: I-35W, 2000

During the reconstruction of a portion of I-35W, the Minnesota Department of Transportation (MN/DOT) designed a pavement for a 60-year service life. Stainless steel clad dowel bars and solid stainless steel dowel bars were utilized within the experimental pavement, along with epoxy-coated steel dowels. Each dowel type had 1.5 and 1.75 inch diameter dowel sections. The pavement was designed as a 13.4 inch thick concrete slab with 15 foot transverse joints. The construction began in the summer of 2000 and no preliminary results were available.

MN/Road Low Volume Road Facility, 2000

The MN/Road is a research facility to study the performance of asphalt, concrete, and aggregate surface roadways. The low volume road runs parallel to I-94 and is exposed to controlled truck weight and traffic loading. Within the loop are heavily instrumented test sections. In 2000, three new test sections were added to consider several new topics, of which, included the study of long-term joint load transfer behavior of different dowel bar types. The test section was a 7.5 inch thick pavement with 15 foot transverse joints, and included 1.25 and 1.50 inch diameter FRP dowels, 18 inches in length. These sections are to be compared to 1.0 and 1.25 inch diameter epoxy-coated steel dowels with a 15 inch length.

2.4.4 Wisconsin

In the summer of 1997, the Wisconsin Department of Transportation (WisDOT) constructed two experimental concrete pavements on Highway 29. One section located from Owen to Abbotsford, and the other from Hatley to Wittenberg. The Owen to Abbotsford section pavement design was an 11 inch thick pavement with transverse joints spaced at variable intervals of 17-20-18-19 feet. The Hatley to Wittenberg section was constructed with a variable thickness cross section, with an 8 inch slab at the passing lane edge that transitions to 11 inches at the driving lane pavement edge. Both sections utilized standard epoxy-coated dowel bars, four FRP dowel bars, and solid stainless steel dowels. The Owen to Abbotsford section also tested stainless steel tubes filled with mortar. The pavements have been monitored for three years using FWD testing and conducting visual surveys. The FWD testing indicates that the standard steel bars are performing slightly better than the FRP and stainless steel dowel bars. The visual distress surveys determined that the pavements were in excellent condition, with minor chipping and fraying of the transverse joints caused by joint sawing operations.

2.5 Falling Weight Deflectometer (FWD)

Prior to the evolution of non-destructive testing (NDT), the evaluation of a pavement and subgrade's structural condition required destruction of pavement slabs by coring through the pavement. The condition of the core could then be inspected visually or by microscopy if so desired. The underlying subbase and subgrade soils could be analyzed by conducting in-situ testing, such as a dynamic cone penetrometer, and laboratory testing, including classification and moisture contents determination. Although this type of pavement analysis produces adequate results, it is time consuming and leaves pavements less structurally sound.

The introduction of the FWD and NDT for pavements has increased the speed of the analysis and does not structurally damage the concrete. The FWD generally consists of a tow vehicle and a trailer to house drop weights. The test consists of placing the FWD on the slab of interest and dropping the weight from a given height and measuring the pavement's deflection response. Varying the drop heights result in different applied loads, with typical loads varying from 9,000 to 16,000 pounds for highway pavements. The ability to test the pavement quickly with the FWD allows for a greater amount of the pavement to be evaluated in comparison to the destructive coring methods. With more tests covering a larger area, the pavement can be defined better and changes over the length of pavement may be seen.

As previously stated, the FWD drop weight is typically housed in a trailer. It is mounted on a vertical shaft that allows drop heights ranging from 2 to 20 inches [29]. The weight is dropped onto an 11.8 inch diameter rubber buffer with a thickness of 0.22 inches. The resulting load is a force impulse that last approximately 30 milliseconds, compared to the typical 120 millisecond pulses from a truck traveling at 50 miles per hour [30]. The resulting impulse load has been shown to produce similar deflections caused by moving wheel loads [29].

The deflection response of a pavement when struck with the impulse load is measured by geophones. A geophone measures an output voltage proportional to the velocity of the base of the unit [31]. The basic idea of the geophone is that a mass will tend to stay motionless due to its inertia. In a geophone, the mass is wrapped with a wire and surrounded by a magnet that is fixed or set on the pavement slab. As the slab moves, the magnet will move, thus creating an electrical voltage in the wire that can be amplified and recorded by a voltmeter. The voltage can then be converted into a distance that the magnet moved, which coincides with the slab movement. Figure 2 is a schematic of a geophone.

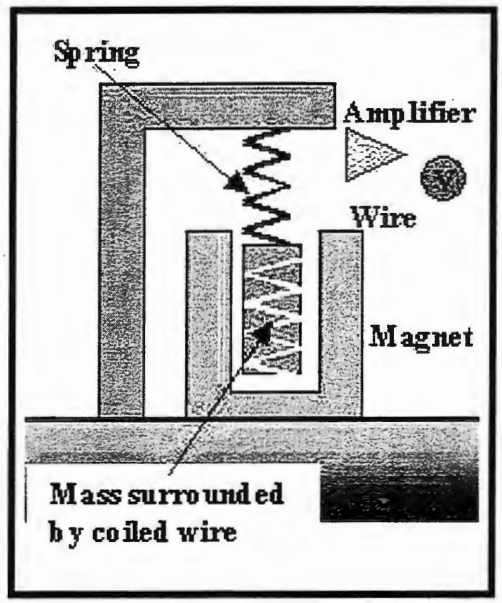

Figure 2. Geophone schematic. [31]

The deflections recorded by the geophones at certain distances from the load plate can be utilized to determine characteristics of the pavement and soil. Several models have been developed to determine the moduli of the pavement and soil. The Strategic Highway Research Program (SHRP) has conducted an exhaustive study comparing two of the most widely used, the Best Fit Method and the AREA Method [32]. The study suggests that the

models are comparable, with the Best Fit Method having a slightly lower coefficient of variability. Both these methods are based on Westergaard's plate theory of a linear elastic, homogeneous, and isotropic material resting a dense liquid foundation [33,34].

The Best Fit Method utilizes an algorithm that finds a combination of concrete modulus of elasticity and modulus of subgrade reaction for which the calculated deflection basin closely matches the measured basin. The AREA method utilizes the AREA parameter based on the Trapezoidal Rule, along with a dimensional analysis based equation for the modulus of subgrade reaction developed by Ioannides [35].

This research project will utilize the AREA method due to the ease of calculation with the closed-form solution, allowing calculations to be performed on a standard spreadsheet without the need of a computer program. The closed-form solution also allows for relatively quick analysis of the vast amount of data to be analyzed.

Along with the material moduli analysis, the deflection responses and corresponding deflection basins provide additional information. The pavement's ability to transfer loads from loaded slabs to adjacent unloaded slabs, termed load transfer efficiency, can be evaluated utilizing deflections from opposite sides of a joint. The deflections are measured by geophones located at equal distances from the joint. The load transfer efficiency is defined as the deflection of the unloaded slab at a distance from the joint equal to the deflection at the load. If the deflections are approximately equal, there is 100% load transfer. The greater the load transfer, the less load each slab will have to support thus reducing fatigue and increasing the pavement's life.

The shape of the deflection basin is also indicative of the strength of the different layers. Foinquinos et al. [29] investigated the effects of varying the layer stiffness of the

pavement, base, and subgrade. It was determined that when compared to a pavement with all three layers stiff, a weaker pavement will result in greater deflections at the joint but sensors at a greater distance from the load will experience little change. A weaker base layer produced similar results, but the increase in deflection at the joint was magnified slightly, along with a greater change at more distant sensors. A weak subgrade will also create larger deflections at the joint, but different from the pavement and base layers, the increased deflections continue as the distance from joint increases. This creates a deeper and wider deflection basin. Figure 3 presents the findings of Foinquinos et al.

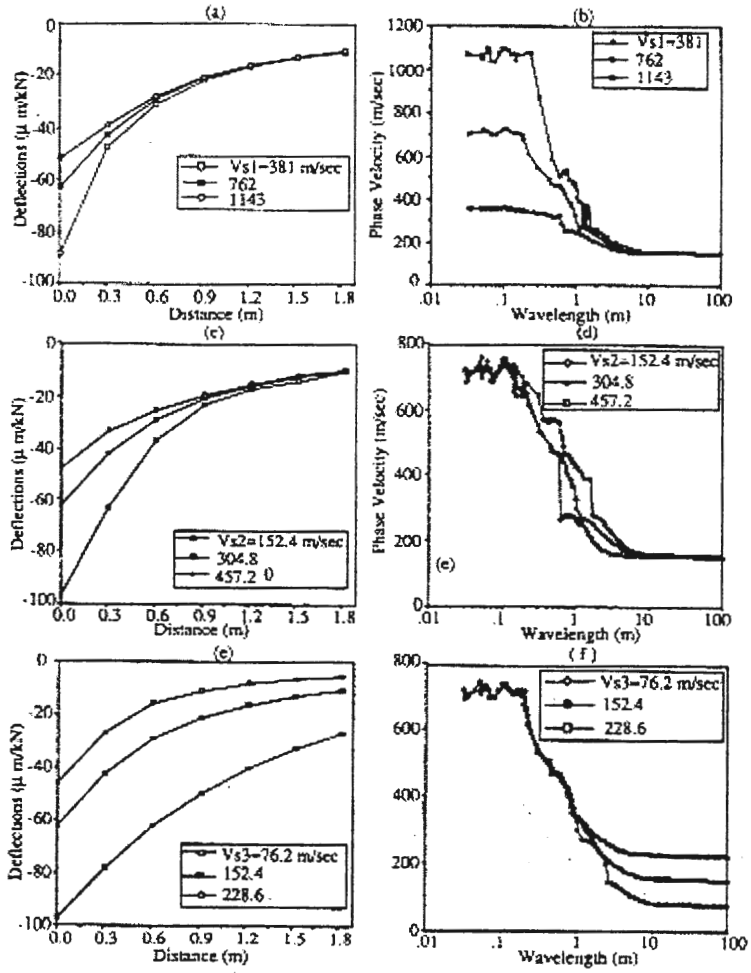

Figure 3. Sensitivity of deflection basins to changes in stiffness of the layers: (a) and (b) surface layer, (c) and (d) base layer, (e) and (f) subgrade layer. [29]

3 RESEARCH PLAN

3.1 Site Review

The research test site is located in the southeast corner of Des Moines, Iowa as part of the US 65 bypass built during the summer of 1997. Figure 4 shows the project location. This portion of the bypass project consisted of both northbound and southbound lanes from the US 65/69 interchange to the IA 5 interchange, totaling 2.69 miles. The concrete pavement was designed as a 12-inch plain jointed pavement on 6 inches of granular base coarse with transverse joints skewed at 6:1 in the counterclockwise direction. The lane widths for the driving and passing lanes were 14 feet and 12 feet, respectively, with 8 inch depth asphalt shoulders extending the highway an additional 8 feet and 6 feet for the driving and passing lanes, respectively. Transverse and longitudinal joints were sealed using a hot-poured sealant. Longitudinal subdrains were installed under the outside shoulder and adjacent to the driving lane. Subdrains were not placed adjacent to the passing lane. The US 65 bypass was designed according to Iowa DOT 1992 specifications.

Of the total 2.69 miles, the project test sections consisted of 2,432 feet of continuous pavement of the southbound lanes between stations 620+03 to 644+35. The pavement was divided into four different test sections: two sections incorporating fiber composite dowels, one stainless steel dowel section, and a control section containing standard epoxy coated bars. Three sections were further subdivided to provide test sections with 8 inch and 12 inch spacing for both the stainless steel and fiber composite dowel bars. The experimental design and layout is illustrated in Table 7 and Figures 5 and 6.

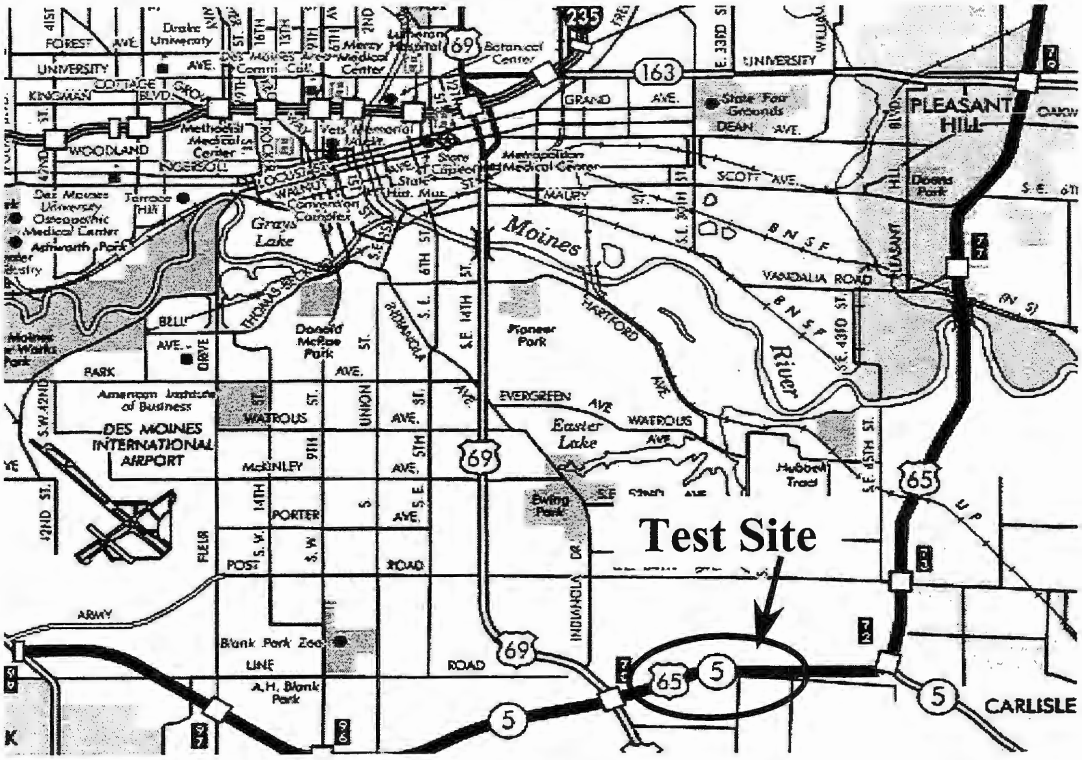

Figure 4. Project site location.

Table 7. Experimental design matrix.

	12-inch Thick JPCP 20-ft Joint Spacing (6:1 skew)			
	8-in Dowel Spacing		12-in Dowel Spacing	
	1.5-in Diameter Dowel	1.88-in Diameter Dowel	1.5-in Diameter Dowel	1.88-in Diameter Dowel
Fiber Composite Dowel Bars		Section 1 Sta. 620+03 to 624+43		Section 2 Sta. 624+63 to 628+80
Fiber Composite Dowel Bars	Section 3 Sta. 629+00 to 630+00		Section 4 Sta. 630+20 to 631+00	
Stainless Steel Dowel Bars	Section 5 Sta. 631+20 to 633+42		Section 6 Sta. 633+82 to 639+38	
Epoxy-Coated Steel Dowel Bars			Section 7 Sta. 639+58 to 644+35	

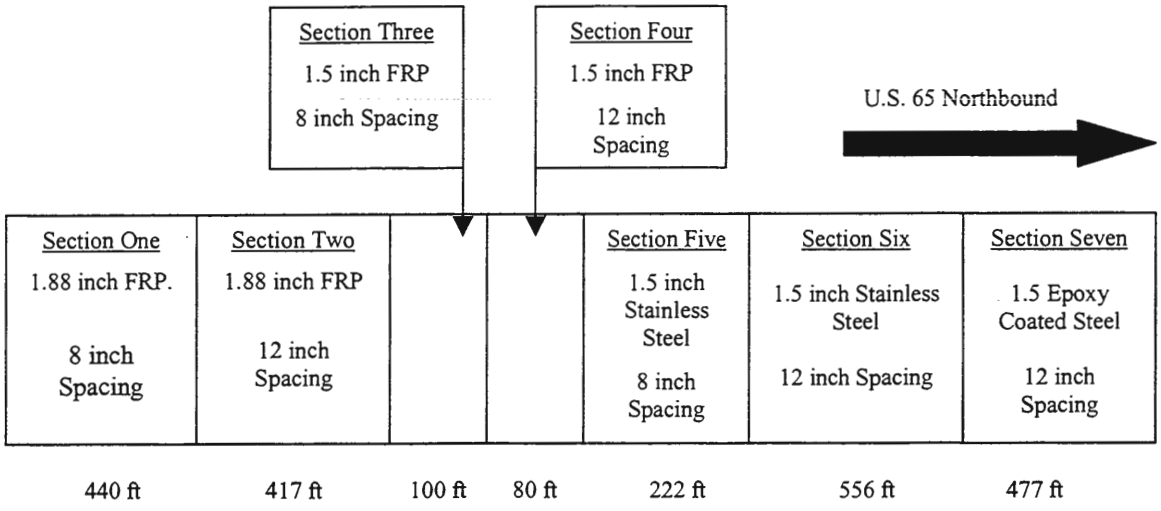

Figure 5. Experimental layout.

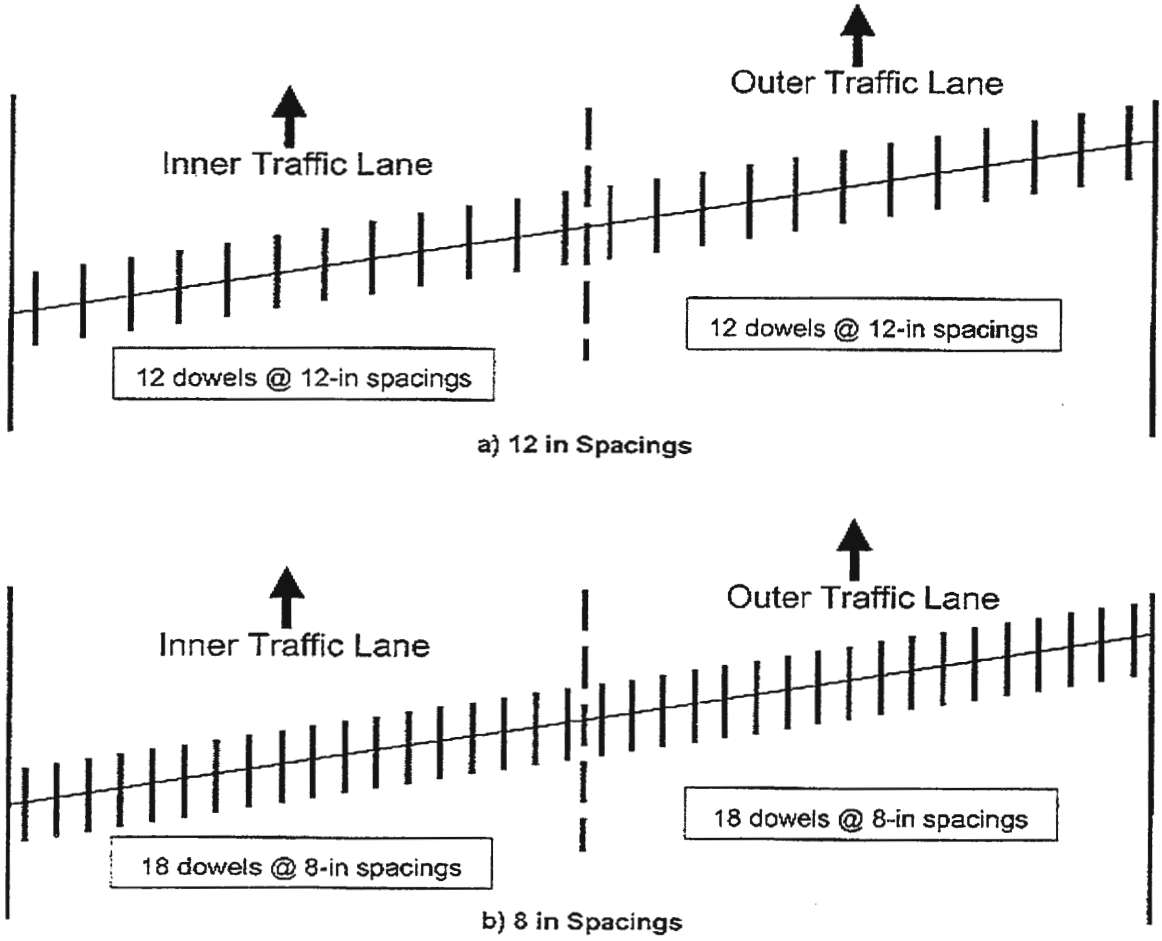

Figure 6. Dowel bar spacing configurations.

The test section is located near the bottom of a vertical curve, with both downhill and uphill sections. The changing vertical grade along with the natural landscape created test sections with subgrade soils consisting of both native soils and structural fill soils. Pavement sections with 1.88 inch diameter FRP dowels are located on fill soils up to approximately station 626+60. At this location the subgrade switches to native soils and continues to the end of the 1.88 inch diameter FRP test sections. The subgrade transitions back to fill at the beginning of the 1.5 inch diameter FRP test section, and continues to station 635+90. The subgrade from station 636+90 to 639+10 consists of native soils. From station 639+10 to 644+35, the remaining portion of the test section is supported by structural fill.

3.2 Dowel Bar Materials

As previously stated, three different dowel bar materials were investigated. Three companies that manufacture fiber composite dowels were interested in supplying their products for project. Two companies were selected based on the speed at which they could provide the dowel bars. In addition to supplying the dowel bars, the FRP dowel companies also supplied tie bars to install across the longitudinal joints. The stainless steel dowel bars with a 1.5 inch diameter were supplied by a separate company selected on similar criteria.

The alternative materials meet the Iowa DOT specifications for flexure, shear, and moment required by IDOT specification #4151, Steel Reinforcement. The alternative dowel diameters were selected to provide similar structural characteristics for load bearing capacity as the standard 1.5 inch diameter steel dowel bar. The dowel diameters utilized were selected by the manufacturer according to their testing and experimental research. Dowel bar properties determined by ISU laboratory testing were provided in Tables 4 and 5.

3.3 Construction

Flynn Construction Company of Dubuque, Iowa constructed the test site in the summer of 1997 with Iowa State University and Iowa DOT staff overseeing the development of the test sections. The location of dowels was recorded for each segment, along with construction procedures used by the contractor to install the dowel bars. Dowel "baskets" were utilized to place the dowel bars at the appropriate height and alignment. Dowels are typically set on the baskets and one end of the steel dowel is spot welded to a brace loop to prevent dowel movement during paving. Also by welding only one end, the pavement is free to move longitudinally due to temperature gradients. Figure 7 is a schematic of the dowel and dowel basket setup. The spot weld on successive dowels within each joint is performed on alternating ends.

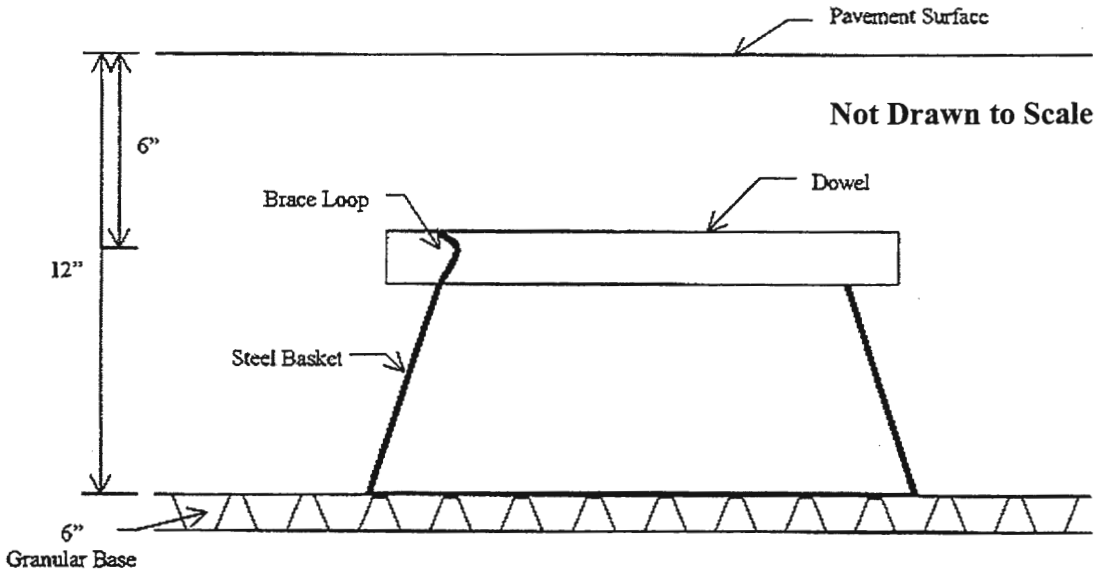

Figure 7. Dowel basket and dowel location schematic. [36]

Steel dowel baskets were utilized for both the epoxy coated steel and FRP dowel bars. Stainless steel baskets were used for the stainless steel dowels. All dowels were shipped to the project site mounted on the dowel baskets. During shipment, many of the dowels became

loose and one end of the dowel bar was required to be re-secured to the basket. Spot welding the fiber composite and stainless steel to baskets was not an option due to degradation of the material from the heat generated during welding. Therefore plastic zip ties were tied around each brace loop and end of the dowel, with excess tie length trimmed before paving.

Tie bars were installed across the longitudinal joint separating the two lanes to ensure load transfer between the two lanes. The tie bars were 0.5 inches in diameter and 36 inches long, with 30 inch on center spacing. The tie bars were mechanically inserted by the paver at slab mid-height. While installing the FRP tie bars, the bars tended to "float" up to or through the pavement surface [36]. This problem was attributed to:

- the automatic tie bar inserter on the paver malfunctioning due to the slightly smaller diameter of these tie bars compared to the standard tie bars, and
- the light weight of the FRP tie bars allowed the roll of concrete to move the tie bar longitudinally and allow final vibration to bring them through the surface.

To correct the problem, laborers hand pushed the tie bars back into the pavement to approximately slab mid-depth. The installation of FRP tie bars was then stopped, and epoxy coated steel tie bars were placed in the remainder of the section.

3.4 Testing Program

The research objective was to evaluate the performance of alternative dowel bars and dowel bar spacing, and compare them to standard epoxy coated steel dowels spaced 12 inches on center. The evaluation process consisted of joint faulting, joint opening, and FWD tests and visual monitoring of the pavement over a 5-year testing period. The testing was conducted on a biannual basis with tests conducted once in the spring and once in late summer or early fall. The test times were selected to evaluate the pavement with a typically wet, weak foundation in the spring and a dry, strong foundation in the summer or fall.

3.4.1 Falling Weight Deflectometer

The falling weight deflectometer (FWD) is a trailer mounted machine that uses non-destructive test methods to measure the response of a pavement section to a dynamic load similar in magnitude to that produced by a moving vehicle tire load. A schematic of a FWD machine is shown in Figure 8. The pavement's deflection response due to the dynamic load is measured by geophones, placed at 12 inch intervals, and collected in a computer installed in the tow vehicle. The observed deflection responses of tests performed at the joint provide information of load transfer efficiency, while tests conducted near the center of slabs indicate pavement and subgrade stiffness. The information can then be analyzed to give an indication of the pavements performance and expected life of each joint tested.

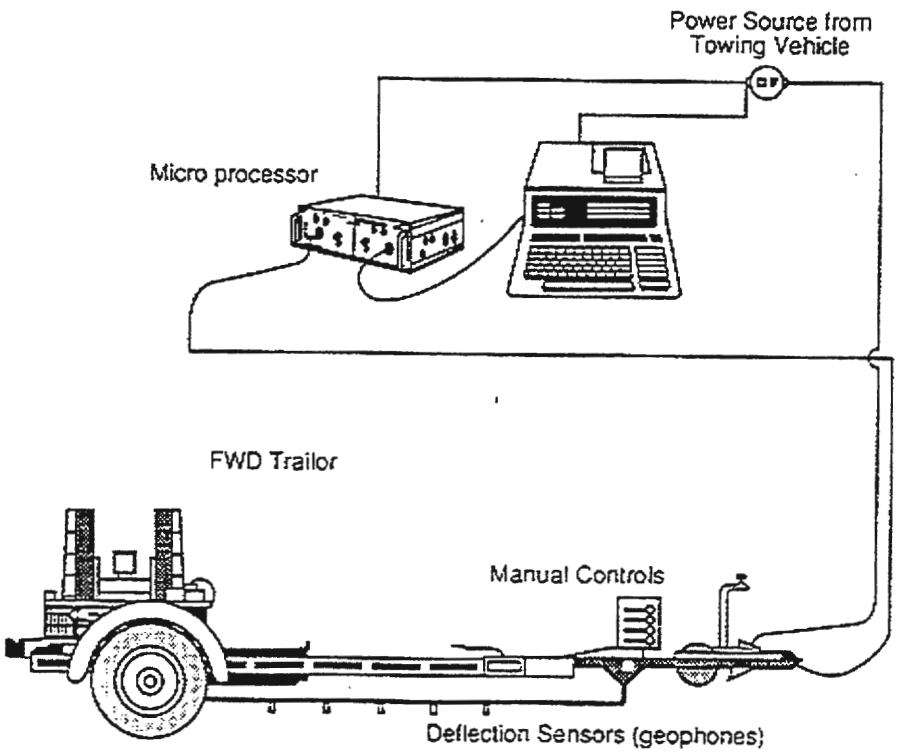

Figure 8. FWD schematic. [8]

FWD tests were conducted in the outside wheel, 2 feet (0.6 meters) from the outer edge, on three transverse joints and three mid-panel locations per test section per lane. Three dynamic loads of 9000, 12000, and 16000 pounds were applied at each test location, with results averaged to provide more accurate information at each location. The variability of the test data at each joint is not important to the scope of the research, but provides a means of statistical analysis to determine any significant difference between joints of different test sections. Figure 9 provides a schematic of a FWD test and a typical pavement deflection at the geophone locations in response to the impact loading.

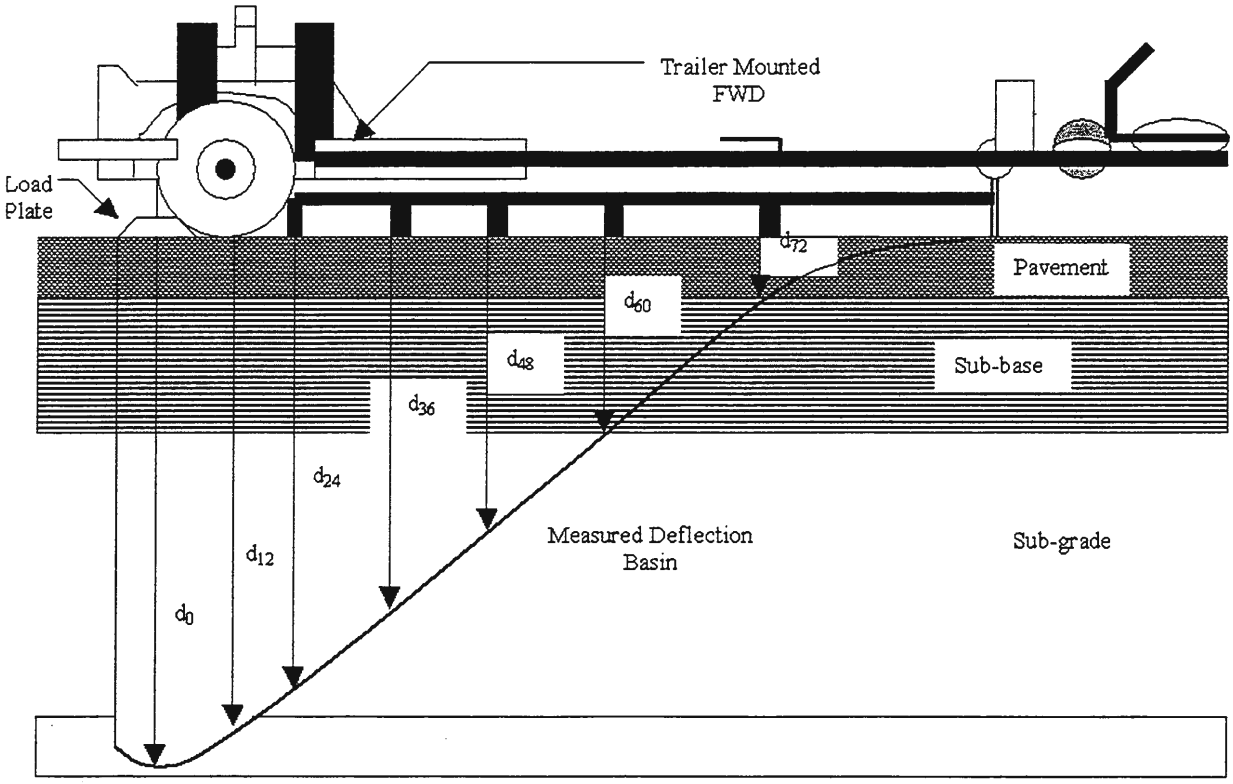

Figure 9. Typical shape of deflection response to loading. [8]

3.4.2 Joint Openings

Concrete pavements will expand or shrink due to temperature changes according to their coefficient of thermal expansion, which is dependent on the materials used in the concrete mix. To avoid problems associated thermal expansion such as cracking or blow-ups, transverse joints are constructed to allow free horizontal movement. Therefore, joint openings were monitored to ensure the joints were allowed to freely move. This testing was conducted by placing surveyor nails into the fresh, plastic concrete at approximately 10 inches apart. The center to center distance between the nails was measured utilizing a digital caliper. The joint openings were measured at approximately the same time as the FWD testing.

3.4.3 Joint Faulting

Over time concrete pavements may start to exhibit joint faulting, which is the presence of a vertical discontinuity between adjacent slabs. If the faulting is severe enough, it will affect the ride quality of the pavement along with creating the possibility of pumping subgrade soils, which in turn will create voids below the pavement and reduce the strength of the pavement system.

Joint faulting was measured using an electronic Georgia Faultmeter (Figure 10) with a digital readout that indicates positive or negative faulting in millimeters. The Faultmeter was set on the pavement in the direction of traffic, with the legs on the "leave side" of the joint and the measuring probe in contact with the approach slab. Movement of the probe is then transmitted to a Linear Variance Displacement Transducer (LVDT) to measure faulting. A slab that is lower on the leave side of the joint will register as a positive faulting, and a slab leaving the joint which is higher, will register as a negative fault. Figure 11 is a schematic of

the positive and negative faulting. Faulting was measured in millimeters for both the inside and outside wheel-paths of the driving lane at 30 inches and 18 inches from the edge, respectively.

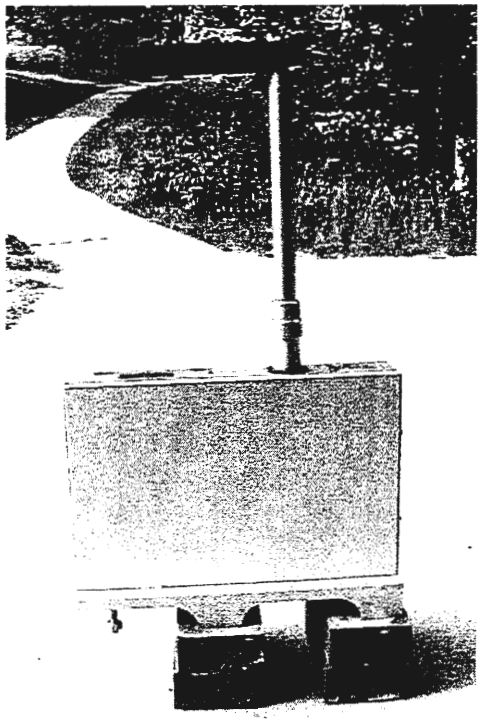

Figure 10. Georgia faultmeter.

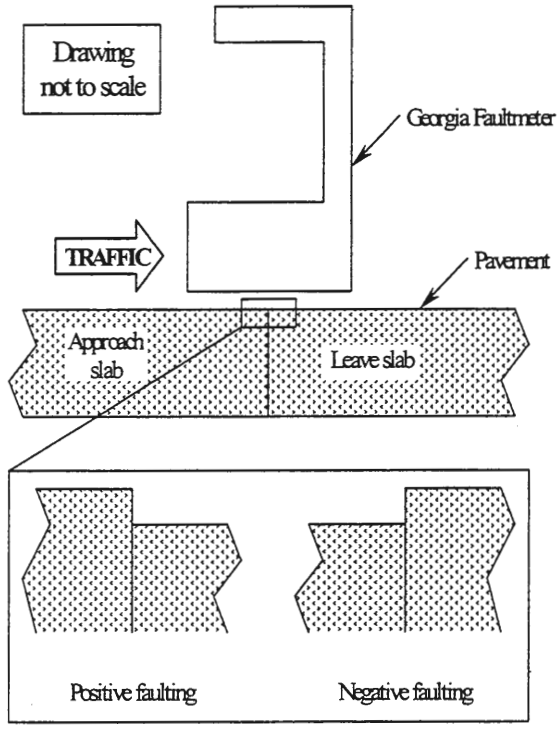

Figure 11. Faulting schematic. [37]

3.4.4 Visual Survey

Along with the quantitative analysis of the pavement's performance, a visual survey of the pavement was performed. The visual surveys identified distresses that occurred between testing periods and were conducted accordance to the Long Term Pavement Performance standards [38]. The surveys were performed at the same time the joint opening and faulting data were collected.

4 DATA ANALYSIS

4.1 Traffic Data

The amount of traffic loading experienced by the highway will impact the performance of a concrete pavement due to fatigue. Therefore traffic was monitored through the use of weigh-in-motion sensors placed in the driving lane of the west bound lane. These sensors are capable of detecting the weight and number of axles of passing vehicles. This information can then be used to determine the number of 18,000 pound Equivalent Single Axle Loads (ESAL's) through the use of an Iowa DOT computer program. Traffic data was available beginning in January of 1999 through the end of the 2001 calendar year, and is presented in Table 8.

Table 8. Traffic data.

Year	Accumulated 18-kip ESAL Applications
1999	651,633
2000	678,767
2001	2,176,982
Totals	3,507,382

The large increase in the number of ESAL's experienced in the 2001 calendar year was mainly due to a large number of 7-axle trucks during the month of August. During this month, the sensors indicated that an average of 9,110, 7-axle or more trucks passed over the sensors on a daily basis. This can be compared to the average of 14.5, 7-axle trucks per day for the other eleven months of the same calendar year, with the second highest monthly average of 72 trucks per day. The large number of 7-axle trucks during August would be

indicative of a construction project utilizing the highway to haul soil, concrete, and other supplies to the project site. The project was most likely the reconstruction of Iowa Highway 5 which consisted of placing structural fill, concrete paving, and bridge construction. The number of 7-axle trucks is consistent and reasonable prior to, and after August, which would indicate the sensors were performing correctly, meaning the data are not erroneous.

4.2 Visual Distress Survey

A visual distress survey was conducted to record any joint or slab deterioration that might affect the transverse joint load transfer. The survey was conducted at the same time joint faulting and opening measurements were obtained. It consisted of identifying changes in joint openings, cracking, or spalling of transverse or longitudinal joints. The survey was conducted in accordance with the Strategic Highway Research Program (SHRP) pavement distress manual.

The visual distress survey indicated that the pavement is in good condition, with no cracking or spalling except for one corner crack. The corner crack was first noticed in the spring of 1999 and extended 3 feet to the south and 1 foot to the west. The crack size or width has not propagated with time.

4.3 Deflection Data

Deflection testing for the project was conducted by Eres Consultants, Inc. of Champaign, Illinois. The testing occurred twice a year, with data from the fall of 1997 through the fall of 2001 available at the time of this thesis. Deflection measurements were recorded at transverse joints and at the mid-slab, for the outside wheelpath for both the passing and driving lanes. Readings were obtained for load levels of 9,000, 12,000, and 16,000 pounds after the load plate was set with a small load to eliminate any voids between

the rubber buffer and pavement. The FWD utilized for this project was composed of 7 sensors spaced at 12 inch intervals as depicted below in Figure 12. All deflection data was recorded in mils, which is equal to one-thousandth of an inch.

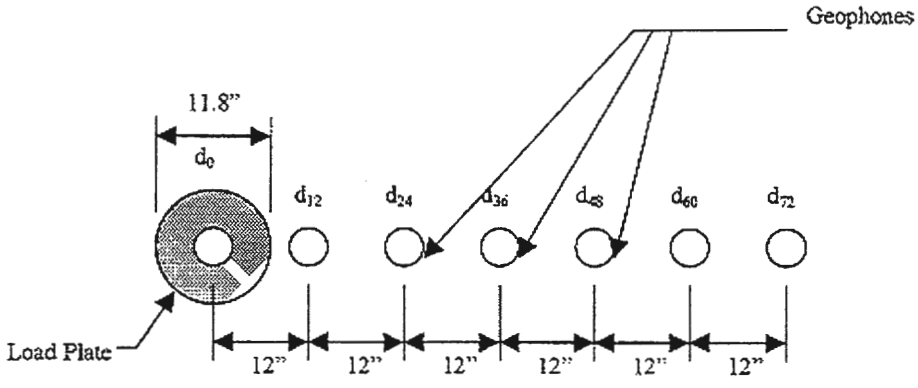

Figure 12. FWD geophone layout. [8]

4.3.1 Load Transfer Efficiency

The FWD deflection testing targeted applied loads of 9,000, 12,000, and 16,000 pounds. However, due to variations in the pavement stiffness the actual loads generated by the FWD will vary slightly from the targeted loads. Therefore, to provide a means to accurately compare the deflections at different locations and joints, the actual pavement deflections were normalized utilizing linear interpolation. Validation of the normalization procedure was conducted by generating a best-fit line through the three data points from each load level for several locations, and determining the coefficient of determination, R-squared. The R-squared values indicate how much of the variance in the deflection data is explained by the load levels. A value close to 1.0 would indicate that the three data points nearly fall on the same line with a constant slope. Thus, most of the variance in the deflections are due to the load levels, validating the normalization procedure. An example of a typical validation graph with equations and R-squared values is presented in Figure 13.

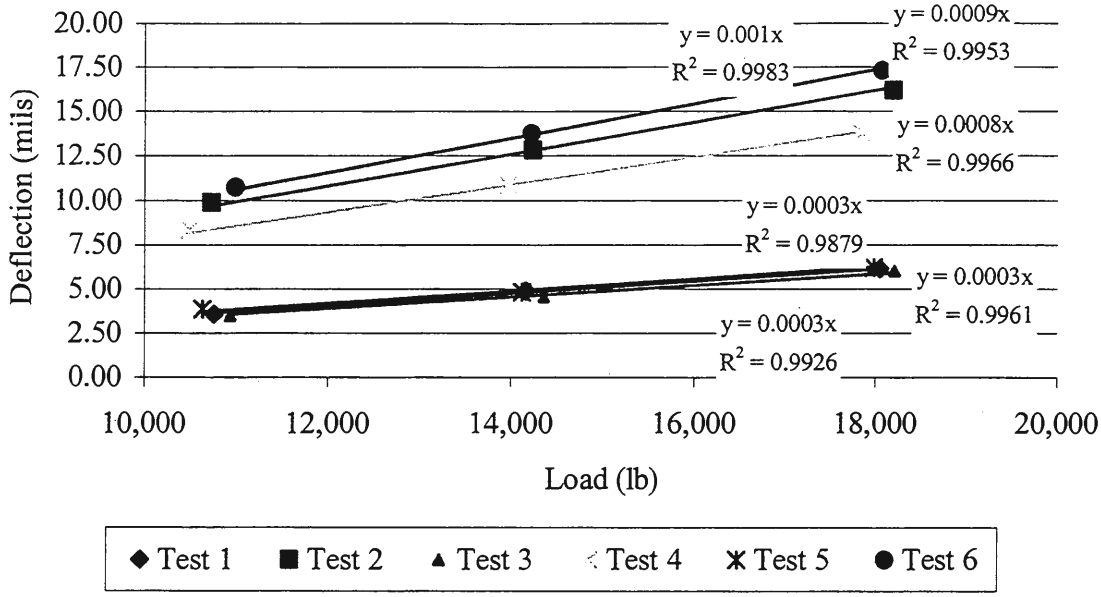

Figure 13. Example verification of normalization by linear interpolation for stainless steel driving lane section in the Fall 1999.

Load transfer efficiency for this project is defined as the ratio of the deflection of an unloaded pavement to that of the adjacent loaded pavement, denoted as a percentage. Load transfer can be defined is this manner because deflections are a function of the stress applied. Therefore, the deflections on either side of the joint, provided they are equal distance from the joint, will give an indication of the load transfer. Using sensors closest to the joint reduce the effects of concrete variability. Deflections were recorded at the load plate, denoted d_0, and every twelve inches up to 72 inches, denoted d_r where "r" is the distance from the load plate in inches. Therefore, the equation to determine load transfer efficiency is:

$$L.T. = d_{12}/d_o * 100\%. \qquad \textit{Equation 1}$$

The load transfer analysis was broken into the driving and passing lanes due to differences in construction, in which only the driving lane had longitudinal drains. The data are shown graphically in Figure 14, which present the research lifetime averages for each of

the dowel bars and spacing. Additional graphs breaking the data down into fall and spring averages over the pavement research life can be found in the Appendix A.

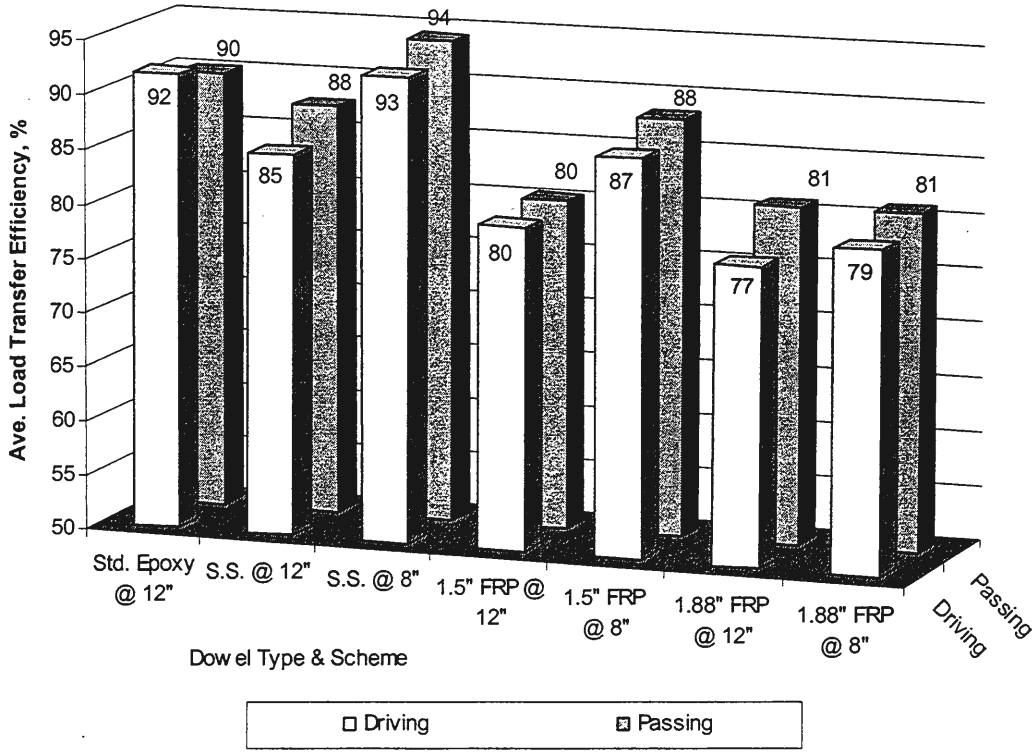

Figure 14. Average load transfer efficiency for pavement research lifetime.

By analyzing Figure 14 and the figures in the Appendix A, several general comparisons can be made between the current dowel design standard of epoxy coated steel spaced at 12 inches and the alternative dowels. The current design standard is currently outperforming the alternatives in load transfer with the exception of stainless steel dowels spaced at 8 inches. Stainless steel at 12 inches and 1.5 inch FRP dowels spaced at 8 inches load transfer efficiency is slightly lower than the epoxy coated steel.

The similar load transfer efficiency between the stainless steel and epoxy coated steel is expected due to their similar stiffness and shear capacities. However, the lower pullout strength (bond strength) for the stainless steel dowel bars may have influenced the lower load

transfer. Increased load transfer efficiency from decreased dowel spacing is also expected due to presence of more dowels near the loaded area. A somewhat unexpected result is the similar performance between the 1.5 and 1.88 inch diameter FRP dowels at 12 inch spacing. If the dowel bar diameter is increased, the result should be a lower bearing stress which intuitively one would think should result in better load transfer. However, Porter et al.[16] concluded that this may not happen due to smaller modulus of dowel support for larger dowel diameters. The modulus of dowel support is defined as reaction per unit area when the deflection is equal to unity. A lower modulus of dowel support will result in a lower relative stiffness of a dowel bar encased in concrete.

The figures also illustrate that for almost all alternative dowel types, the 8 inch spacing is performing better than the 12 inch spacing. The load transfer efficiency increased between 6 to 8 percentage points for the stainless steel and 1.5 inch FRP. The 1.88 inch FRP test results indicate very little to no increase in load transfer efficiency.

These results compare favorable to the laboratory investigation conducted by Porter et. al [16]. From their research, Porter et al. proposed a design scheme as presented in the literature review of this paper, in which they recommend that for pavements greater than 10 inches in thickness, FRP dowel diameters should remain the same as the standard but the spacing be reduced from 12 inches to 6 inches. The results of this field study, utilizing the same FRP dowels, indicate that compared to the current standard dowel design, increasing the FRP dowel diameter does not affect the load transfer efficiency but decreasing the spacing of the 1.5 inch diameter dowel increases the load transfer efficiency.

The results were also analyzed to determine if a trend was developing for load transfer efficiency over time. Figure 15 illustrates the average load transfer efficiency over the nine testing periods.

Figure 15 does not indicate any general trend exists for load transfer over time for the dowel bars or spacing. The data indicate that the alternative dowels with both spacings were performing nearly as well as the standard epoxy coated steel for the first three testing periods. The load transfer was generally in the mid to upper 80 percentile for each test section with the exceptions of the stainless steel and 1.88 FRP dowels at 12 inch spacing during the spring of 1998, with load transfers of 79% and 76%, respectively. After the third testing period most test sections experienced a decrease, but a larger decrease was experienced by the 12 inch spaced stainless steel and 1.5 inch FRP dowels, along with both 12 inch and 8 inch spaced 1.88 FRP dowels. Figure 15 also shows that the spring testing periods generally produced load transfer results lower than the fall, which was expected due to the softer subgrade soil.

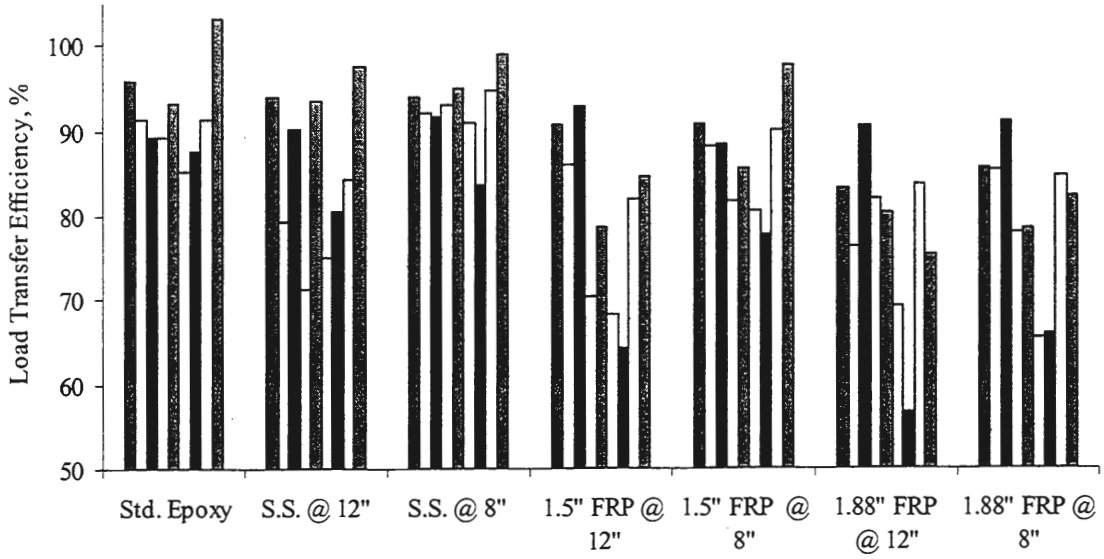

(a)

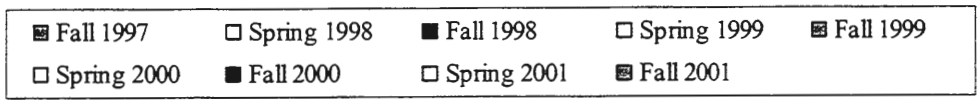

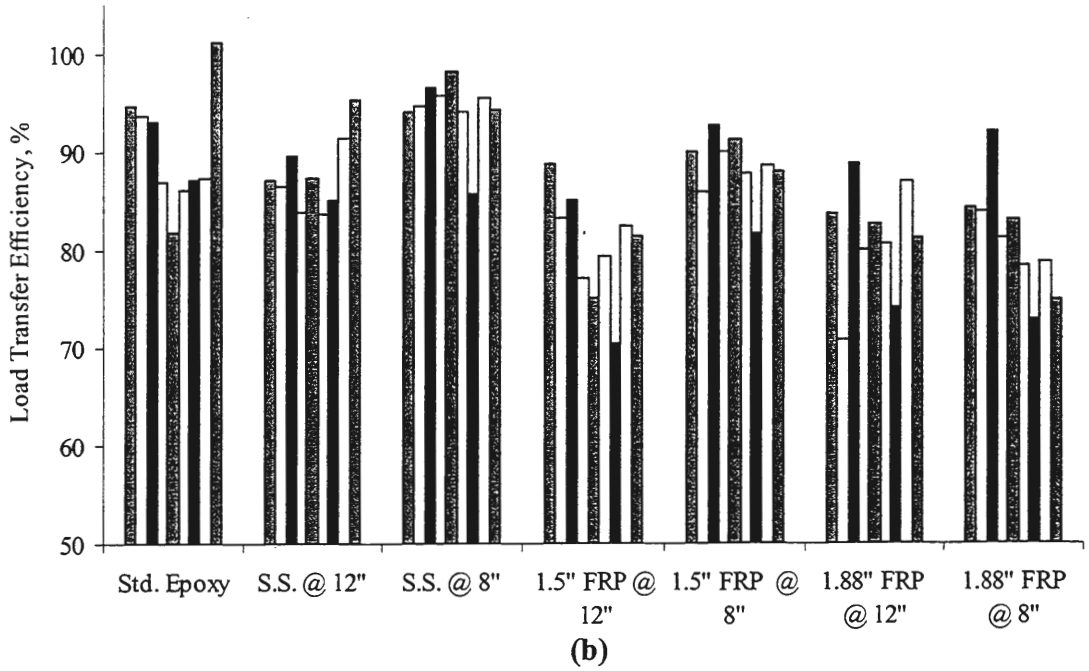

(b)

Figure 15. Chronological average load transfer efficiency over all testing periods. (a) driving lane, (b) passing lane.

4.3.2 Maximum Joint Deflections

The normalized data was also utilized to analyze the differences between the maximum joint deflections for each dowel type and spacing. The point of maximum deflection was recorded by sensor d_0, located directly over the load plate. All deflections were normalized to represent the deflection from a 9,000 pound load.

Figure 16 illustrates the average maximum deflection over the pavement's research life. The joint deflections for the passing lane are higher than the driving lane for all dowel types and spacing, with all passing lane deflections more than 1 mil larger, except the 1.88 inch diameter FRP section at 8 inch spacing. The most likely explanation to why the passing lane deflections are great is due to the absence of the longitudinal drains along the passing lane. The drains expatiate the removal of water from the subgrade soils, thus increasing the soil stiffness. Also, as will be discussed in Section 4.3.5, the concrete modulus of elasticity is larger in the driving lane than for the passing lane. The modulus of elasticity describes the materials stiffness, therefore the lower modulus of elasticity of the passing lane will correspond to greater deflections at the same load levels.

When comparing the treatments within each lane in Figure 16, the maximum joint deflections are generally within 0.5 mils. The only sections varying significantly more than 0.5 mils are the 1.88 inch diameter FRP at 8 inch spacing in the passing lane and stainless steel dowels spaced at 8 inches in the driving lane. Additional joint deflection graphs can be found in Appendix B.

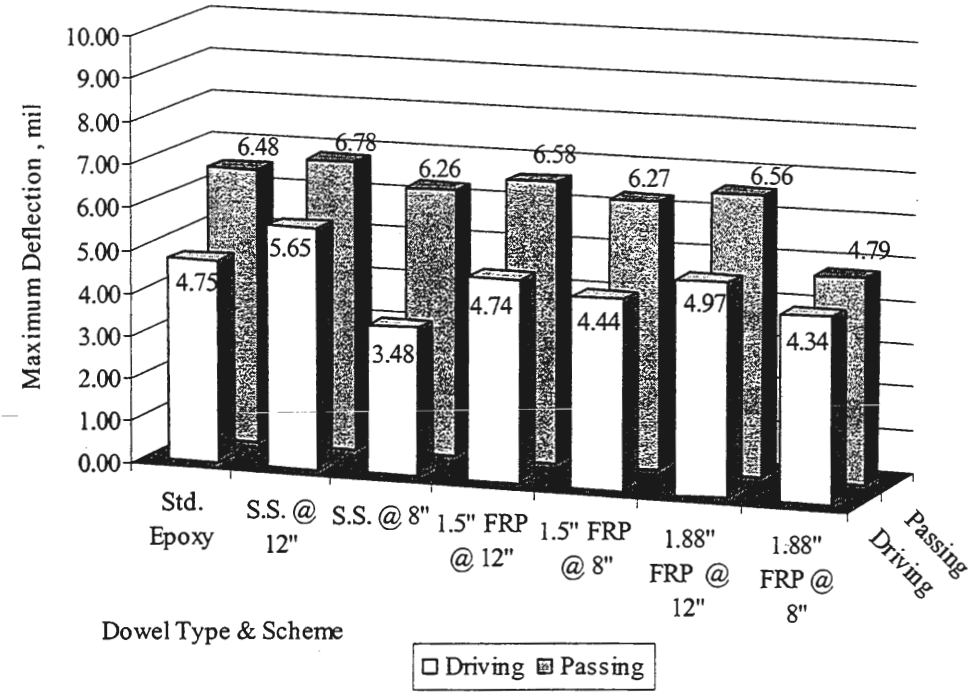

Figure 16. Average maximum deflection for the pavement research lifetime.

4.3.3 Backcalculation of Layer Moduli

The FWD tests conducted at the section's mid-slab can be utilized to analyze the pavement and subgrade moduli. The moduli are determined through a closed form backcalculation procedure based on Westergaard's plate theory model. Several parameters must be calculated during this procedure. They include the area of the deflection basin (AREA), radius of relative stiffness (l_k), modulus of subgrade reaction (k), and the concrete's modulus of elasticity (E). The deflection basin area calculation is based on the trapezoidal rule using the following equation:

$$AREA = 6 + 12(d_{12}/d_0) + 12(d_{24}/d_0) + 12(d_{36}/d_0) + 12(d_{48}/d_0) + 12(d_{60}/d_0) + 6(d_{72}/d_0) \qquad \textit{Equation 2}$$

where d_r = deflection measured r inches from the applied load.

The AREA parameter is calculated using raw data, not the normalized data discussed above and used for the load transfer and maximum deflection analysis. The AREA is normalization by dividing each deflections at each sensor by the maximum deflection, d_0. Therefore, any variations in the deflections due to the applied loads are removed.

Prior to the determination of the moduli, the AREA parameter must be used to estimate the radius of relative stiffness, l_k. Westergaard defines the radius of relative stiffness as the ratio of the stiffness of the slab or pavement to the stiffness of the foundation soils. If the foundation is modeled as a dense liquid, the radius of relative stiffness can be calculated using the following equation:

$$l_k = \sqrt[4]{\frac{E_c h_c^3}{12(1-\mu_c^2)k}} \qquad \textit{Equation 3}$$

Where: E = Concrete modulus of elasticity
μ = Concrete Poisson ratio
k = Modulus of subgrade reaction.
h_c = Concrete thickness.

However, it has been shown that the radius of relative stiffness can be estimated utilizing the AREA parameter of a seven sensor FWD by utilizing the following equation [39]:

$$l_k = \left[\frac{\ln\left(\frac{72-AREA}{242.385}\right)}{-0.442}\right]^{2.205} \qquad \textit{Equation 4}$$

The modulus of subgrade reaction, k, provides an estimation of the soils ability to carry loads and is the ratio of the stress applied to induce a displacement of unity, meaning one unit of the measurement system employed, such as inches or centimeters. The modulus of subgrade reaction is reported as a load per area per unit of deflection and can be estimated from the measured deflections in pounds per cubic inch with Equation 5 [39]:

$$k = \frac{P d_r^*}{d_r l_k^2}$$ *Equation 5*

Where: P = Load magnitude
d_r = Measured deflection at distance r from the load plate
d_r^* = Nondimensional deflection coefficient for radial distance r:

$$d_r^* = a \text{ Exp } [-b \text{ Exp } (-c\, l_k)]$$

where a, b, and c are constants based on the distance from the applied load.

Equation 5 requires deflection measurements at only one sensor location to determine the subgrade reaction, with the sensor distance from the load plate taken into account by the nondimensional deflection coefficient. Therefore, the deflections from each of the seven sensor locations were utilized to determine the subgrade reaction and then averaged to determine the subgrade reaction for that test. The procedure was followed for each load increment at each test section, with the affect of different loads handled by using the maximum deflections to normalize the data while determine the AREA term.

With the modulus of subgrade reaction and radius of relative stiffness determined, the modulus of elasticity of the concrete pavement can be determined rearranging Equation 3 (Equation 6) if Poisson's ratio is assumed. The concrete modulus of elasticity is the ratio of the stress applied to the strain experienced. Poisson's ratio is the longitudinal strain divided by the transverse strain, and is typically between 0.10 and 0.20 for concrete [40], with this research project assuming a Poisson's ratio of 0.15.

$$E_c = \frac{12(1-\mu_v^2) l_k^4 k}{h_c^3}$$ *Equation 6*

4.3.4 Modulus of Subgrade Reaction

The modulus of subgrade reaction determined from FWD testing is a dynamic modulus calculated from an impact load. The effect of a dynamic load on the modulus of subgrade reaction results in a value approximately double the static modulus of subgrade reaction utilized for pavement design. Therefore, the presented values should be divided by 2 if they were to be used in a design or compared to typical values.

The modulus of subgrade reaction was analyzed to find differences with in test sections, testing season, lane, and type of subgrade material. The changes in subgrade over time were also investigated and presented in Appendix C.

Figure 17 illustrates the modulus of subgrade reaction over the pavement's research lifetime. The figure is broken into driving and passing lanes. There appears to be little difference between treatment types within a lane. However, a significant difference exists between the driving and passing lane for each treatment, with the driving lane having soils with much larger modulus of subgrade reactions.

The driving lane was constructed with longitudinal drains in all test sections, but the passing lane did not. The drains allow for water to escape from the subgrade soils quicker, alleviating any excess pore pressures that may develop, particularly in the spring when soils thaw. A soil that does develop excess pore pressures that cannot be alleviating quickly, will be weaker due to lower effective stress.

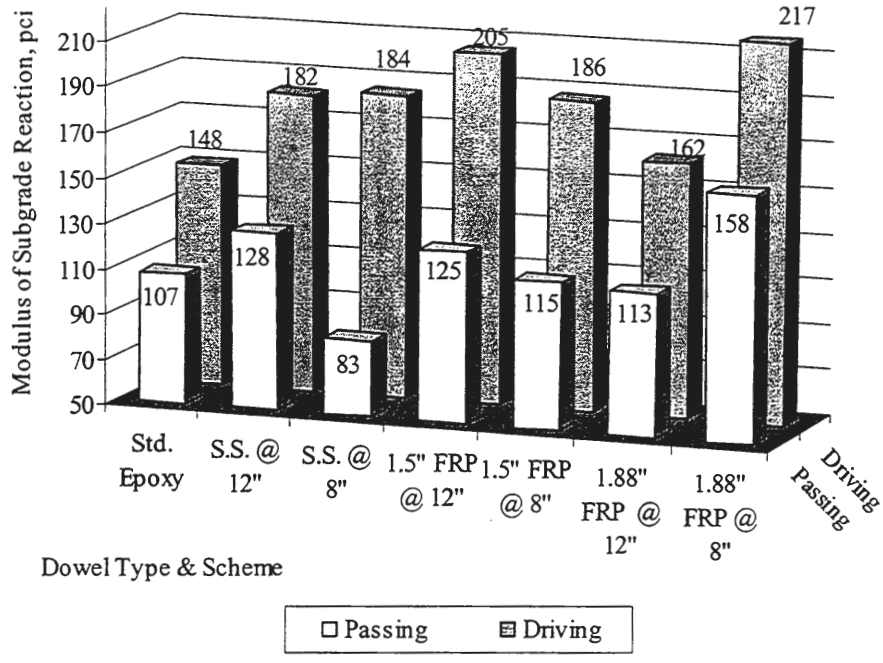

Figure 17. Research lifetime average modulus of subgrade reaction.

Change in the modulus of subgrade reaction over time was analyzed in Figures 1C through 3C, which can be found in Appendix C. The figures indicate that the subgrade modulus of reaction changed over time, but do not show a trend indicating loss of subgrade support. A loss of subgrade support would be expected if pumping occurred due to inadequately performing dowels.

Figures 18 and 19 illustrate the change in modulus of subgrade reaction between testing periods. Figures 18 and 19 indicate the majority of the test sections did not experience a large change between the spring and fall testing periods. The stainless steel placed in the driving experienced the greatest amount of change, on the order of 40 pounds per cubic inch (pci). Also of interest is that in the driving lane, the spring values are generally higher than the fall. It is typically expected that a pavement subgrade would be

weakest in the spring due thawing and the development of excess pore pressures. In the passing, the only treatments indicating change between seasons were the epoxy coated steel and 1.88 inch diameter FRP, which had spring values approximately 20 and 25 pci higher, respectively. The spring values in the passing lane generally follow the expected trend of lower spring values, but the differences are very small.

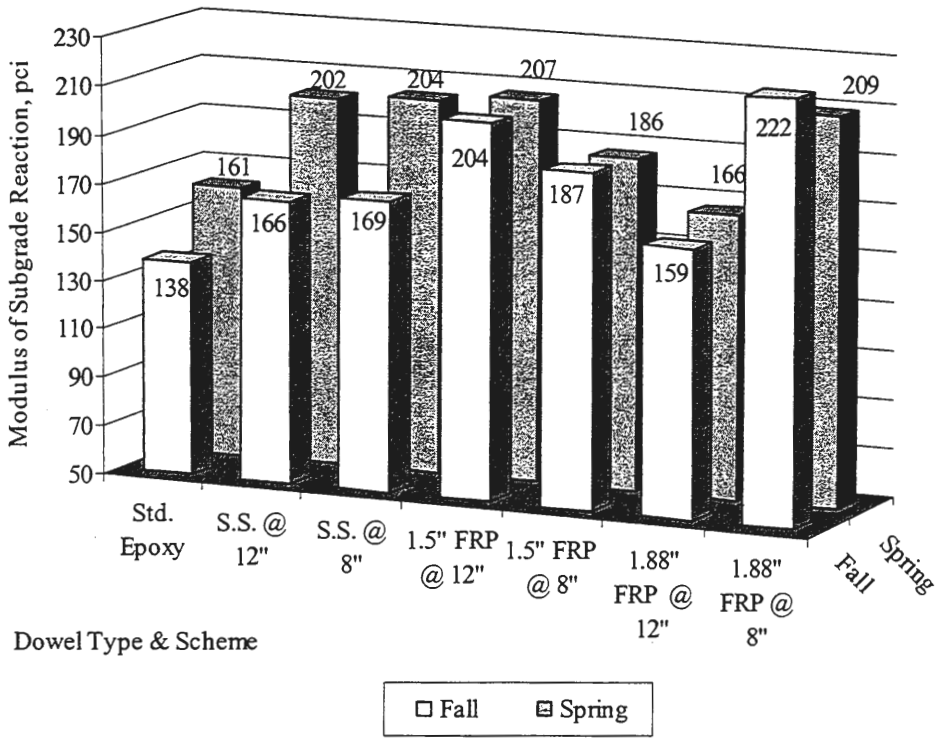

Figure 18. Comparison between the research lifetime averages of the modulus of subgrade reaction in the fall versus spring for the driving lane.

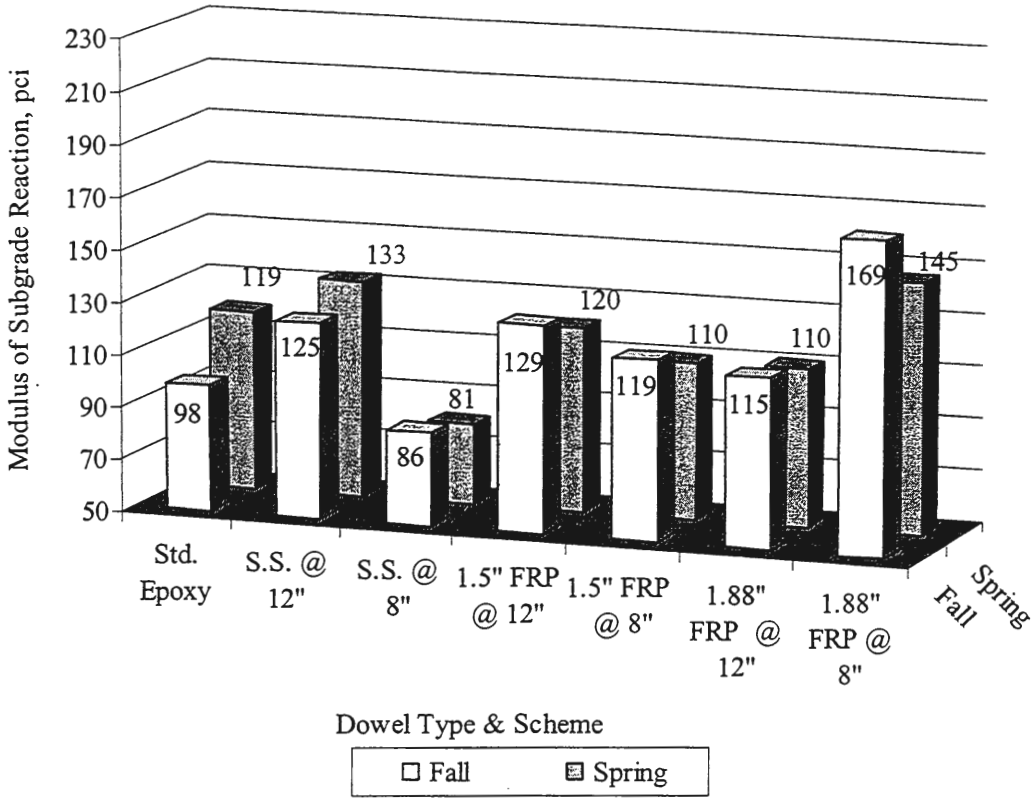

Figure 19. Comparison between the research lifetime averages of the modulus of subgrade reaction in the fall versus spring for the passing lane.

The effect of the subgrade material on the modulus of subgrade reaction was also analyzed. The project site subgrade consisted of sections with both natural existing soils and structural fill. An analysis of the location of soil types concluded that the only treatment constructed on native soils was the section with 1.88 inch diameter FRP dowels with 12 inch spacing. When the modulus of subgrade reaction for that section was compared with all others, it was concluded that the fill soils have a slightly higher modulus than the corresponding structural fill soils. Figure 20 illustrates the differences for several means of comparison, such as an overall mean, fall mean, spring mean, and differences in the driving and passing lane.

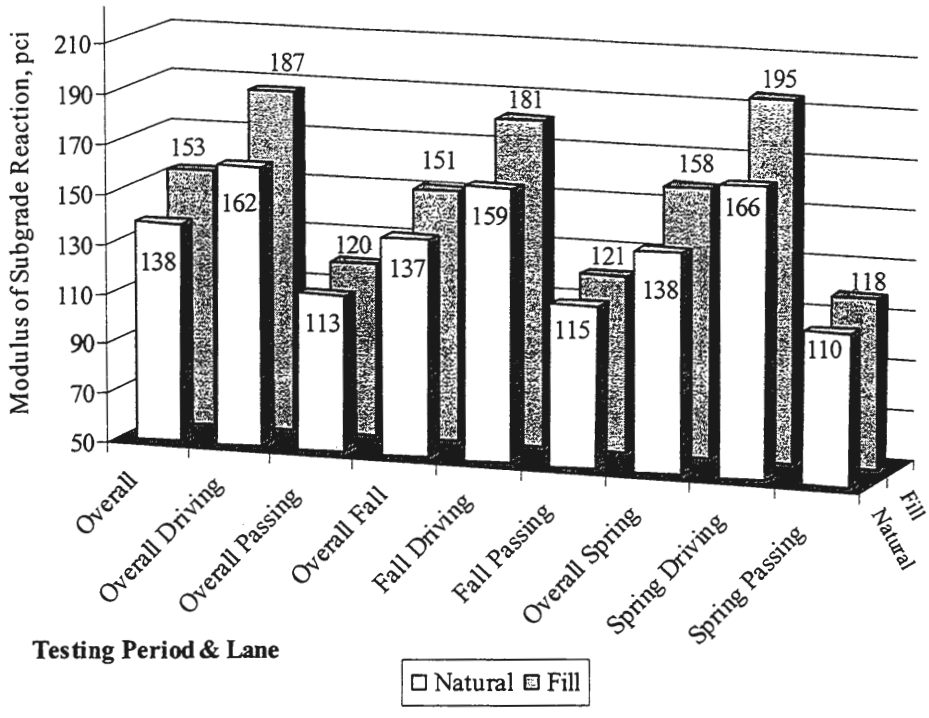

Figure 20. Effect of subgrade type.

The final analysis conducted for the modulus of subgrade reaction was to analyze the effects the modulus had on load transfer and joint deflections. Figure 21 displays both the modulus of subgrade reaction and load transfer efficiency for each dowel bar type and spacing. The modulus of subgrade reaction was consistently lower in the passing lane, but the load transfer efficiency was higher. Also, there is no correlation between increasing or decreasing the modulus of subgrade reaction resulting in increased or decreased load transfer. This would indicate that the modulus of subgrade reaction was not a controlling variable in the pavement's ability to transfer load.

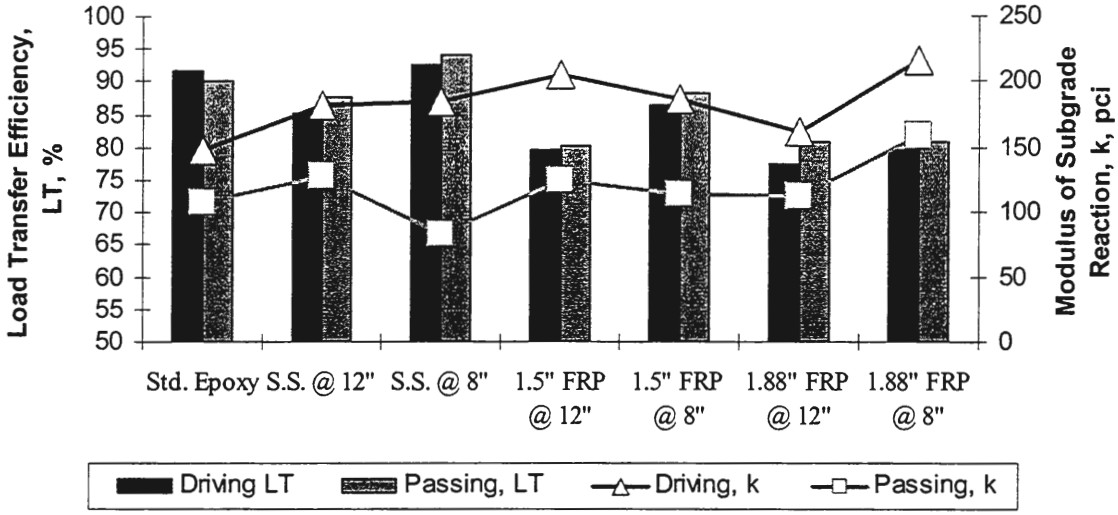

Figure 21. Effect of modulus of subgrade reaction on load transfer efficiency, based on research lifetime averages.

Figure 22 illustrates the relationship between the modulus of subgrade reaction and joint deflections for each dowel bar type and spacing. The figure depicts that when compared to the driving lane, the lower modulus of subgrade reaction of the passing lane corresponded with larger joint deflections. Greater joint deflections occur at lower modulus of subgrade reaction due to a less stiff soil, which will deflect more under similar loads. The increased joint deflection also is affected by the decrease in lower concrete modulus of elasticity in the passing lane, as will be discussed in Section 4.3.5. Figure 22 also depicts that within each lane, there is not a strong pattern indicating that increasing modulus of subgrade reaction will result in decreased joint deflection.

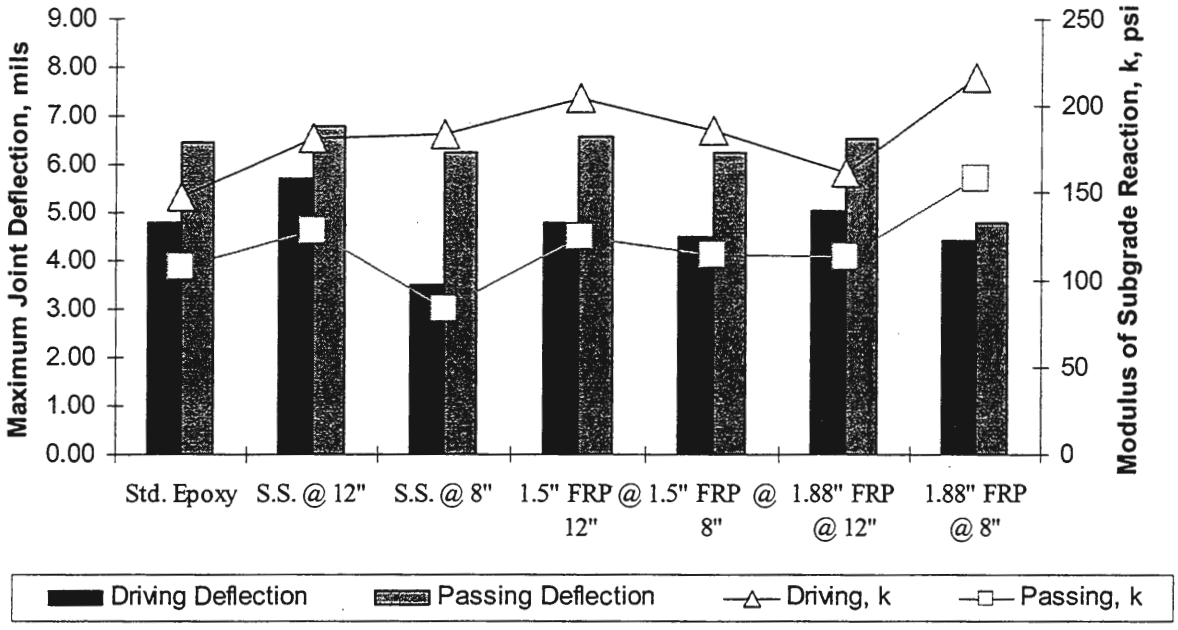

Figure 22. Effect of modulus of subgrade reaction on joint deflection, based on research lifetime averages.

4.3.5 Concrete Modulus of Elasticity

The results of the backcalculation procedure for the concrete modulus of elasticity for each treatment type is presented in Figure 23. The values presented are the research lifetime average for each treatment type, broken into driving and passing lanes. A graphical comparison of the concrete modulus of elasticity over the pavement lifetime is presented in Appendix D. The graphs indicate all treatment types are changing in approximately the same way over time.

The values recorded are higher than what is normally expected for concrete. Mindess and Young [40] suggest the modulus of elasticity for concrete should range between 2 to 6 million psi. However, they also indicate that moduli determined from dynamic loading will generally be 20 to 30% higher, resulting in a modulus of elasticity ranging between 2.4 and 7.8 million psi. Review of the equation used to calculate the modulus of elasticity (Equation

6), will show that the modulus of subgrade reaction is found in the numerator. As discussed in the previous section, the dynamic modulus of subgrade reaction is approximately double the static modulus of subgrade reaction. If this is taken into account and the modulus of elasticity values are divided by two, the results are within the typical values stated by Mindess and Young, indicating the FWD and backcalculation procedures are a valid analytical process.

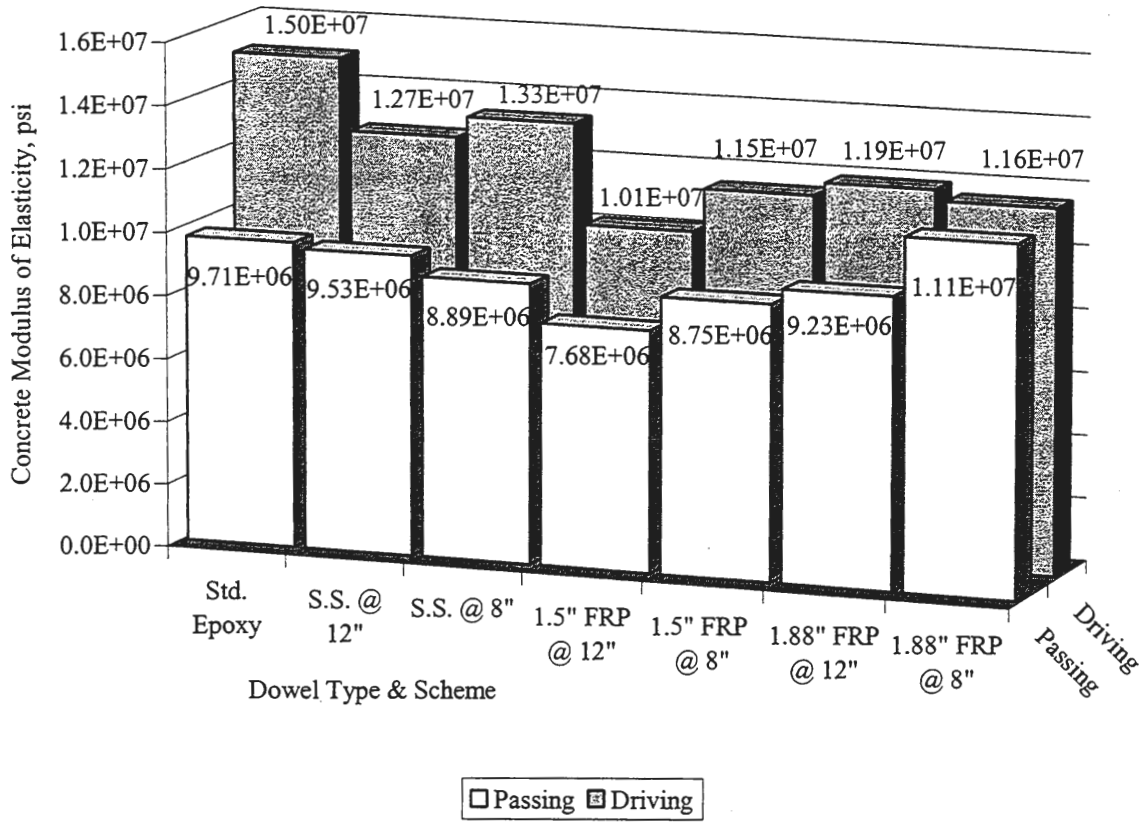

Figure 23. Average concrete modulus of elasticity for the pavement research lifetime.

Figure 23 also indicates that the concrete modulus of elasticity in the driving lane is larger than the passing lane for each dowel bar type and spacing. In the driving lane, the

epoxy coated steel sections exhibited the largest modulus of elasticity, followed by the stainless steel sections, and finally the FRP sections. The 8 inch spacing for the stainless steel and 1.5 inch diameter FRP resulted in higher modulus of elasticity values if compared to the 12 inch spacing. The modulus of elasticity in the passing lane did not show as much deviation between the different test sections. The 1.88 inch diameter FRP with 8 inch spacing had the highest moduus of elasticity, followed by 5 treatments with similar results, and then the 1.5 inch diameter FRP sections having the lowest values.

Figure 24 provides a comparison between the concrete modulus of elasticity and load transfer efficiency. A general trend exists between the modulus and load transfer, with a higher load transfer efficiency corresponding with a higher modulus of elasticity. The trend is more defined for the driving lane than the passing. This is most likely due the small variation in concrete modulus of elasticity of the test sections within the passing lane. The higher load transfer with higher modulus of elasticity can be explained by the effects of load transfer and fatigue. If a pavement slab has a high load transfer efficiency, lower stresses will be observed within the slab. Lower stresses from repetitive traffic loads will result is less fatigue, which is the loss of elasticity and strength due to cyclic stresses.

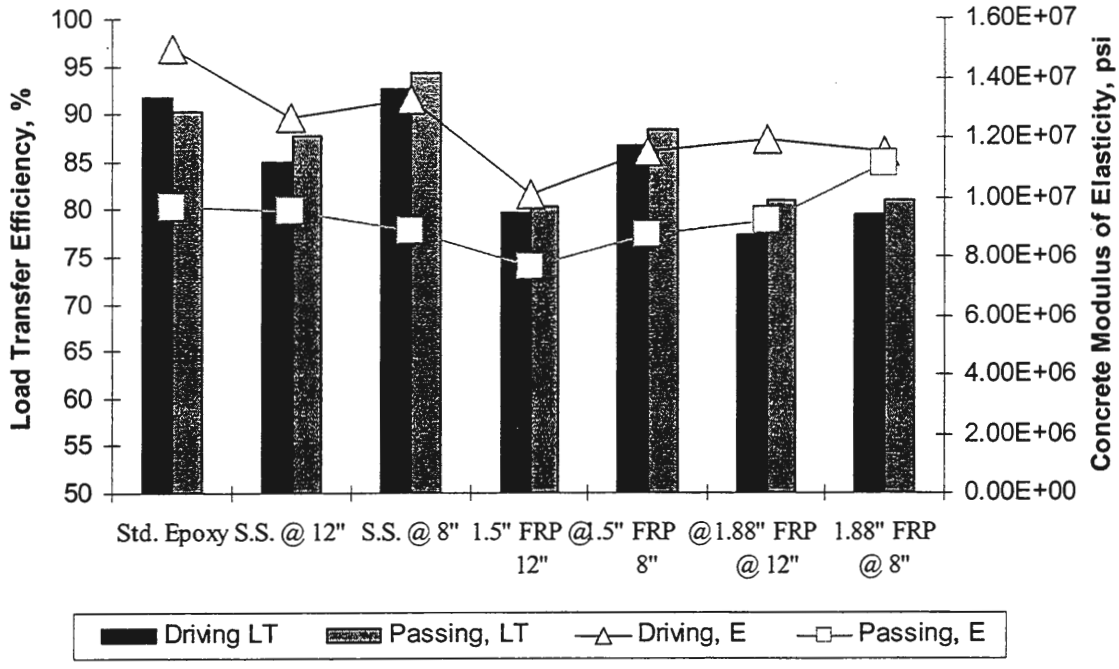

Figure 24. Comparison between the research lifetime averages of the concrete modulus of elasticity and load transfer efficiency.

Figure 25 compares the concrete modulus of elasticity to the maximum joint deflections for each of the dowel bar types and spacings. The passing lane consistently has lower modulus of elasticity values in comparison to the driving lane, while at the same time the joint deflections are greater for the passing lane. The lower modulus of elasticity in the passing lane is most likely the result of increased stresses in the slab due to the lower modulus of subgrade reaction in the passing lane. The effects of fatigue on the passing lane is therefore a result of lower modulus of subgrade reaction, not due to traffic loads, which would generally be lower in the passing lane. If the treatment types within each lane are compared, the general trend continues, with higher modulus values corresponding to smaller joint deflections.

The result of increased joint deflection with decreasing concrete modulus of elasticity is exactly what would be expected. Modulus of elasticity, by definition, is the stress divided by the strain. A higher modulus of elasticity should therefore result in the material deforming less under the same loading conditions.

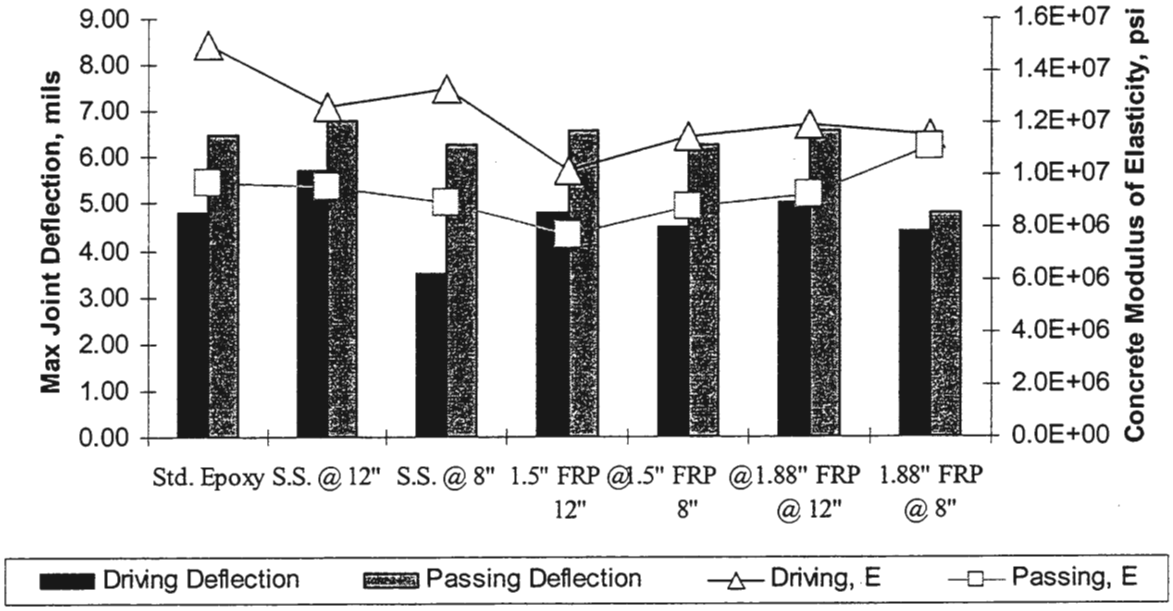

Figure 25. Comparison between research lifetime average maximum joint deflection and concrete modulus of elasticity.

4.3.6 Joint Faulting

As stated in the research plan, the pavement faulting was monitored with the Georgia Faultmeter. Faulting measurements were obtained for both the inside and outside wheel path in the driving lane only. The analysis consisted of looking at the overall research lifetime average and wheel path averages for all treatment types, with the results illustrated in Figure 26.

Figure 26 indicates the epoxy coated steel sections experienced the least amount of faulting. The also appears that decreasing dowel spacing from 12 to 8 inches for the 1.5 inch

diameter FRP and 1.88 inch diameter FRP resulted in less faulting. The decreased spacing for the stainless steel dowels had little effect, but the average faulting of stainless steel with either spacing combination is less than the two FRP dowel sections with 12 inch spacing.

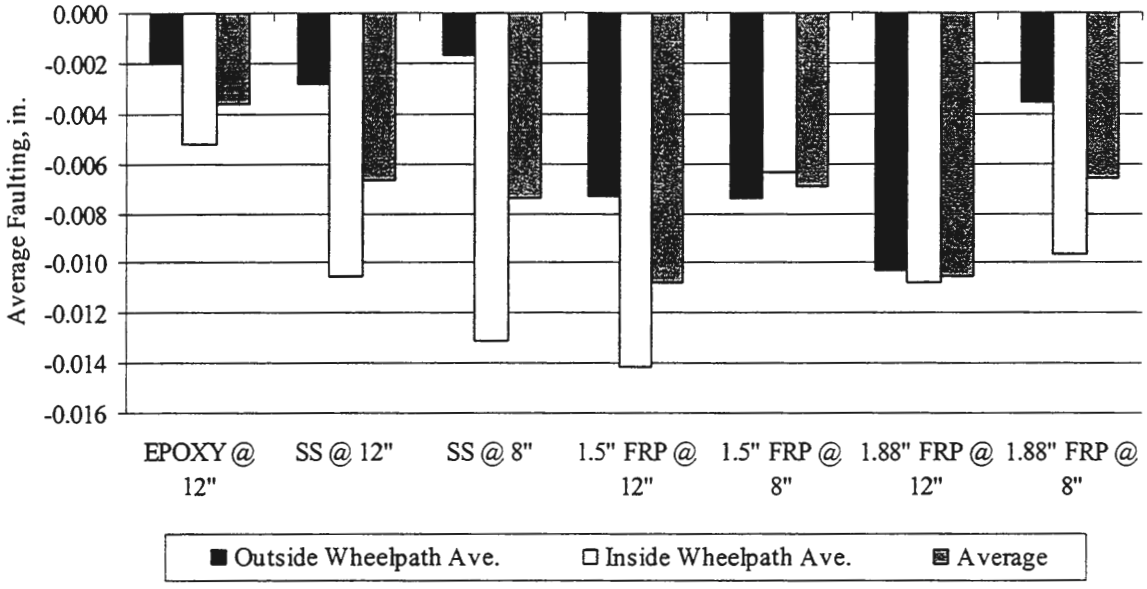

Figure 26. Average joint faulting over the pavement research lifetime.

Along with the effect of dowel type and spacing, the faulting data was analyzed with regard to the grade of the pavement sections. Pavement sections epoxy coated steel dowels and stainless steel dowels with 12 inch spacing were construction on an uphill grade. The stainless steel with 8 inch spacing and 1.5 inch diameter FRP dowels with 12 and 8 inch spacing are located on a flat subgrade The downhill grade of the vertical curve was constructed with 1.88 inch diameter FRP dowels with both 8 and 12 inch spacing.

Figure 27 illustrates the results of the analysis. The analysis shows that the uphill section with the least amount of faulting, with the flat and downhill grades approximately equal. However, the grade should not be considered the only attributing factor to the

faulting. The graph is influenced by the type of dowel bars and spacing used. The uphill section consisted of the two types of dowel bars and spacing with the lowest faulting.

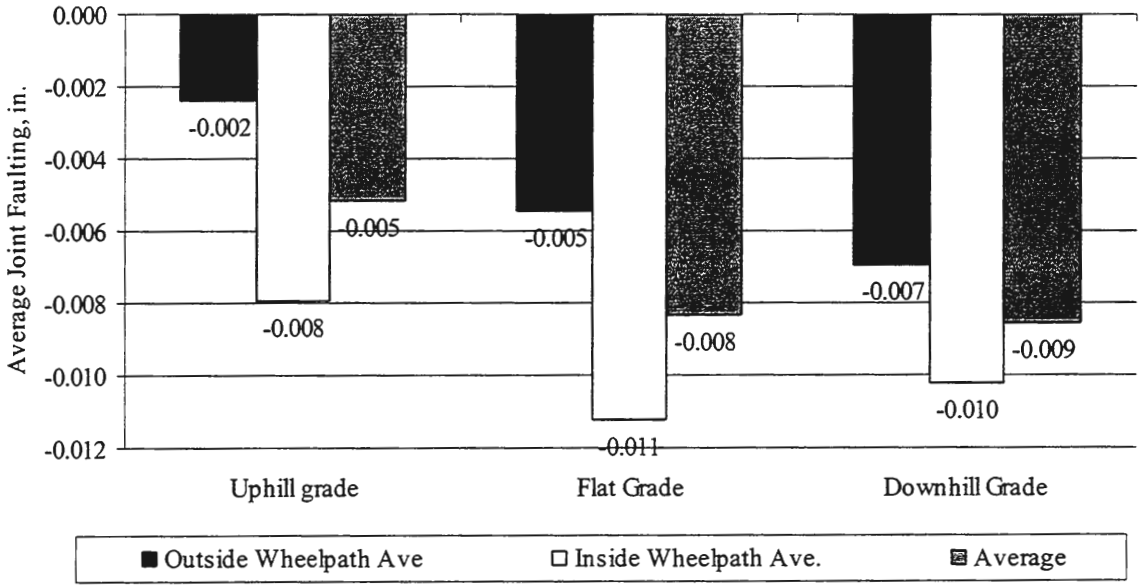

Figure 27. Effect of pavement grade on joint faulting.

Lastly, the faulting was analyzed to determine the effect of the season of testing. Figure 28 indicates that joint faulting was greater during the spring testing periods in comparison to the fall testing periods. There are two possible explanations for the difference between testing periods. The most probable cause for the difference is due to a missing data in the fall of 2000. The springs of 2000 and 2001 both have large negative deflections in comparison to the other testing periods. Joint faulting data for the fall of 2000 may have increased fall average, resulting less difference between the seasons

The second possibility could be the affect of warping and curling from temperature gradients created by the pavement surface expanding or contracting prior to the pavement bottom. A pavement will warp (convex shape) when the pavement surface is expanding and

curl (concave shape) if the surface contracts. In the spring, temperature changes are generally larger than temperature changes in summer months, resulting in larger temperature gradients and thus more curling and warping which will effect faulting measurements.

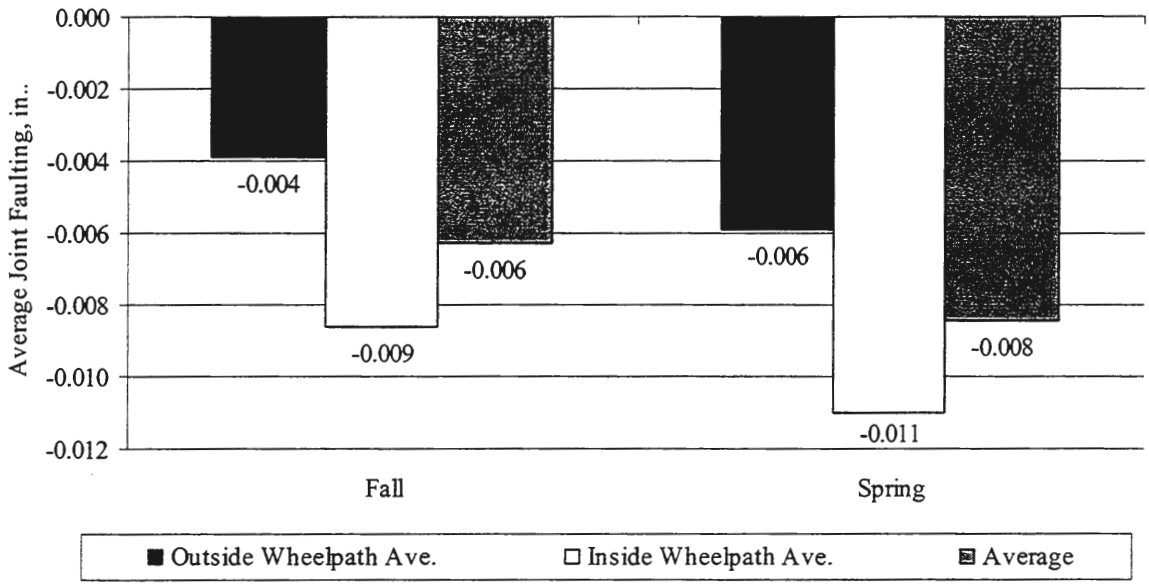

Figure 28. Seasonal variation of average research lifetime joint faulting.

Graphs indicating the maximum, minimum, and average faulting for each test section are provided in Appendix E. Also in Appendix E are graphs showing the relationship of faulting over time, for each test section. These graphs indicate a general downward trend, with values becoming more negative with time.

4.3.7 Joint Opening

Joint openings were measured to ensure the pavement slabs were able to move from expansion and contraction caused by thermal gradients. If pavements were not allowed to move, distresses within the pavement would develop, such as spalling and cracking. The openings were determined by measuring the distance between surveyors nails with a digital

caliper. The nails were placed in the fresh concrete, on either side of the joint, 10 inches apart. Figure 28 is a graph of the differences between adjacent testing periods (i.e. Spring 1998 signifies Spring 1998 joint opening minus Fall 1997 joint opening). The graph illustrates the all pavement test sections were able to expand or contract. This corresponds with the visual distress survey in which no spalling has occurred.

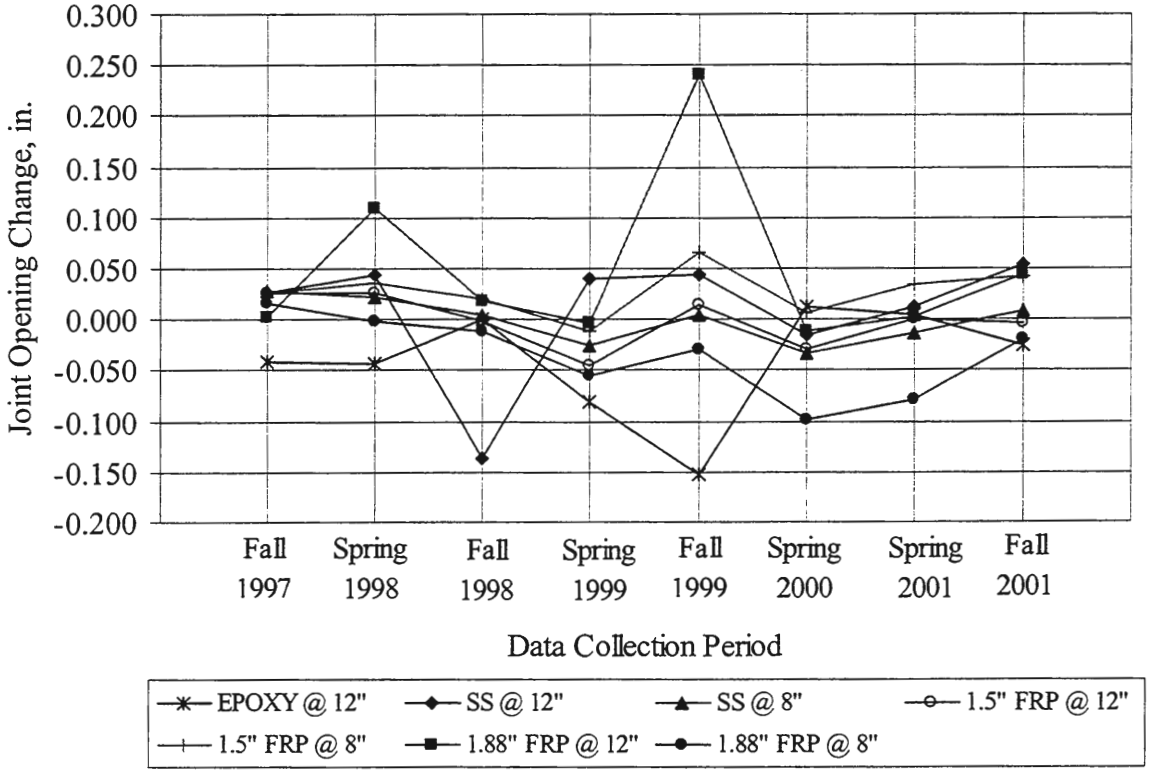

Figure 29. Difference in joint opening between current and previous testing period.

4.4 Statistical Inferences

The statistical analysis performed with the experimental data was limited due to the complexity of the experimental design and the nature of the materials involved. The variables of interest in this experiment are: material, diameter, and spacing of dowel bars. The materials evaluated were stainless steel (M1), fiber reinforced plastic (M2), and epoxy coated steel (M3). Two dowel diameters, 1.5 inch diameter (D1) and 1.88 inch diameter (D2), and two dowel spacings, 8 inch on center spacing (S1) and 12 inch on center spacing (S2), were evaluated:. There were seven different combinations (treatments) investigated, which are summarized in Table 9.

Table 9. Treatment descriptions.

Treatment	Material	Dowel Diameter	Basket Spacing
1	M2	D2	S1
2	M2	D2	S2
3	M2	D1	S1
4	M2	D1	S2
5	M1	D1	S1
6	M1	D1	S2
7 (Control)	M3	D1	S2

An analysis of variance (ANOVA) and Scheffe' multiple comparison tests were used to compare load transfer efficiency, concrete modulus of elasticity, modulus of subgrade reaction, maximum joint deflection, and joint faulting for the seven treatments. A comparison of means was conducted for the individual lanes in addition to a comparison of individual treatment testing periods. The results of these statistical analyses can be found in tabular form in Appendix F.

The objective of the ANOVA test is to determine if there is a significant difference between the means (averages) of the variable of interest. The analysis considers the variance

within treatment types, as well as the variance between the treatment types. When the variability between the treatment types is significantly more than the variability within the treatment types, it can be concluded that the difference between the means is due to the treatment type and is not a result of testing variability. The point at which the variability between the treatment types becomes significant is based on a significance level specified by the researcher. The significance level specified for this experiment was a 0.05 level, meaning it is acceptable to the author that there is a 5% probability that two groups deemed significantly difference are in fact not different. This test method will not distinguish which test methods are different, only if there is a significant difference between the treatment types on the variables of interest.

Scheffe' comparison tests are used after an ANOVA analysis has been conducted to determine which variables are significantly different between which pairs of treatment types. The Scheffe' test is one of many possible tests that could be conducted to determine significance between individual treatments. The difference between the comparison testing methods is the ease at which significance can be shown. For example, the liberal Fisher Least Significant Difference method, with a 0.05 significance level, would expect that 5% of the group comparisons would be misidentified as significantly different. On the conservative side, the Bonferroni method requires the desired significance level to be divided by the number of tests being performed. For example, for this experiment the significance level tested would be 0.05 divided by 21. This will result in fewer treatments deemed significantly different. The Scheffe' method is a compromise between the two extreme methods mentioned.

4.4.1 ANOVA Tests

ANOVA tests were conducted to determine if the differences between the treatments were significant for the following variables: load transfer efficiency, concrete modulus of elasticity, modulus of subgrade reaction, maximum joint deflection, and joint faulting. The ANOVA tests indicated that the difference in treatment types were significant for all the variables except for joint faulting in the inside wheel path. The ANOVA tests also indicated that the differences between testing periods for each treatment type is significant. The significance between treatment types of all ANOVA tests was 0.000 for all variables, except the inside and outside wheel path faulting. The significance for faulting in the outside wheel path was 0.024, which is within the 0.05 significance level set by the author. The ANOVA test for faulting in the inside wheel path determined a 0.282 significance, well outside the 0.05 level.

4.4.2 Scheffe′ Tests

The results of the Scheffe′ tests can be found in Appendix F, Tables 1A through 15A. The following sections will discuss the results of the analysis for each variable investigated.

4.4.2.1 Load Transfer Efficiency

Tables 1A and 2A present the Scheffe′ results for the comparison between treatments over the pavement's lifetime. The results are broken down into driving and passing lanes. The results for the driving lane indicate:

- Standard epoxy coated steel dowels significantly outperform all other dowel types and spacings, except for the stainless steel dowels spaced on 8 inch centers for which no significant difference was found.
- The stainless steel dowels spaced at 8 inches significantly outperform all other dowel bar materials and spacings, except for the standard epoxy coated steel.

- The stainless steel dowels spaced at 12 inches perform significantly less than the stainless steel dowels spaced at 8 inches, but significantly better than 1.5 inch diameter FRP dowels spaced at 12 inches and 1.88 inch diameter FRP dowels spaced at both 8 and 12 inches.

- The load transfer for 1.5 inch diameter FRP dowels spaced at 12 inches is significantly less than the same dowel bars spaced at 8 inches. Also, no significance was found between the 1.5 inch diameter FRP dowels spaced at 12 inches and the 1.88 inch diameter FRP dowels with 8 or 12 inch spacing.

- No significance was found for the difference between the 1.88 inch diameter FRP dowels spaced 12 inches and 8 inches.

Passing lane results are similar to the driving lane results. The only comparisons in the passing lane found to be different than the driving lane are between the standard epoxy coated steel and stainless steel spaced at 12 inches, and the standard epoxy coated steel and 1.5 inch diameter FRP dowels spaced at 8 inches. In both instances, the driving lane indicated the epoxy coated steel dowels were outperforming the other two treatments. The results of the passing lane indicate that no significant difference exists between the treatments.

Tables 9A through 15A present the Scheffe' test results in which the difference in testing periods were compared. This analysis was conducted to see if a trend had developed over the treatment's lifetime or between spring and fall testing periods. The test results indicate:

- No significant trend has developed over the research lifetime of the epoxy coated steel dowels. The only significant changes were noted between the fall of 1999 and spring of 2000, and the spring of 2001 and fall of 2001 for the driving lane. The passing lane experienced significant changes between the fall of 1998 and spring of 1999, and the fall of 1999 and spring of 1999, in addition to significant changes of the driving lane. A slight seasonal trend, but not to the 0.05 level, has developed with spring testing periods generally indicating lower load transfer than in the previous fall testing period.

- Stainless steel dowels spaced at 12 inches developed the same seasonal trend as the standard dowel bars, with significant changes found between the first five testing periods for the driving lane. No significant changes have occurred for the passing lane, but the general trend still exists. The stainless steel dowels spaced at 12 inches exhibited greater variability between testing periods with greater differences between testing periods.

- No seasonal trend developed for stainless steel dowels spaced at 8 inches. Variability between testing periods was much lower for stainless steel spaced at 8 inches when compared to 12 inches. Significant differences were found only between the fall of 2000 and spring of 2001 and the spring of 2001 and fall of 2001 for both lanes.

- The 1.5 inch diameter FRP dowel spaced at 12 inches exhibited significant changes between the fall of 1998 and spring of 1999, and the fall of 2000 and spring of 2001 in the driving lane only. A seasonal trend with lower load transfer in the spring exists for the first six test periods, but an opposite trend exists for the last three.

- The 1.5 inch diameter FRP dowel spaced at 8 inches indicated the same general seasonal trend as the 1.5 inch diameter dowel spaced at 12 inches. A significant change occurred only between the spring of 2001 and fall of 2000 for the driving lane, however, the difference in means between periods for the 8 inch spacing was generally lower than the 12 inch spacing.

- The 1.88 inch diameter FRP dowel spaced at 12 inches exhibited a general downward trend in the driving lane for load transfer over the pavement research lifetime. The load transfer of the driving lane decreased every testing period except from the spring of 1998 to the fall of 1998 and from the fall of 2000 to the spring of 2001. However, only one difference of means between testing periods was found to be significant. The passing lane did not show any downward trend, with only one difference of means found to be significant.

- 1.88 inch diameter FRP dowels spaced at 8 inches exhibited the same general decrease in load transfer over the pavement research lifetime as the 1.88 inch diameter FRP dowels spaced at 12 inches. The downward trend was more pronounced in the driving lane with slight increases in load transfer in the fall testing periods offset by large decreases in the spring. However, only one difference of means between testing periods between both lanes was found to be significant

4.4.2.2 Maximum Joint Deflections

The comparison of the maximum joint deflections, located at d_0, is presented Tables 3A and 4A for the driving lane and passing lane, respectively. The results of the treatment comparisons are:

- The maximum joint deflections for the stainless steel dowels spaced at 12 inches were significantly larger than all other treatment types in the driving lane.
- The stainless steel dowels spaced at 8 inches experienced joint deflections significantly smaller than all other treatment types in the driving lane.
- In the passing lane, the 1.88 inch diameter FRP dowels spaced at 8 inches exhibited significantly smaller joint deflections than all other treatment types except for stainless steel spaced at 12 inches.

Tables 9F through 15F in present the Scheffe' results for the comparison of testing periods. The passing and driving lanes for all treatment types exhibited significant differences between many testing periods, but no pattern has developed. An increase in maximum joint deflection for a given testing period was generally followed by a decrease in joint deflection. Also, the maximum joint deflection is generally lower in the spring testing periods when compared to fall testing periods. This observation follows with the unexpected result of higher modulus of subgrade reaction values in the spring. Typically soils will have a lower modulus of subgrade reaction in the spring due to the thawing of soil and excess pore pressures.

4.4.2.3 Modulus of Subgrade Reaction

The results of the modulus of subgrade reaction statistical analysis can be found in Tables 5A and 6A, along with Tables 9A through 15A. The statistical analysis determining the following:

- Driving lane pavements with epoxy coated steel dowels have significantly lower subgrade reactions than all other treatments except 1.88 inch diameter FRP dowels spaced at 12 inches.

- Driving lane pavements with 1.88 inch diameter FRP dowels spaced at 12 inches are significantly lower than stainless steel dowels at 8 inch spacing, and 1.5 inch diameter dowels with 12 and 8 inch spacing.

- Driving lane pavements with 1.88 inch diameter FRP dowels spaced at 8 inches exhibit subgrade reactions significantly higher for all other treatments except 1.5 inch diameter FRP dowels spaced at 12 inches.

- Passing lane pavements with 1.88 inch diameter FRP dowels spaced at 8 inches exhibit subgrade reactions significantly higher for all other treatments.

- Passing lane pavements with stainless steel spaced at 8 inches are significantly lower than all other treatments.

- Passing lane pavements with epoxy coated steel are significantly lower than stainless steel at 12 inch spacing, 1.5 inch diameter FRP at 12 inch spacing, and 1.88 inch diameter FRP at 8 inch spacing.

- The comparison of testing periods within each treatment type did not reveal any trends over time for the modulus of subgrade reaction.

The effect of the subgrade material below the pavements was also investigated. As stated in the research plan, due to the highway layout and cut-and-fill requirements, the pavement is supported on a combination of natural soils and structural fill placed during construction. A statistical comparison of the modulus of subgrade reaction was conducted without regard for the type of dowel. The modulus of subgrade reaction with natural soils is significantly lower than three sections supported on structural fill in the driving lane, but is not significantly different than the structural fill sections in passing lane. Therefore, it can be concluded that the difference in subgrade material impacted the test results only slightly, if at all.

4.4.2.4 Concrete Modulus of Elasticity

The concrete modulus of elasticity was backcalculated from FWD deflection data from the pavement's mid-slab to reduce edge effects created by transverse joints. The results of the statistical analysis can be found in Tables 7A and 8A, along with Tables 9A through 15A. The treatment comparison for the driving lane indicated:

- The epoxy coated steel dowel pavement is significantly larger than all other treatment types.
- The pavement with stainless steel dowels with 8 inch spacing is significantly larger than all pavements containing FRP dowels.
- Pavement with 1.5 inch diameter FRP dowels with 12 inch spacing exhibits significantly greater modulus of elasticity than all other sections with FRP dowels.

Results of the passing lane comparison tests reveal only one treatment is significantly different than the others. Pavements with 1.88 inch diameter FRP dowels at 8 inch spacing have significantly larger modulus of elasticity than all other treatment types. Three other comparisons from different treatments display significance, but no pattern exists.

The comparison between testing periods of the driving lane did not revealed any significant trends for any treatment over the concrete lifetime. Significant differences were obtained between various testing periods, but significant trend has developed. The passing lane comparisons reveal a slight decreasing trend during the first three to four testing periods. Although the trend exists, most of the treatment differences were not found to be statistically significant. After the fourth testing period, no trend developed.

4.4.2.5 Joint Faulting

As stated earlier, the ANOVA tests indicate that there is no significance between the treatment types and pavement faulting for the inside wheel path. Significance was found for

the outside wheel path, but the Scheffe' tests revealed no significance exists between individual treatment types

Due to definition of faulting, both positive and negative faulting occurs with an average that tends to be near a zero reading. Therefore an analysis was conducted using the absolute value of the faulting. The ANOVA test results for this analysis also indicate that no significance between treatment types exists in the inside wheel path (0.282 level), but the outside wheel path did show significance at a 0.024 level. Although the ANOVA testing showed significance between all treatment types for the outside wheel path, the Scheffe' tests comparing individual treatment types indicated no significance to the 0.05 level exists.

A third analysis of faulting was conducted in which the effect of the pavement grade was considered. The location of the test site is within a valley with downhill, uphill, and relatively flat sections. The ANOVA comparison indicated no significance between grade and faulting with significance of 0.626 and 0.061 for the inside and outside wheel path, respectively.

5 CONCLUSIONS

The research focused on the evaluation of alternative dowel bar materials due to problems associated with corrosion of today's standard steel or epoxy coated steel dowel bars in pavements. Both fiber reinforced plastic (FRP) and stainless steel were evaluated as alternative dowel bar materials within a highway pavement. Previous laboratory research indicated the materials were corrosion resistant with desirable mechanical properties. The goal of the research is to compare the performance of highway joints reinforced with FRP and stainless steel dowel bars to the performance of conventional epoxy-coated steel dowel bars, under the same design criteria and field conditions.

Along with the type of dowel material, the influence of dowel bar spacing was evaluated with alternative dowel bars spaced at both 12 (standard) and 8 inches on center. The hypothesis being, distributing traffic loads over more FRP dowels will result in the less stiff (lower modulus of elasticity) FRP dowels performing similarly to the standard steel dowel bars. The effect of the FRP dowel bar diameter was evaluated to validate previous research, which indicated increasing the FRP dowel diameter would not enhance pavement performance. Both 1.5 and 1.88 inch diameter FRP dowel bars were evaluated.

The dowel bar treatments were evaluated biannually by conducting visual surveys, monitoring joint opening and joint faulting, and performing FWD tests. The FWD deflection data were graphically analyzed using load transfer efficiency, joint deflection, modulus of subgrade reaction, and concrete modulus of elasticity. A statistical analysis utilizing ANOVA and Scheffe' comparison tests, evaluated the differences between dowel type and spacing for each measurement type.

5.1 Load Transfer Efficiency

The effect of the type of dowel bar material on load transfer efficiency is best illustrated when comparing dowel types with the same 12 inch spacing. For pavement sections with dowels spaced at 12 inches, the epoxy coated steel significantly outperforms all other dowel types with an average load transfer of 91%. The stainless steel dowel bars outperform the FRP dowels with a load transfer of 87%. However, there is no significant difference between the 1.5 and 1.88 inch diameter FRP dowels at the 12 inch spacing with load transfers of 80% and 79%, respectively.

The analysis of dowel spacing, 12 inches versus 8 inches, was conducted by comparing the same dowel material with both spacings. Stainless steel and 1.5 inch diameter FRP dowels spaced at 8 inches outperform stainless steel and 1.5 inch diameter FRP dowels with 12 inch spacing by 13.5% and 7.5%, respectively. The 1.88 inch diameter FRP dowels did not show any significant difference between the 12 and 8 inch spacing, with load transfer different by only 1%.

An overall comparison of load transfer efficiency for dowel bar types and spacings reveal that the epoxy coated steel with the standard 12 inch spacing, and stainless steel spaced on 8 inch centers, outperform all other alternatives with load transfer above 90%. The stainless steel with 12 inch spacing and 1.5 inch diameter FRP dowels spaced at 8 inches, have a load transfer efficiency approximately 5% lower than the epoxy coated steel and stainless steel spaced at 8 inches. The 1.88 inch diameter FRP dowels spaced at 12 and 8 inches perform at the lowest load transfer efficiency at approximately 80%, which is 11% lower than the epoxy coated steel and 13.5% lower than the stainless steel spaced at 8 inches.

5.2 Joint Deflection

The joint deflection is a function of the stiffness of the pavement system, which includes subgrade, concrete, pavement design, and load transfer mechanisms. The type of dowel bar material does not appear to be the controlling factor in joint deflection magnitude. The average joint deflections are similar for dowel material within each lane as shown in Table 11. However, a difference between lanes is apparent. The difference is most likely due to the lack of longitudinal drains along the passing lane, resulting in weaker subgrade soils. A slight difference in joint deflections exists between the 12 and 8 inch spacings, but the differences are not large enough to conclude the difference is caused by dowel spacing.

5.3 Modulus of Subgrade Reaction

The modulus of subgrade reaction is dependent on the type of subgrade soil and its moisture condition. However, if the pavement system is not functioning properly, such as poor joint sealing or inadequate drainage, pumping may occur and a decrease in modulus of subgrade reaction would be expected. Analyses performed do not indicate any trend of decreasing modulus of subgrade reaction over time. Moduli of subgrade reaction of the treatment types were also compared over time, and there are no noticeable differences between treatments. A pavement system not functioning properly would have moduli values that do not follow the same trends as properly performing pavement. The statistical analyses indicate that significant differences between dowel type and spacing exist, but this is most likely due to variations in moisture content and soil type.

Specific information on soil type was not available, however an analysis of modulus of subgrade reaction for sections with cut and fill was conducted. The results show fill materials have a higher modulus of subgrade reaction, on the order of 15 pci, than natural

soils. Fill soils are typically stronger because they have been reworked and compacted under ideal moisture conditions. Also, modulus of subgrade reaction for the passing lane was significantly lower than the driving lane. As previously discussed, this is due to the presence of longitudinal drains next to the driving lane.

An analysis of the effect of subgrade stiffness on the pavement load transfer and joint deflection was also conducted. The less stiff subgrade in the passing lane resulted in greater joint deflections, along with slightly higher load transfer efficiency. The higher load transfer is most likely due to the loads being distributed downward to the underlying soil, instead of being transferred to the adjacent slab.

5.4 Concrete Modulus of Elasticity

Concrete modulus of elasticity is affected by dowel type and spacing, as can be seen in Table 13. The modulus of elasticity values presented are the result of dynamic testing, which will result in higher moduli values when compared with static loading. Therefore, if the data are compared to standard values, it should be modified according to Section 4.3.5.

The driving lane of the pavement section containing epoxy coated steel dowels has a significantly higher modulus of elasticity in comparison with other dowel types and spacing in the driving lane. The modulus of elasticity is approximately 2 to 3 million psi stiffer than other sections. Sections with stainless steel dowels exhibit a concrete modulus of elasticity approximately 1 million psi stiffer than the four FRP dowel sections.

The same differences are not observable in the passing lane. The most likely reason the differences are not duplicated in the passing lane is due to traffic loading. The driving lane typically will experience more traffic than the passing lane. Therefore, the decrease in modulus of elasticity from fatigue will not be as significant.

The concrete modulus of elasticity was also compared with load transfer and joint deflection. Results indicate that a higher concrete modulus of elasticity generally correspond with greater load transfer efficiency. It was also shown that concrete modulus of elasticity effects the joint deflection, with higher concrete moduli resulting in less joint deflection.

5.5 Joint Faulting and Joint Opening

Joint faulting was analyzed to determine the effects of dowel type and spacing, along with the pavement grade. Statistical ANOVA tests show no significance between the type of treatment and faulting, and pavement grade and faulting. Graphical analyses indicate that epoxy coated steel dowels experience the least amount of faulting, with all other treatment types exhibiting approximately equal faulting. A season by season comparison within each test section does not reveal any pattern to the magnitude or direction of faulting. A seasonal analysis of the average faulting over the entire project indicates more faulting in the spring season. This is likely due to the absence of data for the fall of 2000, with the spring periods prior to and after the fall of 2000 having large negative faulting. The other possible explanation is the seasonal variation is due to the effects of curling and warping.

Joint openings were also monitored during the research to ensure the pavement slabs were allowed to expand and contract due to temperature changes. The joint openings varied from testing period to testing period, indicating the slabs were free to expand and contract. This corresponds to the minimal amount of pavement distress observed during the biannual visual distress surveys.

6 RECOMMENDATIONS

6.1 Dowel Bar Design

The results of this study indicate that the current dowel bar material and spacing standard should continue to be implemented for concrete pavements requiring dowels as load transfer devices. The load transfer efficiency, concrete modulus of elasticity, and joint faulting of the epoxy coated steel perform better than the alternative materials and spacings studied. However, if it is known the concrete pavement will be exposed to severe corrosive agents or a longer than normal design life is desired, both stainless steel spaced at 12 inches and 1.5 inch diameter FRP spaced at 8 inches should be considered.

6.2 Further Study

It is recommended that future studies evaluate new methods of attaching FRP and stainless steel dowels to dowel baskets. The solution should permanently attach the dowel bars to the baskets and minimize dowel movement within the basket during assembly, shipping, and pavement construction. A possible solution to investigate would be the use of a quick setting epoxy.

The observational time for this research was limited to 5 years. It is recommended evaluation of the pavement continue during its lifetime to monitor any changes in the test sections. Although the epoxy coated steel may outperform the alternative dowels early in a pavements life, corrosion problems resulting in decreased performance, and continued performance of stainless steel and FRP dowels may result in a different dowel bar recommendation. Also, the results of the research should be verified by findings of other research currently being conducted.

Due to the limited information on FRP dowel performance, they should be monitored to determine the effects the cyclic traffic loading and resulting pavement fatigue. Monitoring should be established to evaluate the pavement integrity, and should include structural analyses such as FWD tests and coring of dowels to inspect their condition

Finally, a stress analysis of the dowels in a concrete pavement system, considering both the concrete slab and subgrade, should be studied. The results should provide a better understanding of the dowel bar performance.

APPENDIX A – LOAD TRANSFER

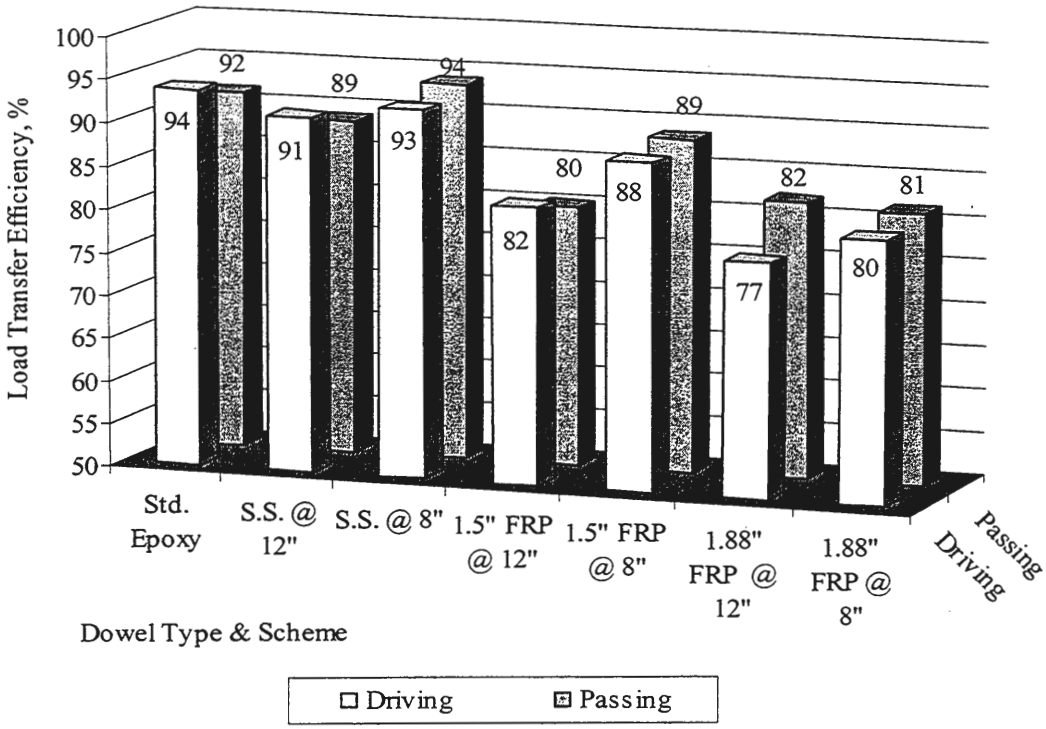

Figure 1A. Average load transfer for fall testing periods.

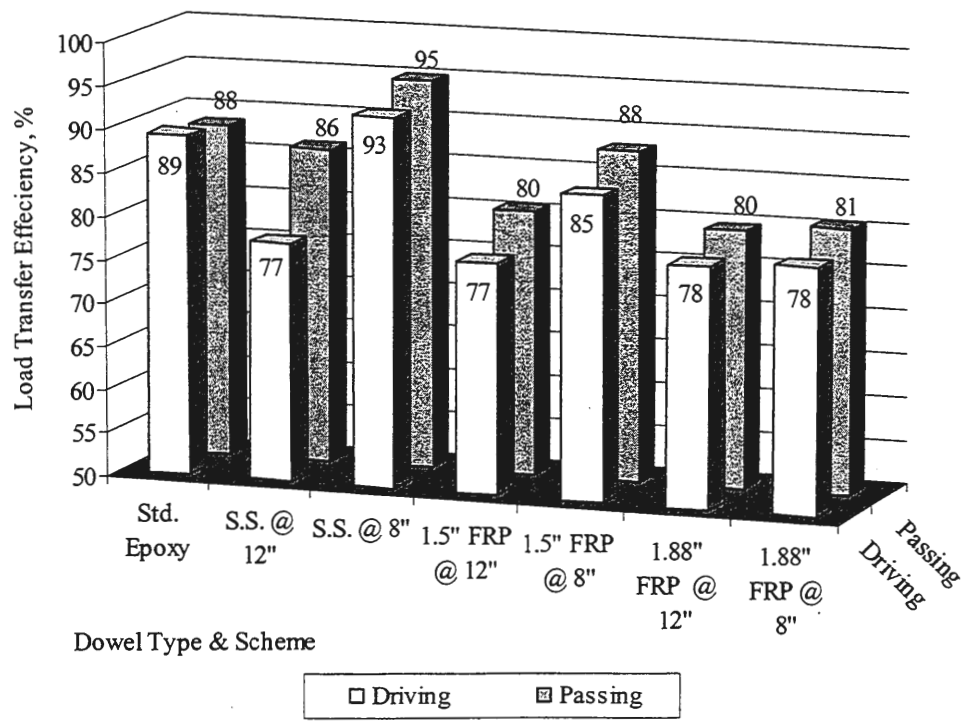

Figure 2A. Average load transfer for spring testing periods.

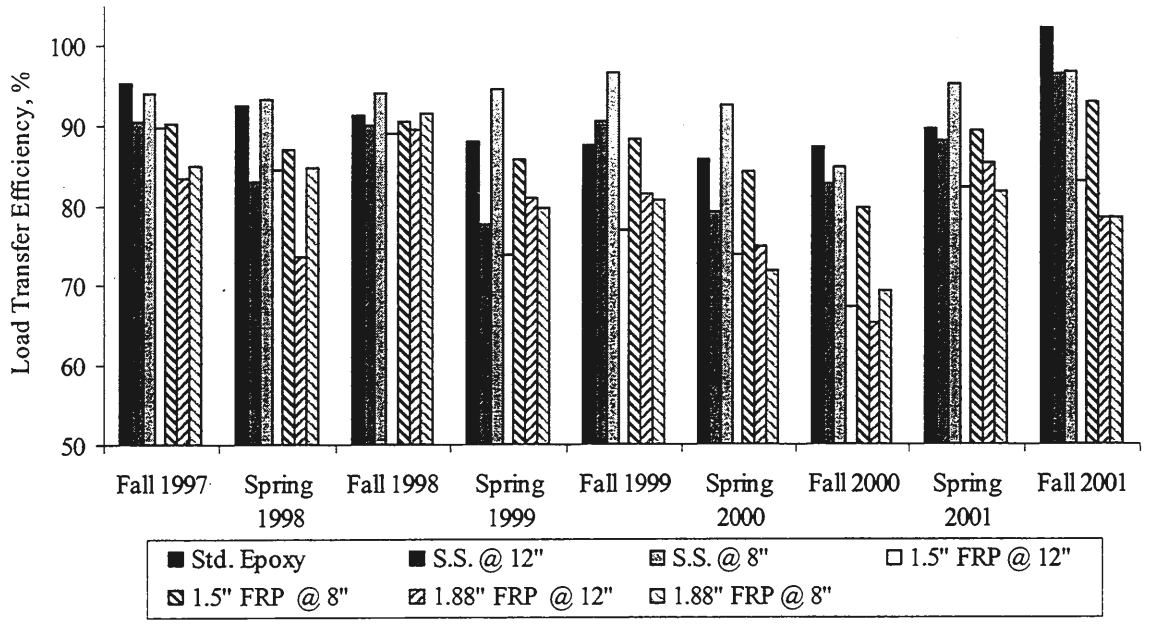

Figure 3A. Seasonal variations of overall average load transfer.

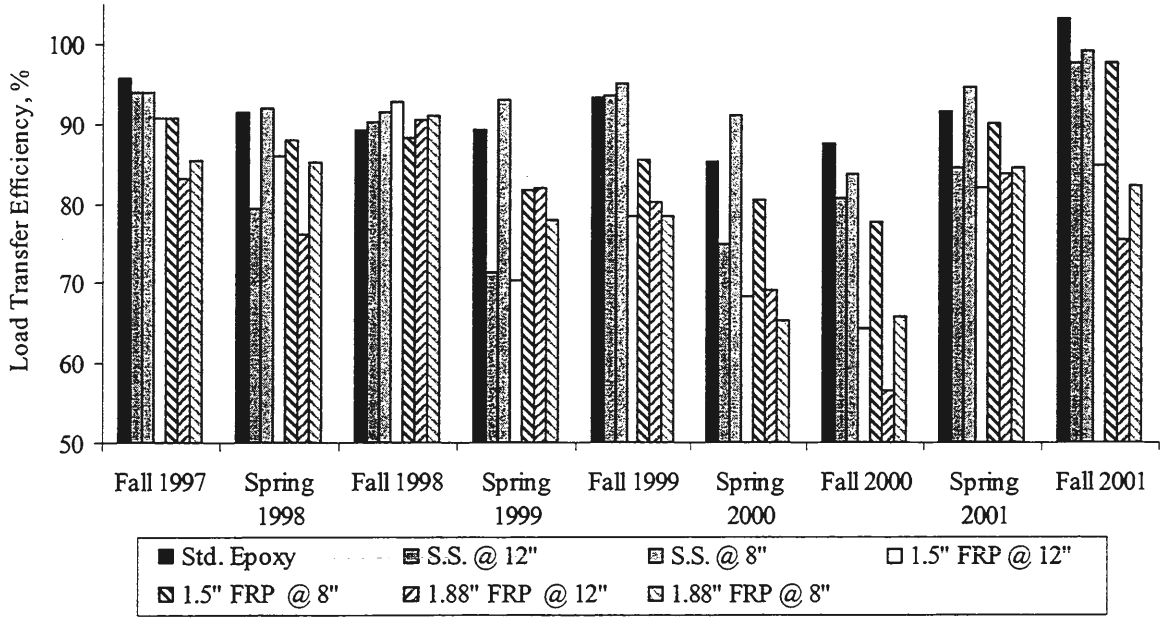

Figure 4A Seasonal Variations of average load transfer in the driving lane.

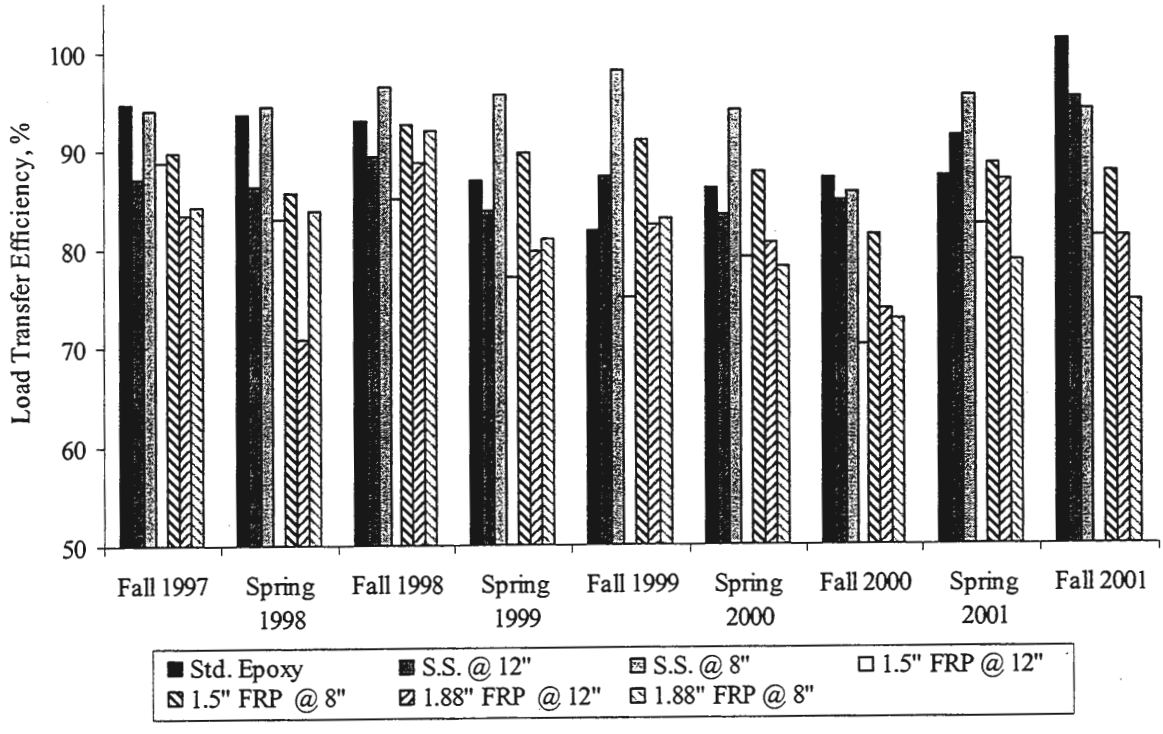

Figure 5A. Seasonal variations of average load transfer for the passing lane.

APPENDIX B – MAXIMUM JOINT DEFLECTION

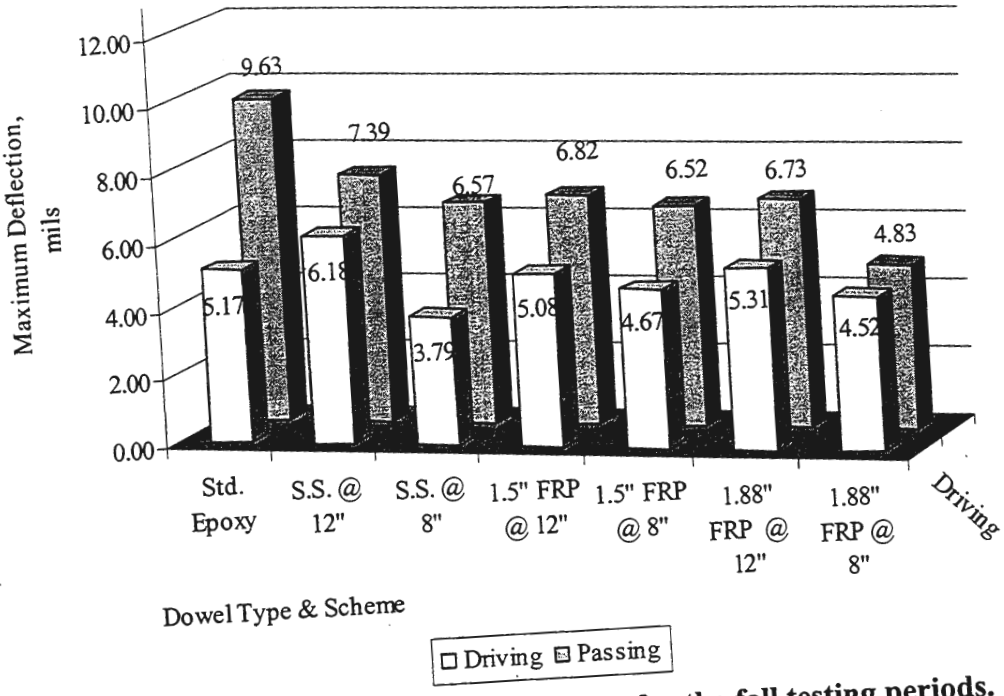

Figure 1B. Average joint deflections for the fall testing periods.

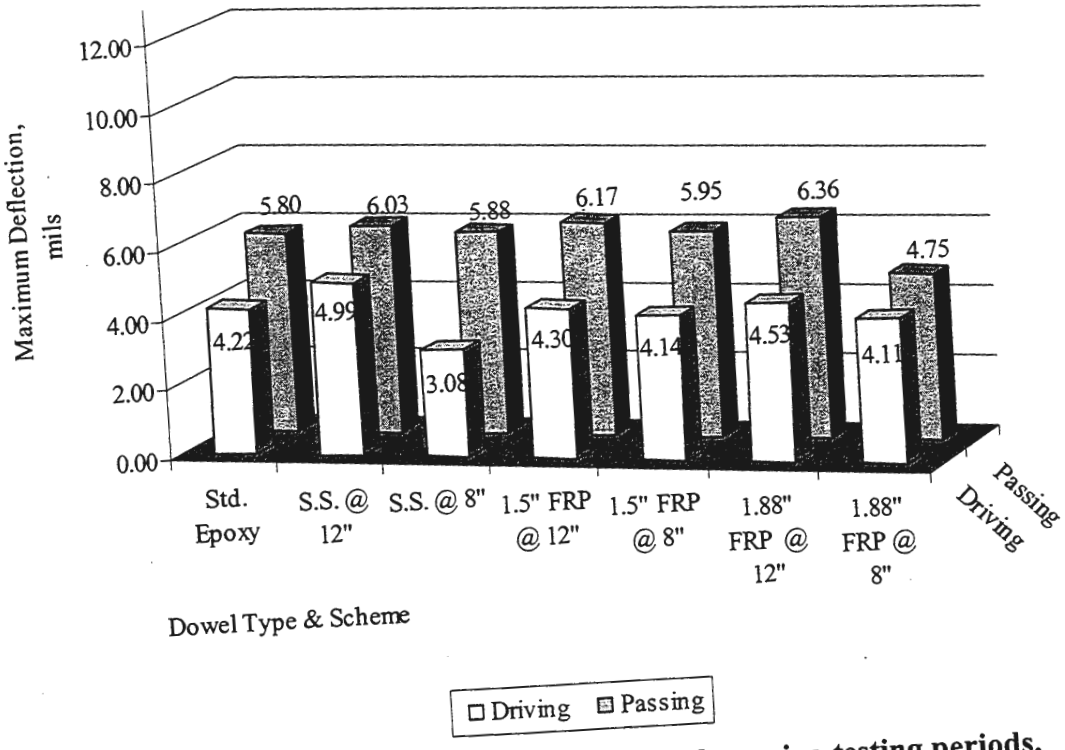

Figure 2B. Average joint deflections for the spring testing periods.

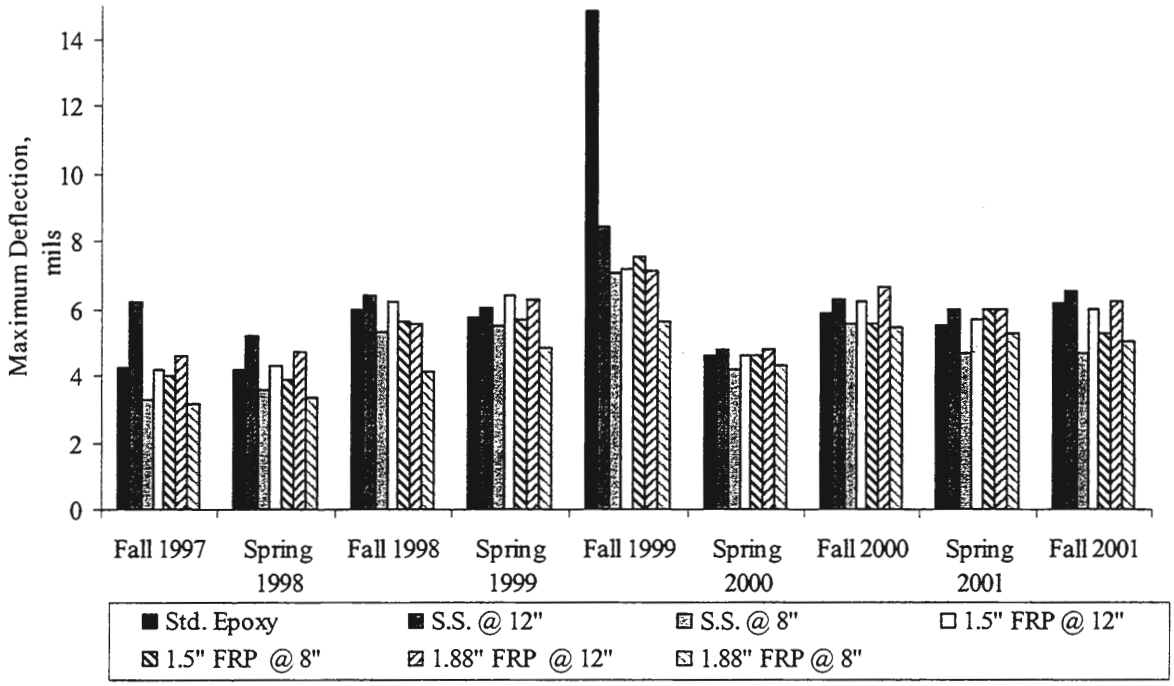

Figure 3B. Seasonal variation in overall average joint deflections.

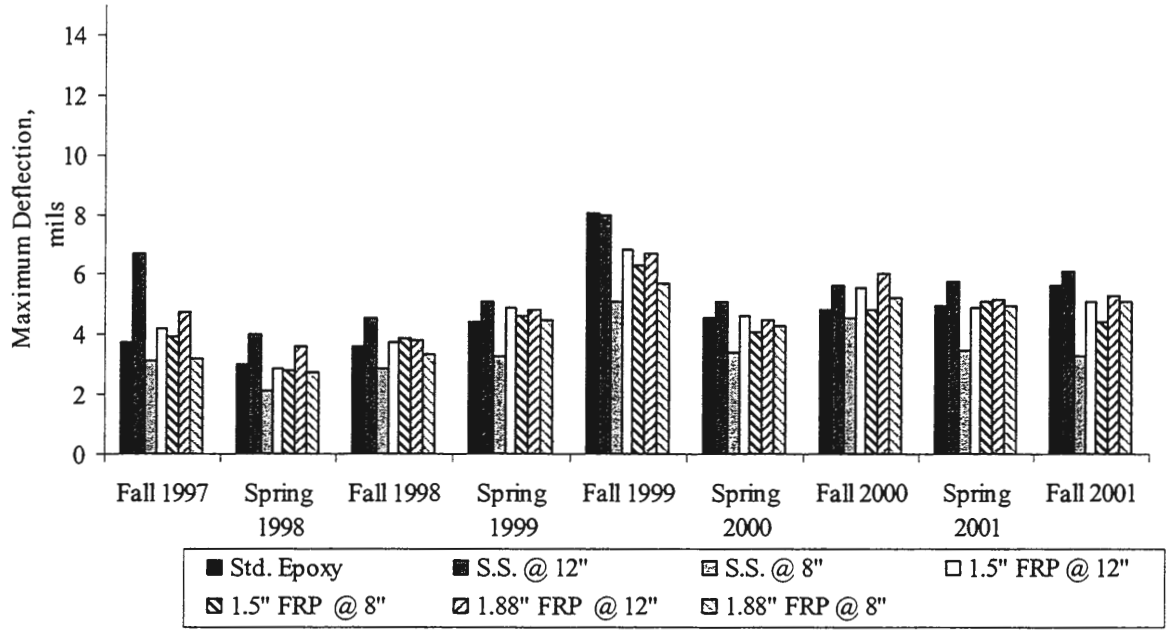

Figure 4B. Seasonal variation in average joint deflection for the driving lane.

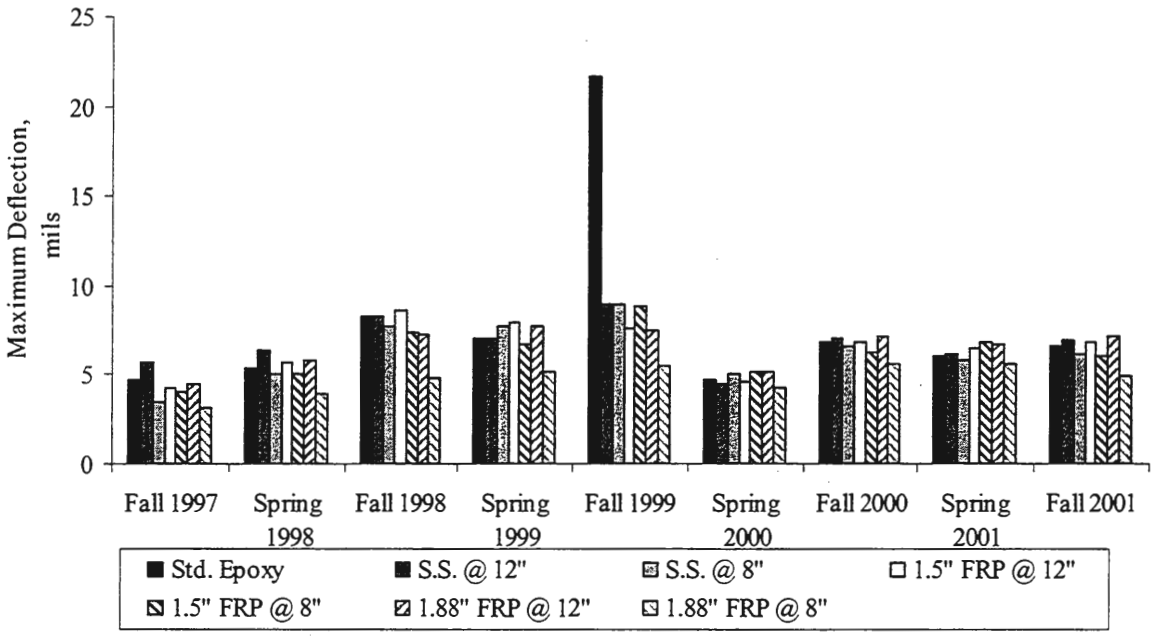

Figure 5B. Seasonal variations in average joint deflection in the passing lane.

APPENDIX C – MODULUS OF SUBGRADE REACTION

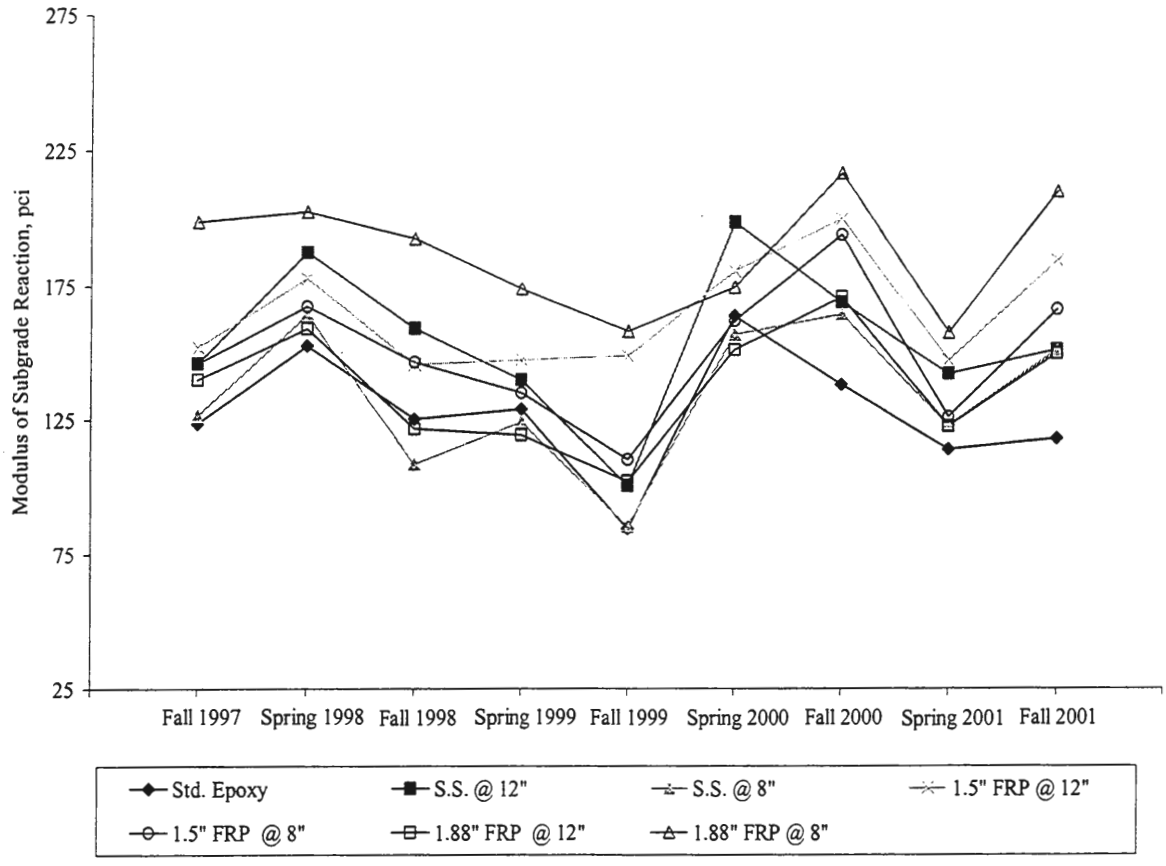

Figure 1C. Seasonal variations of the overall average modulus of subgrade reaction.

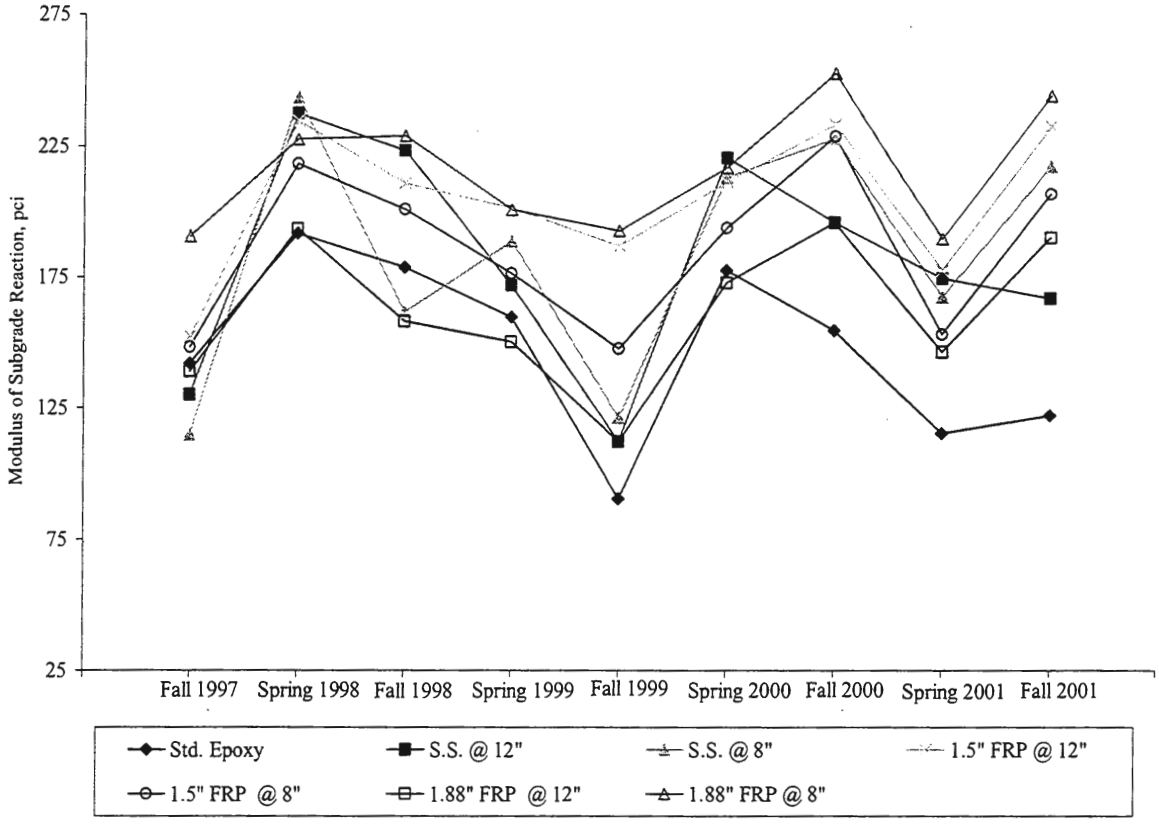

Figure 2C. Seasonal variations of the average modulus of subgrade reaction in the driving lane.

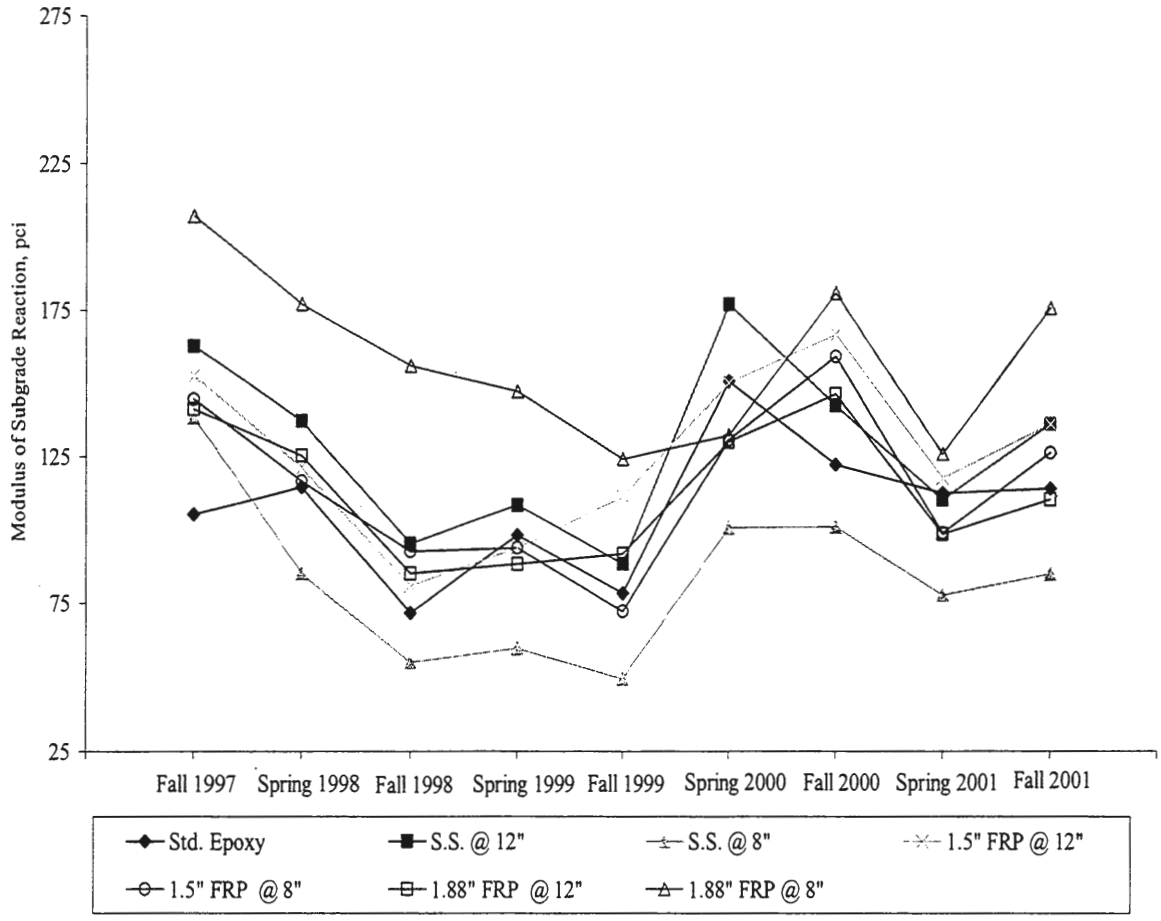

Figure 3C. Seasonal variations of the average modulus of subgrade reaction in the passing lane.

APPENDIX D – CONCRETE MODULUS OF ELASTICITY

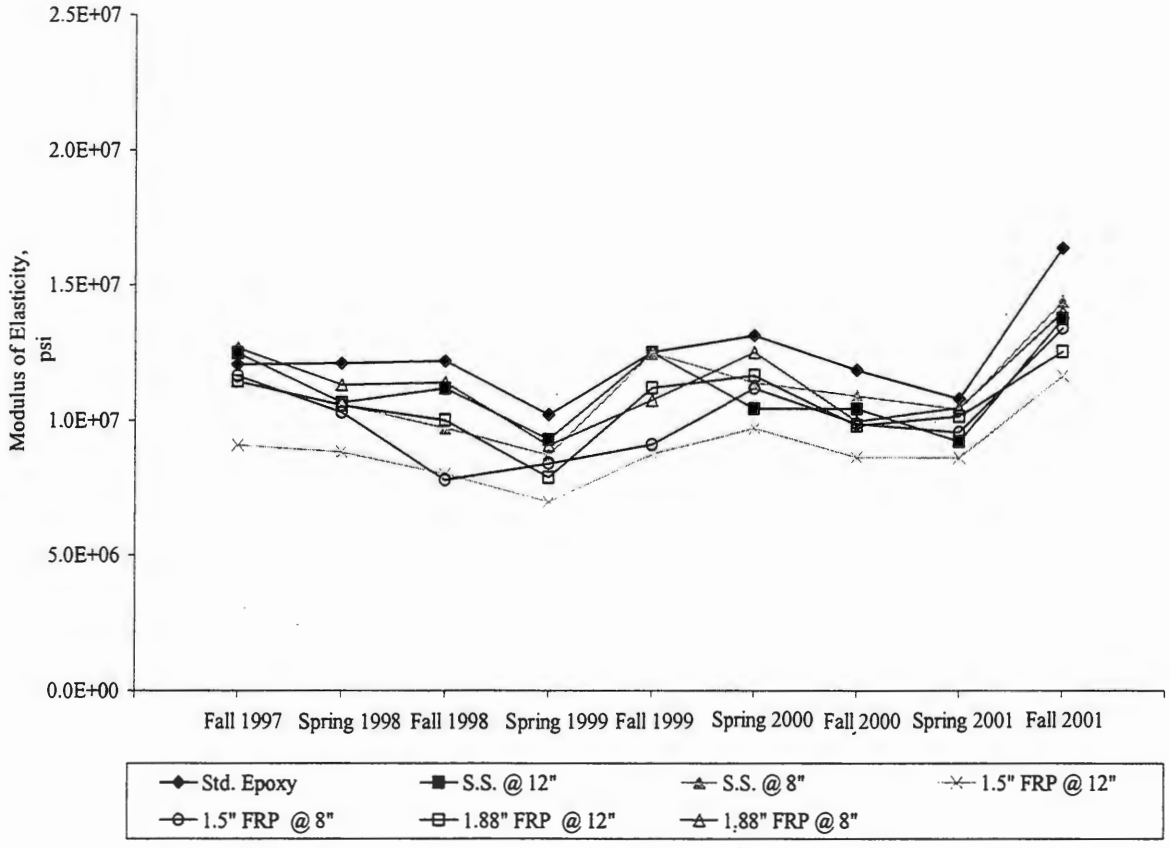

Figure 1D. Seasonal variations of the overall average concrete modulus of elasticity.

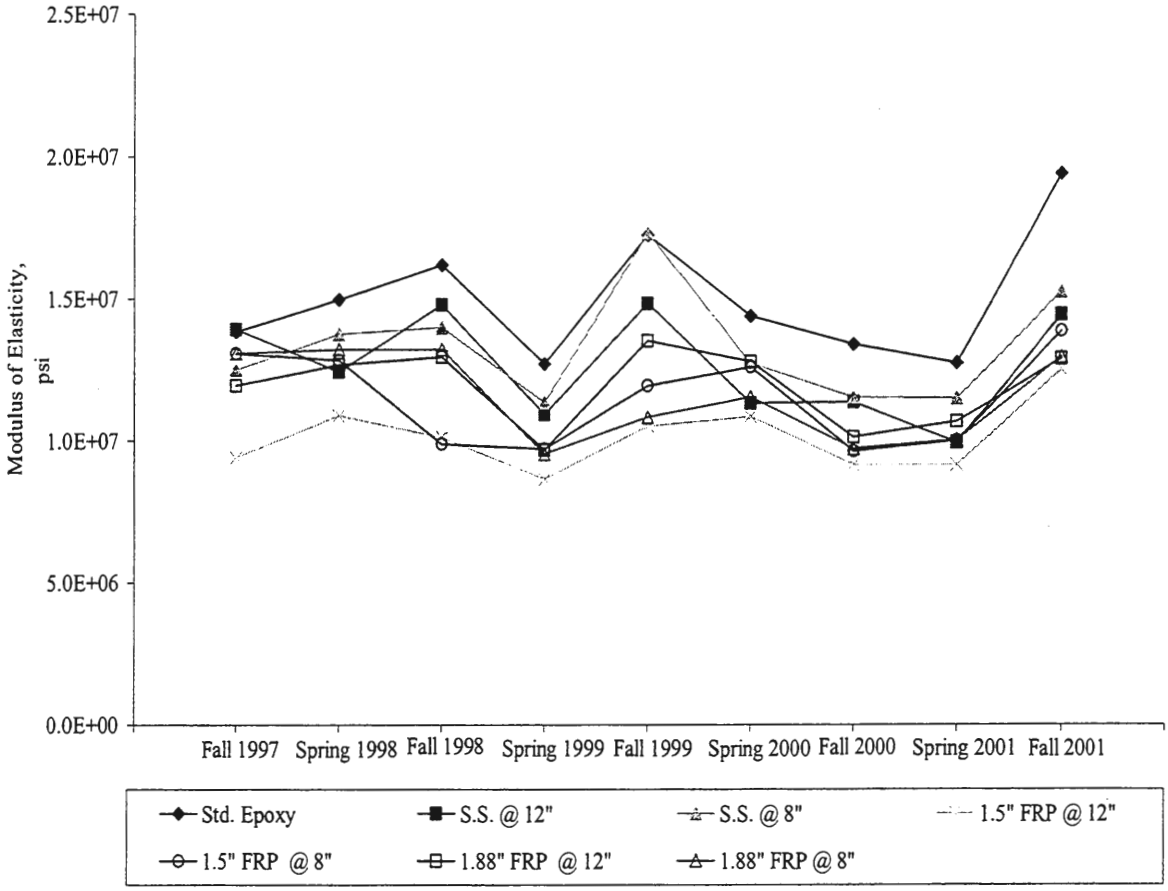

Figure 2D. Seasonal variations of the average concrete modulus of elasticity in the driving lane.

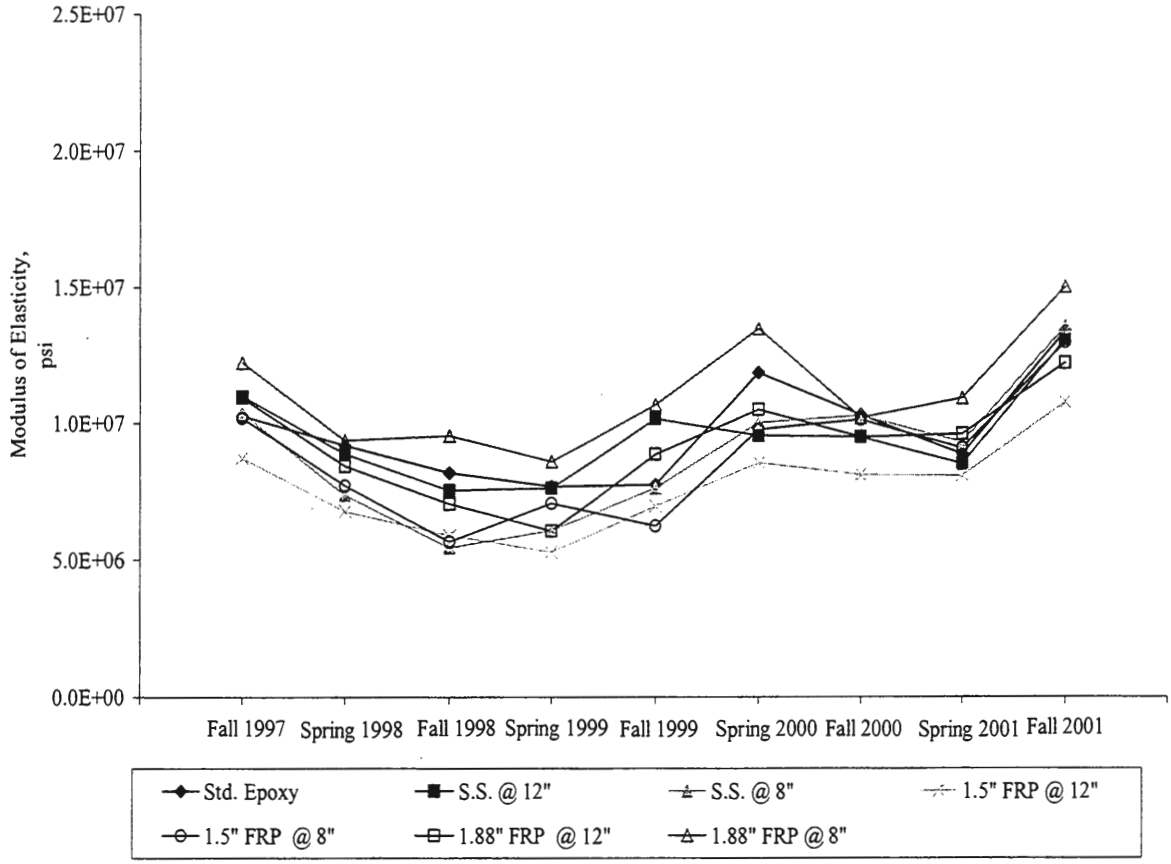

Figure 3D. Seasonal variations of the average concrete modulus of elasticity in the passing lane.

APPENDIX E – JOINT FAULTING

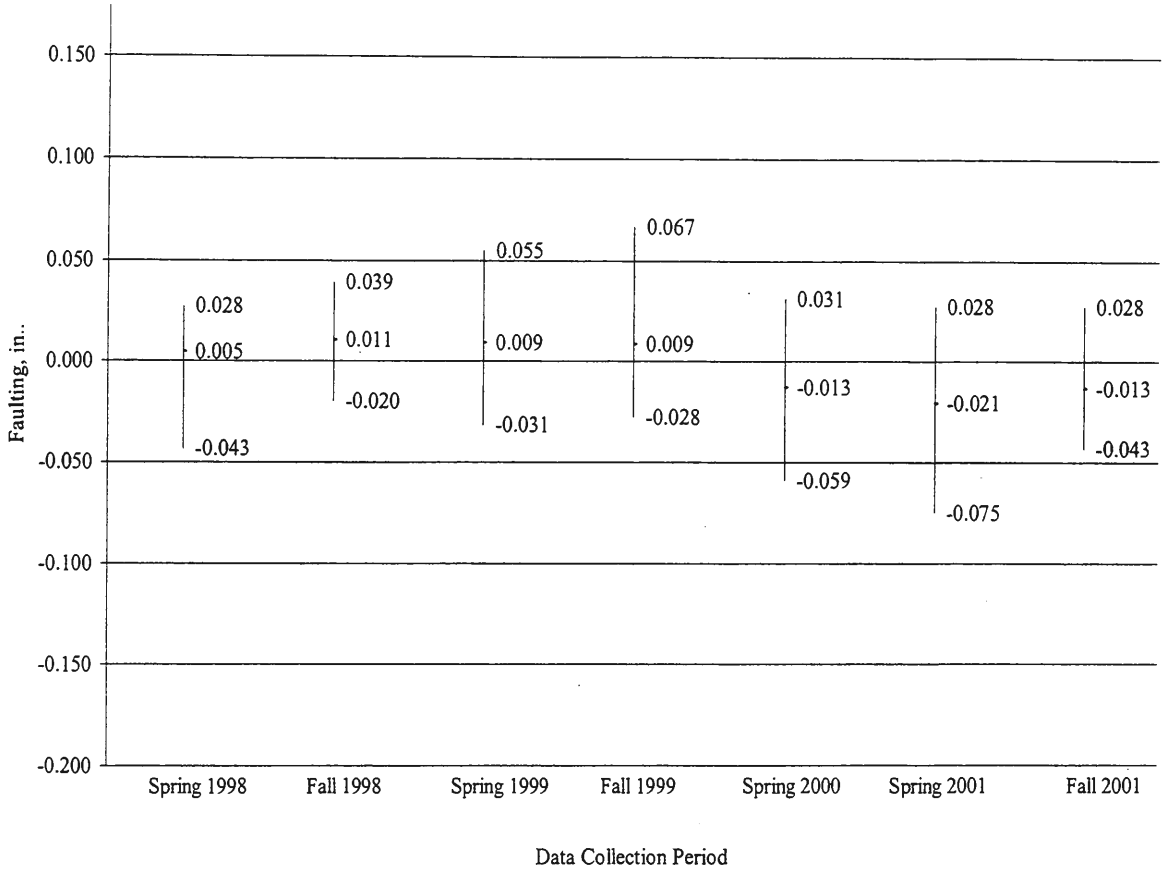

Figure 1E. Maximum, minimum, and average joint faulting for the outside wheel path of epoxy steel with 12 inch spacing.

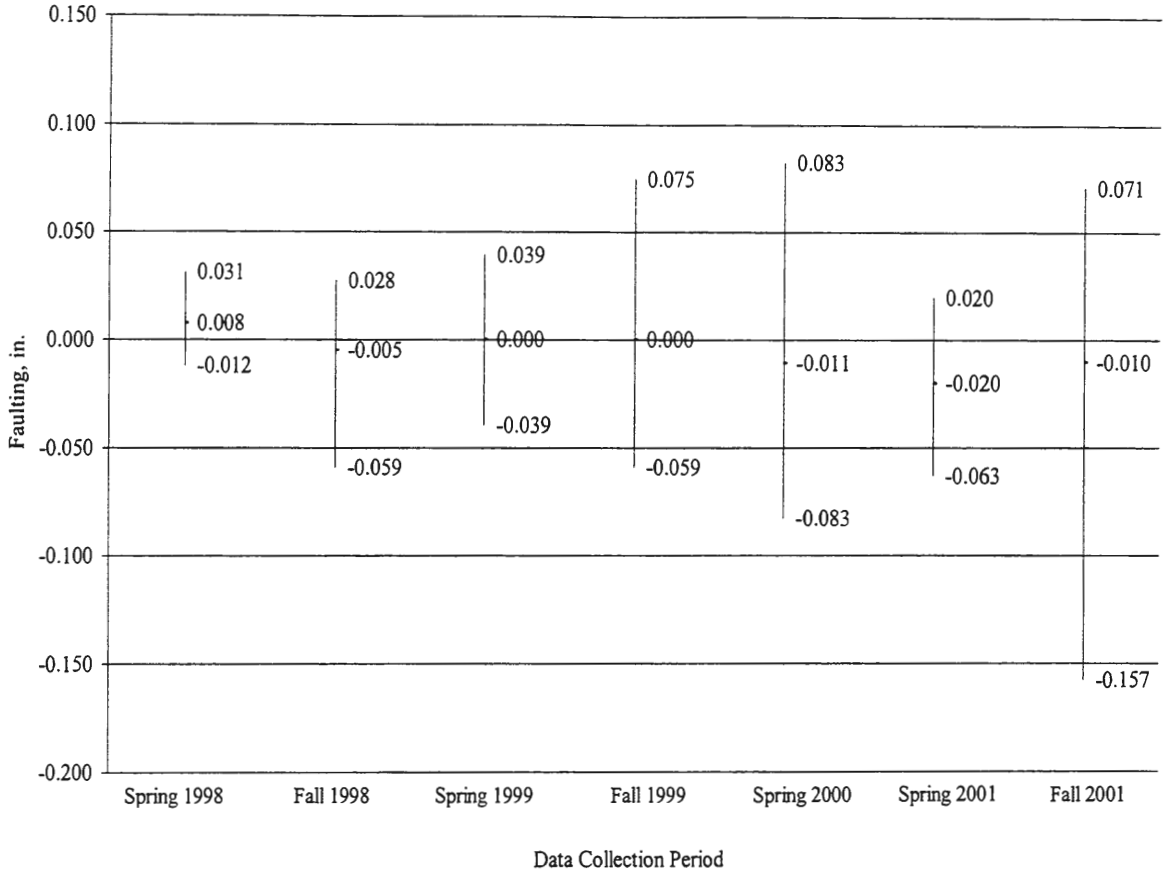

Figure 2E. Maximum, minimum, and average joint faulting for the inside wheel path of epoxy steel with 12 inch spacing.

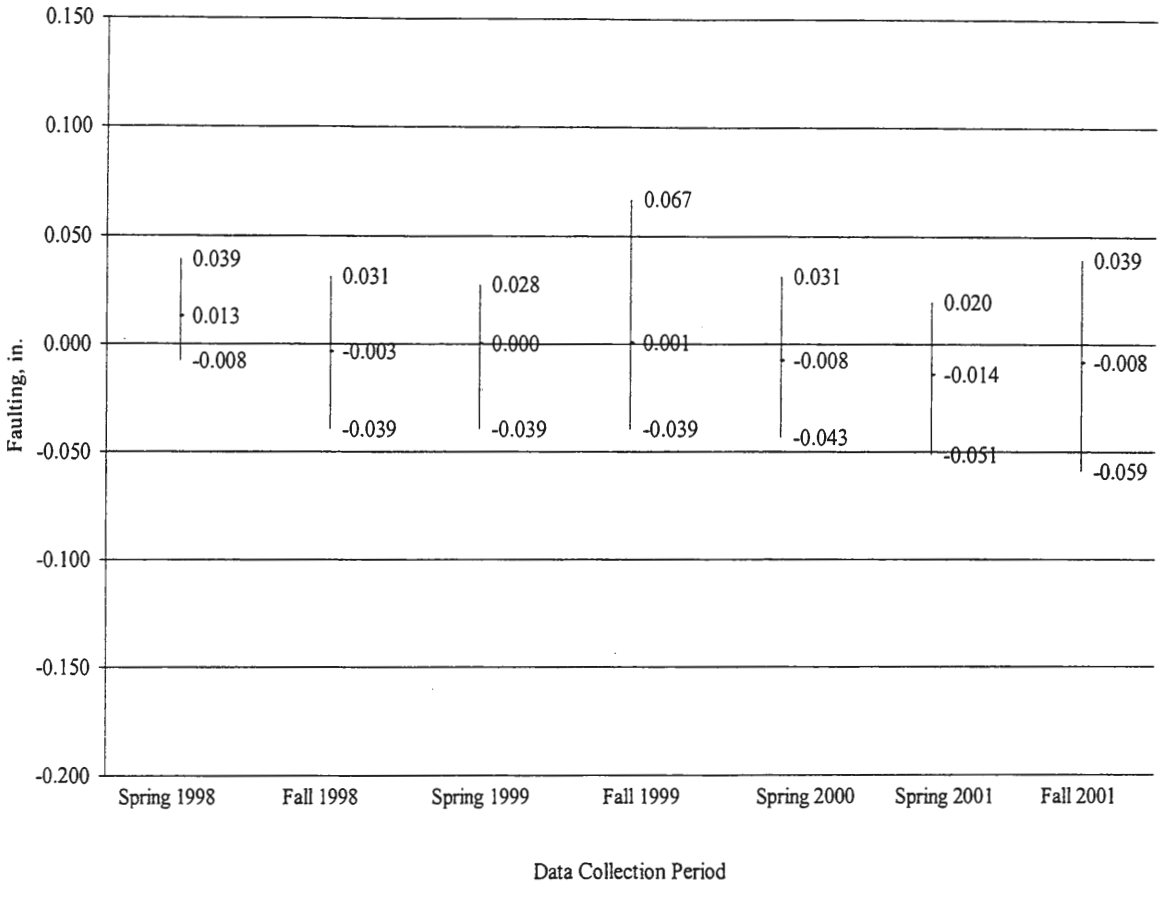

Figure 3E. Maximum, minimum, and average joint faulting for the outside wheel path of stainless steel with 12 inch spacing.

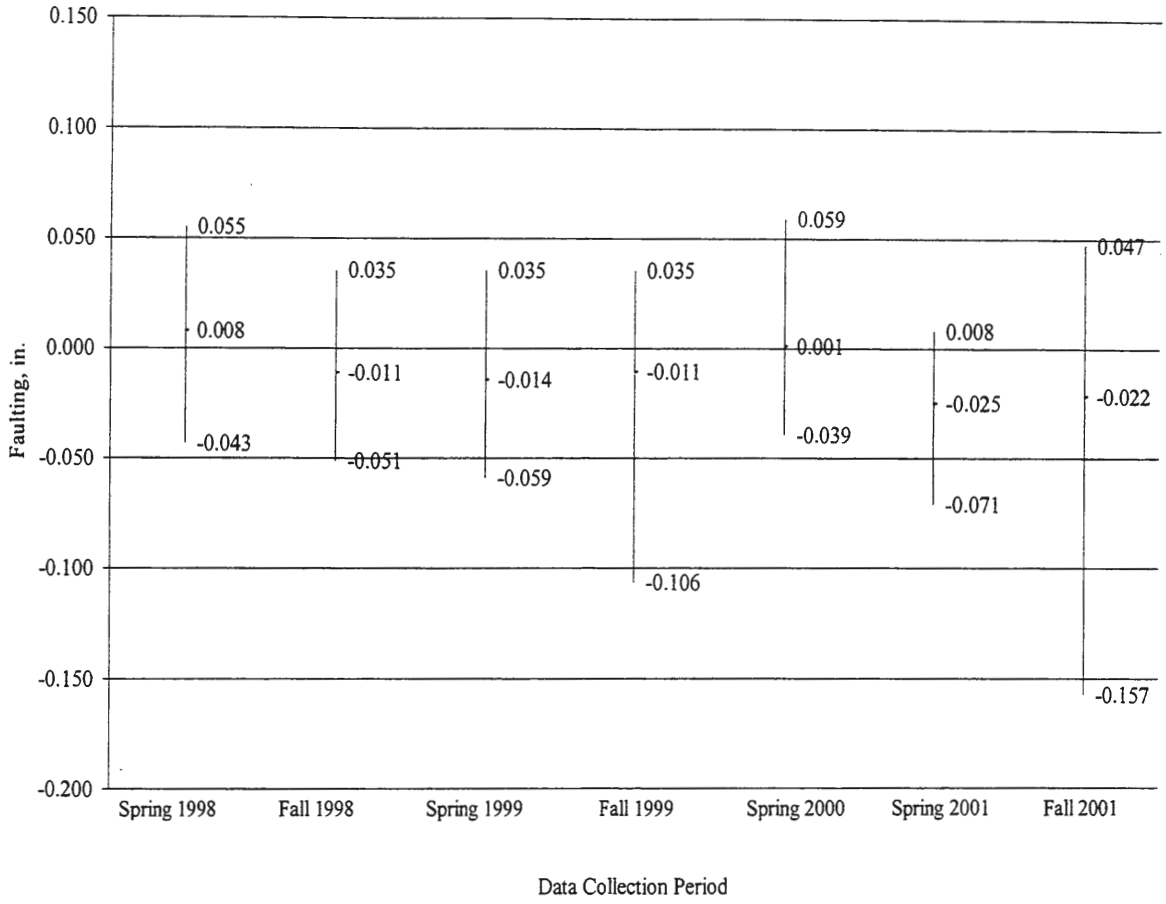

Figure 4E. Maximum, minimum, and average joint faulting for the inside wheel path of stainless steel with 12 inch spacing.

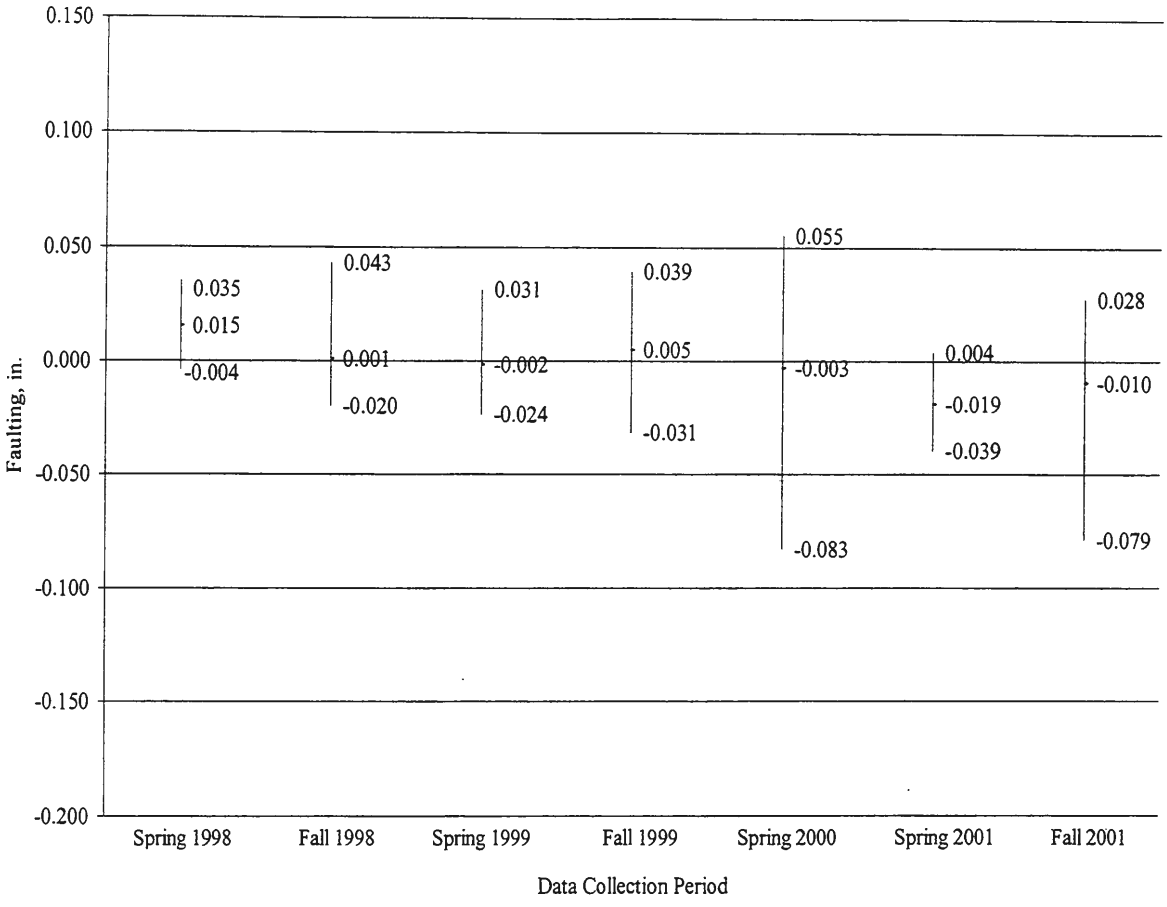

Figure 5E. Maximum, minimum, and average joint faulting for the outside wheel path of stainless steel with 8 inch spacing.

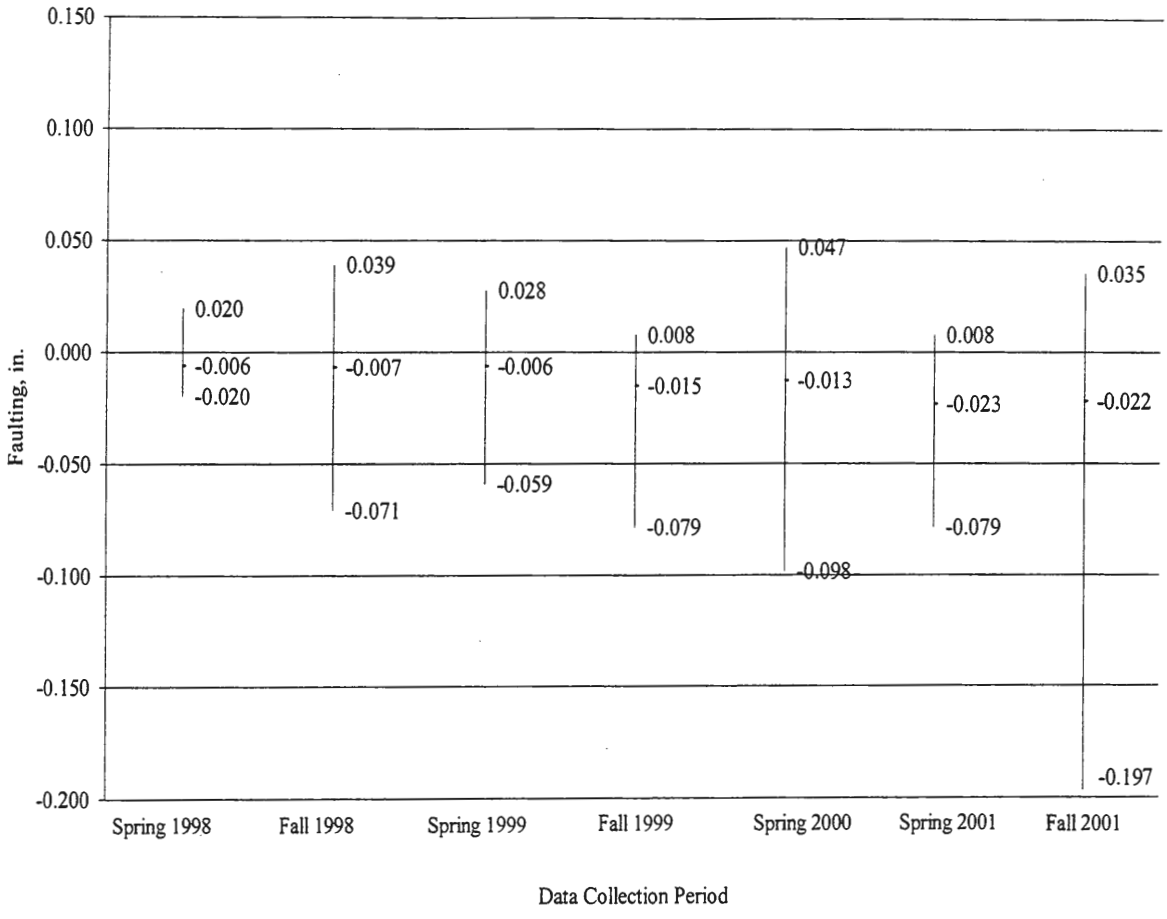

Figure 6E. Maximum, minimum, and average joint faulting for the inside wheel path of stainless steel with 8 inch spacing.

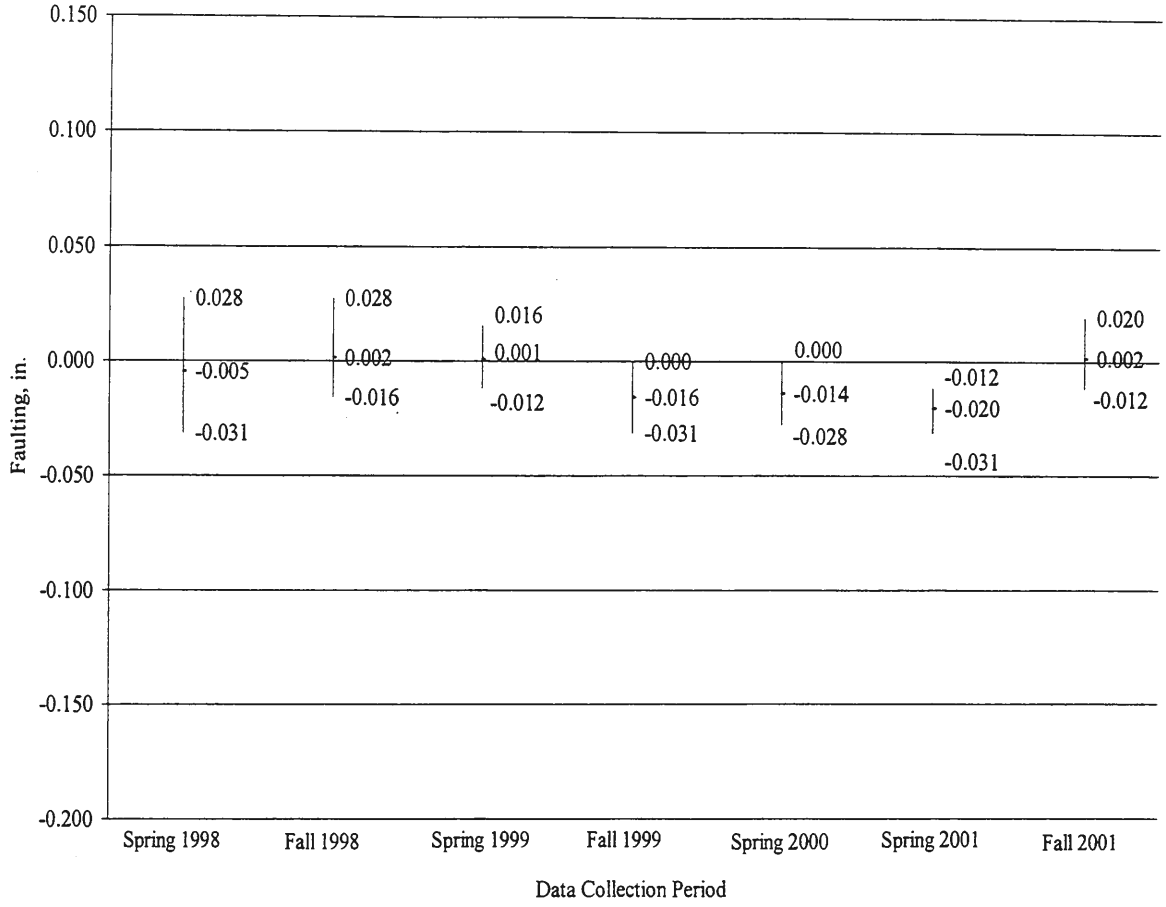

Figure 7E. Maximum, minimum, and average joint faulting for the outside wheel path of 1.5 inch diameter FRP with 12 inch spacing.

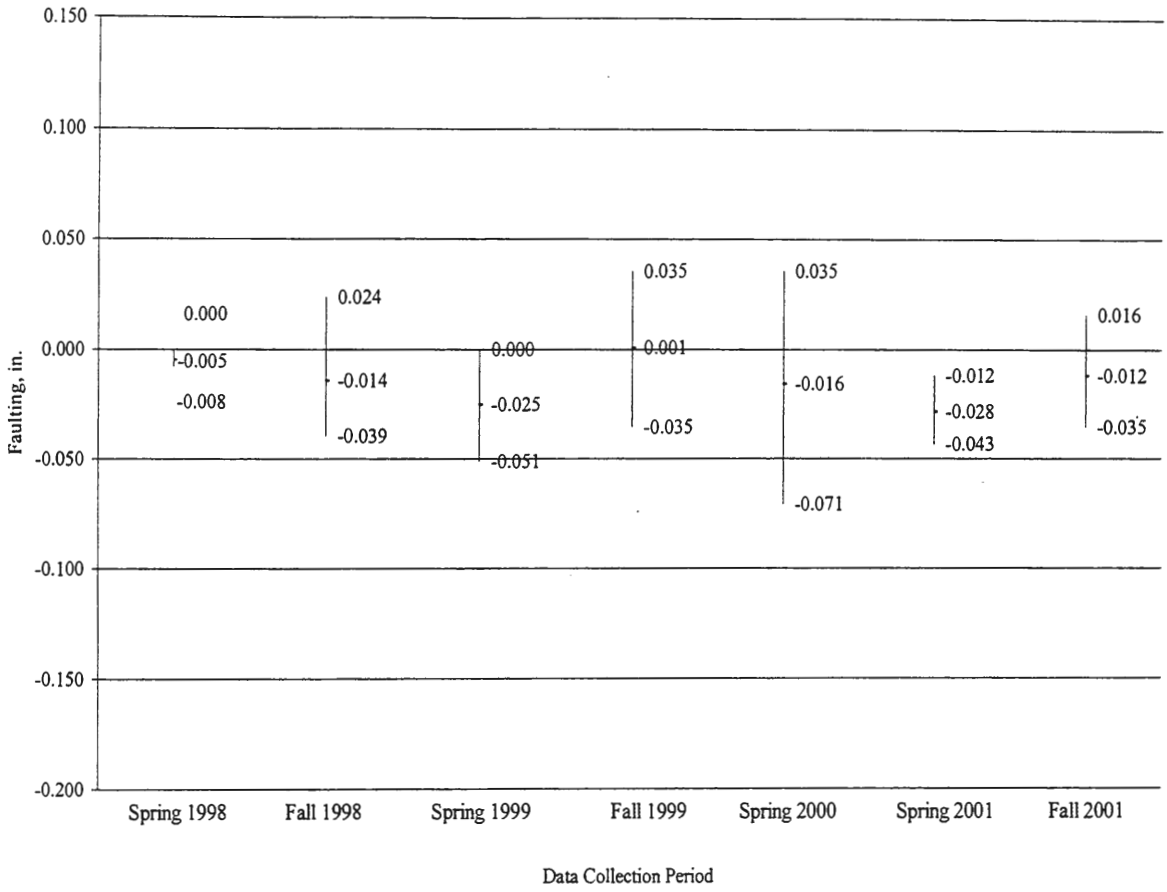

Figure 8E. Maximum, minimum, and average joint faulting for the inside wheel path of 1.5 inch diameter FRP with 12 inch spacing.

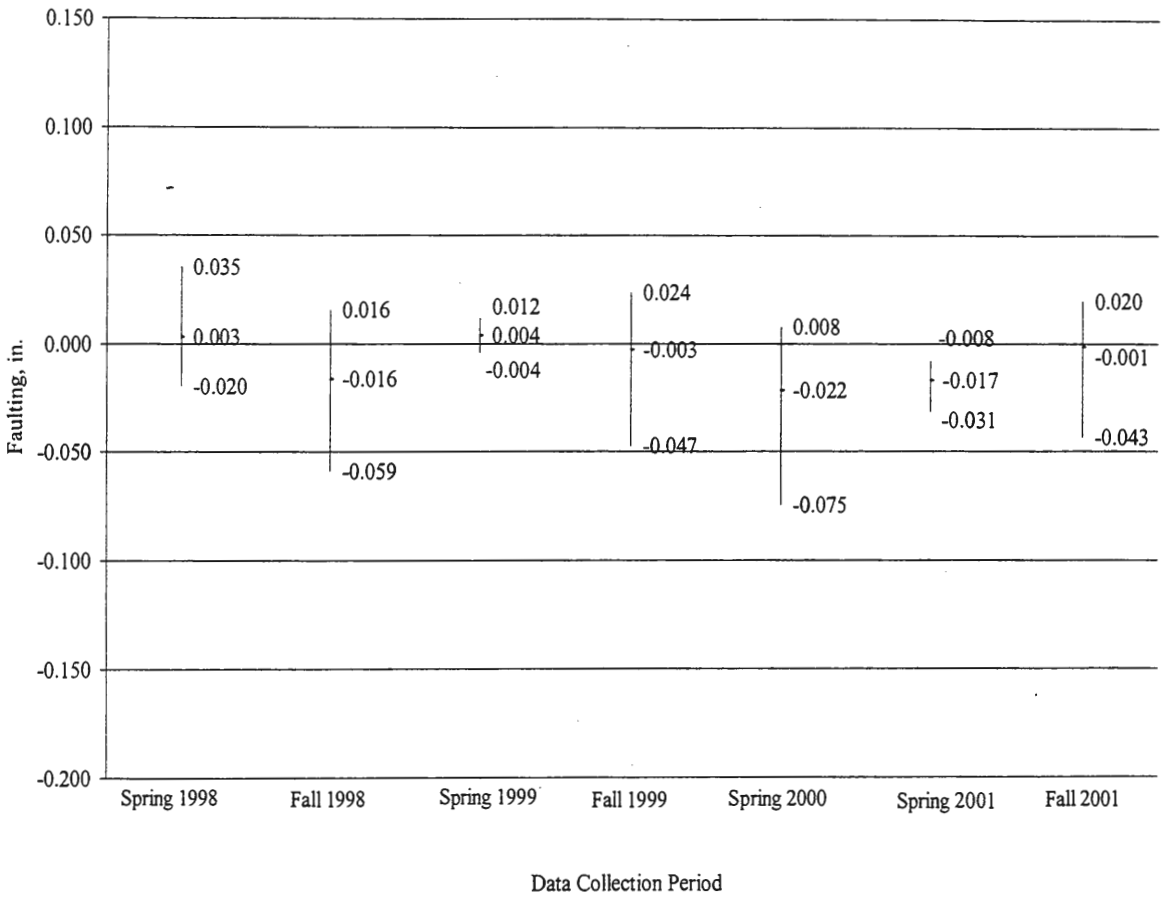

Figure 9E. Maximum, minimum, and average joint faulting for the outside wheel path of 1.5 inch diameter FRP with 8 inch spacing.

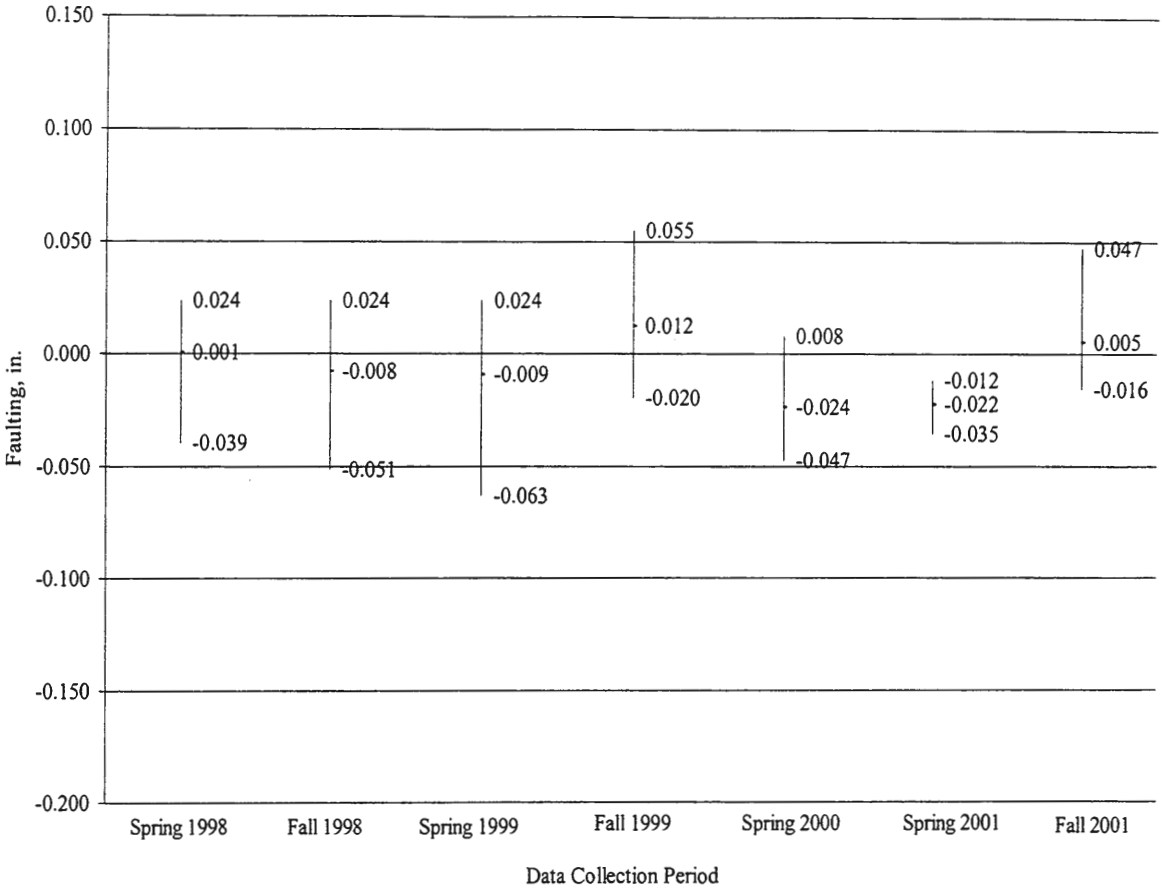

Figure 10E. Maximum, minimum, and average joint faulting for the inside wheel path of 1.5 inch diameter FRP with 8 inch spacing.

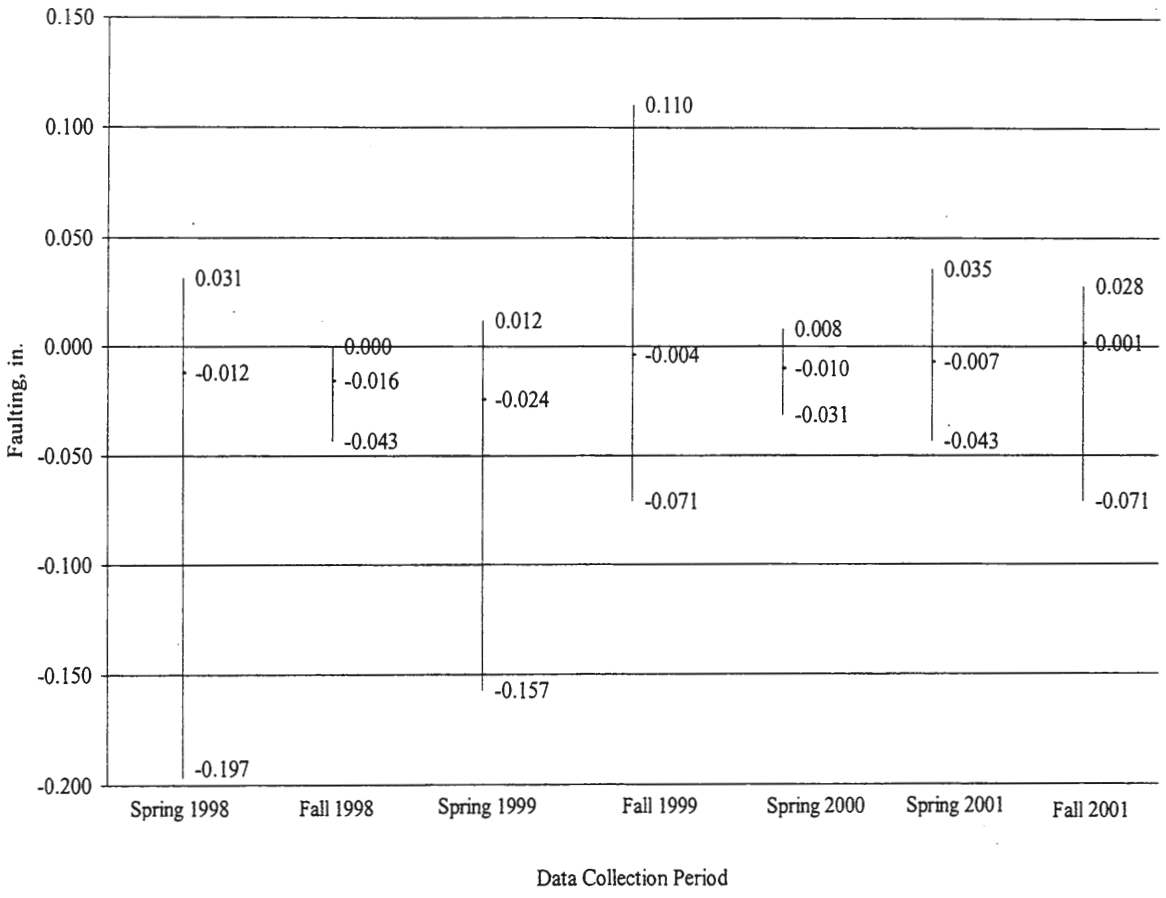

Figure 11E. Maximum, minimum, and average joint faulting for the outside wheel path of 1.88 inch diameter FRP with 12 inch spacing.

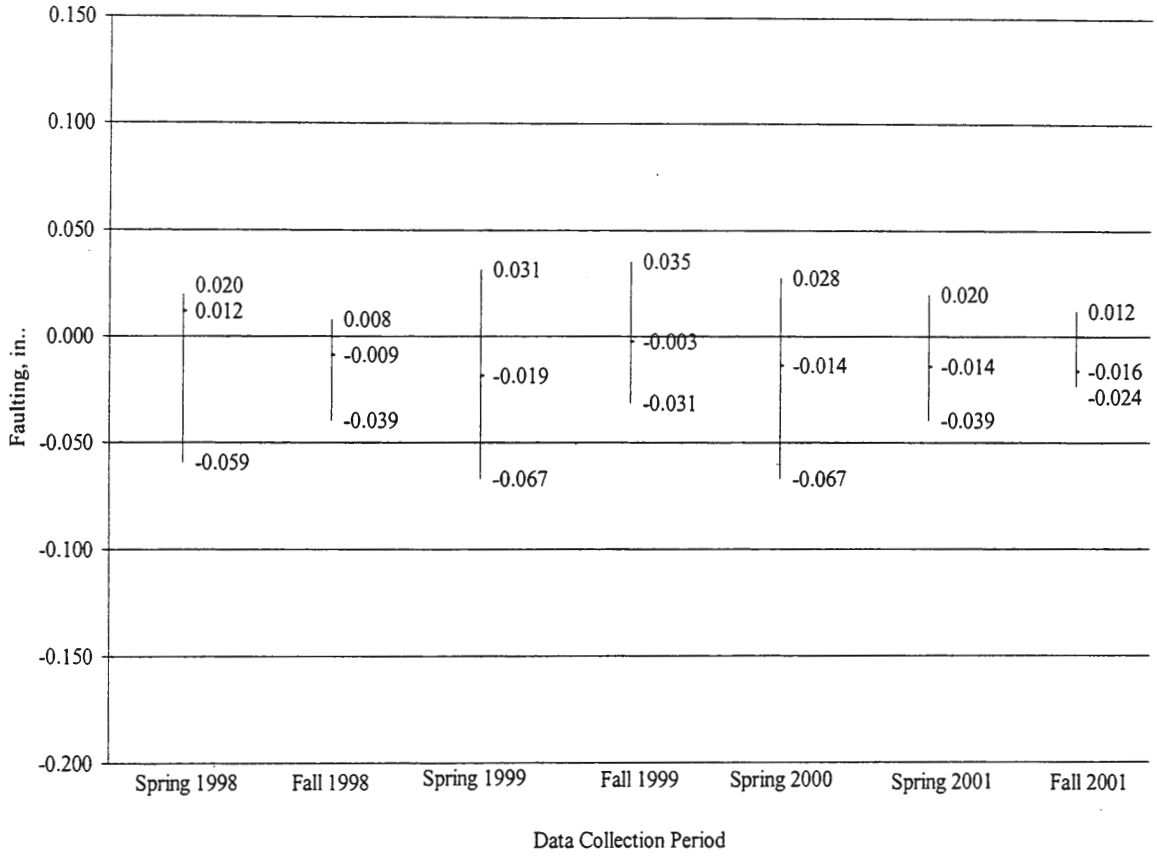

Figure 12E. Maximum, minimum, and average joint faulting for the inside wheel path of 1.88 inch diameter FRP with 12 inch spacing.

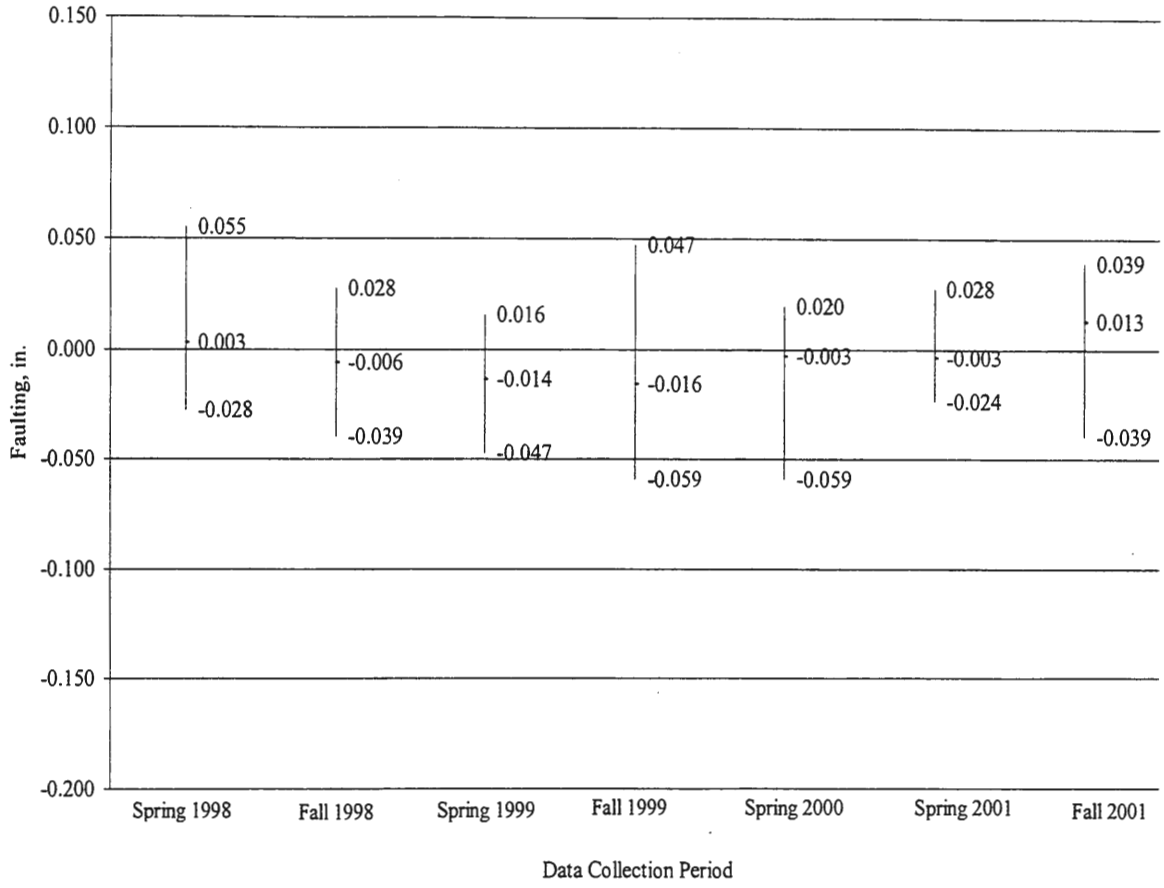

Figure 13E. Maximum, minimum, and average joint faulting for the outside wheel path of 1.88 inch diameter FRP with 8 inch spacing.

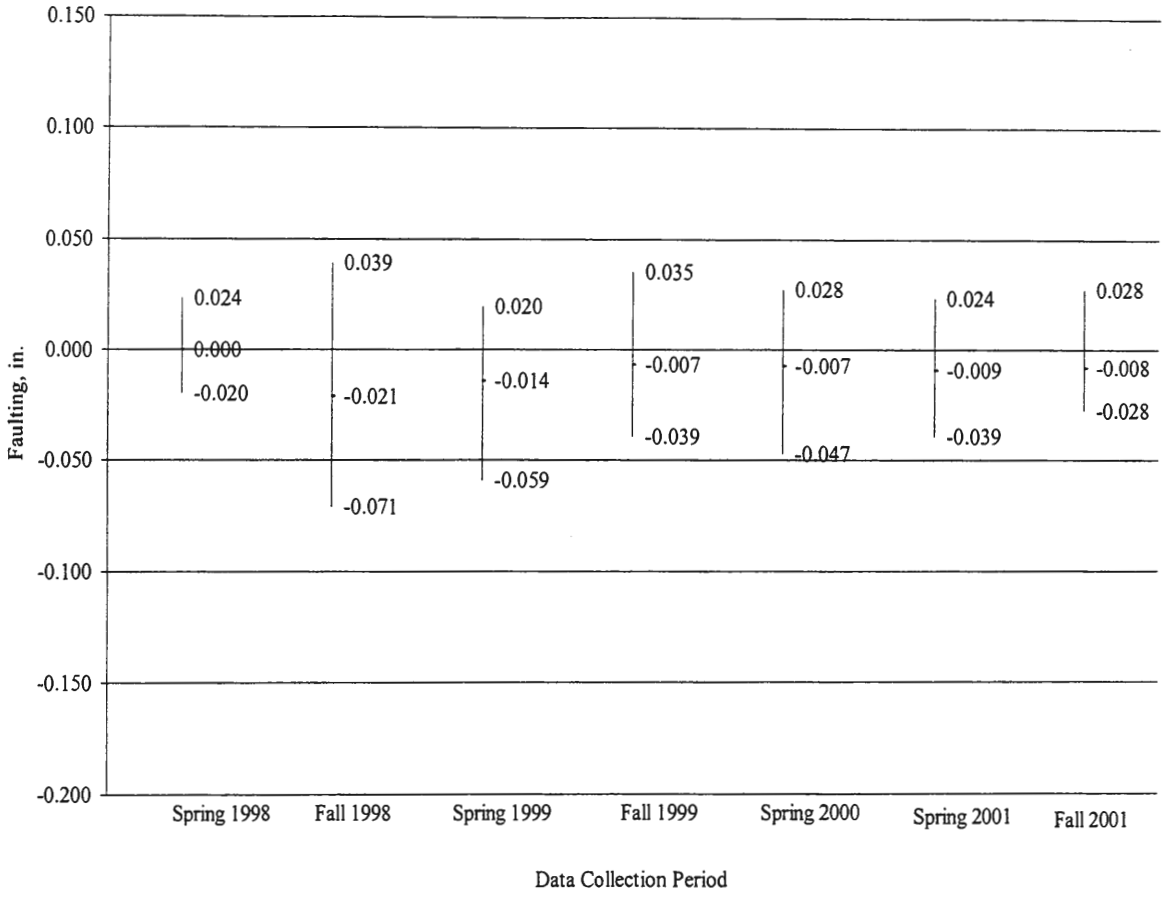

Figure 14E. Maximum, minimum, and average joint faulting for the inside wheel path of 1.88 inch diameter FRP with 8 inch spacing.

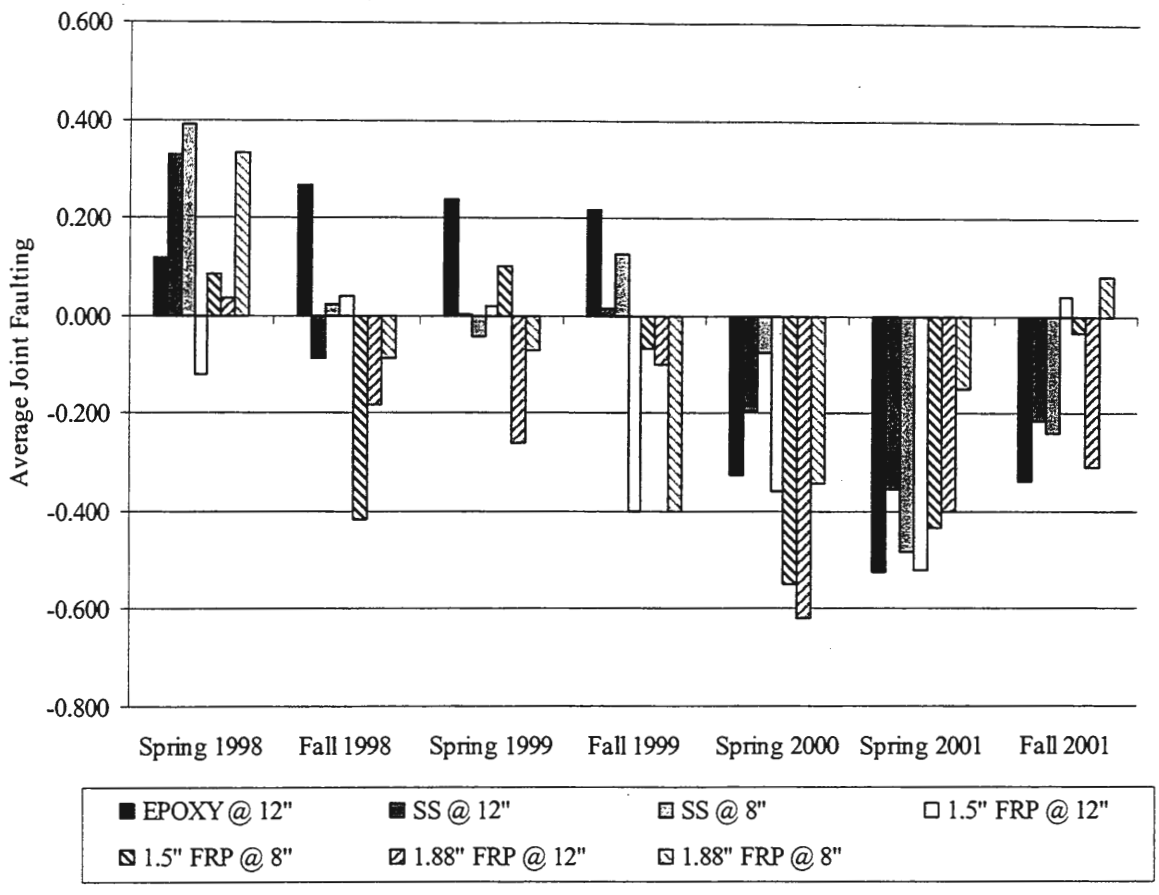

Figure 15E. Seasonal variation in average joint faulting in the outside wheel path.

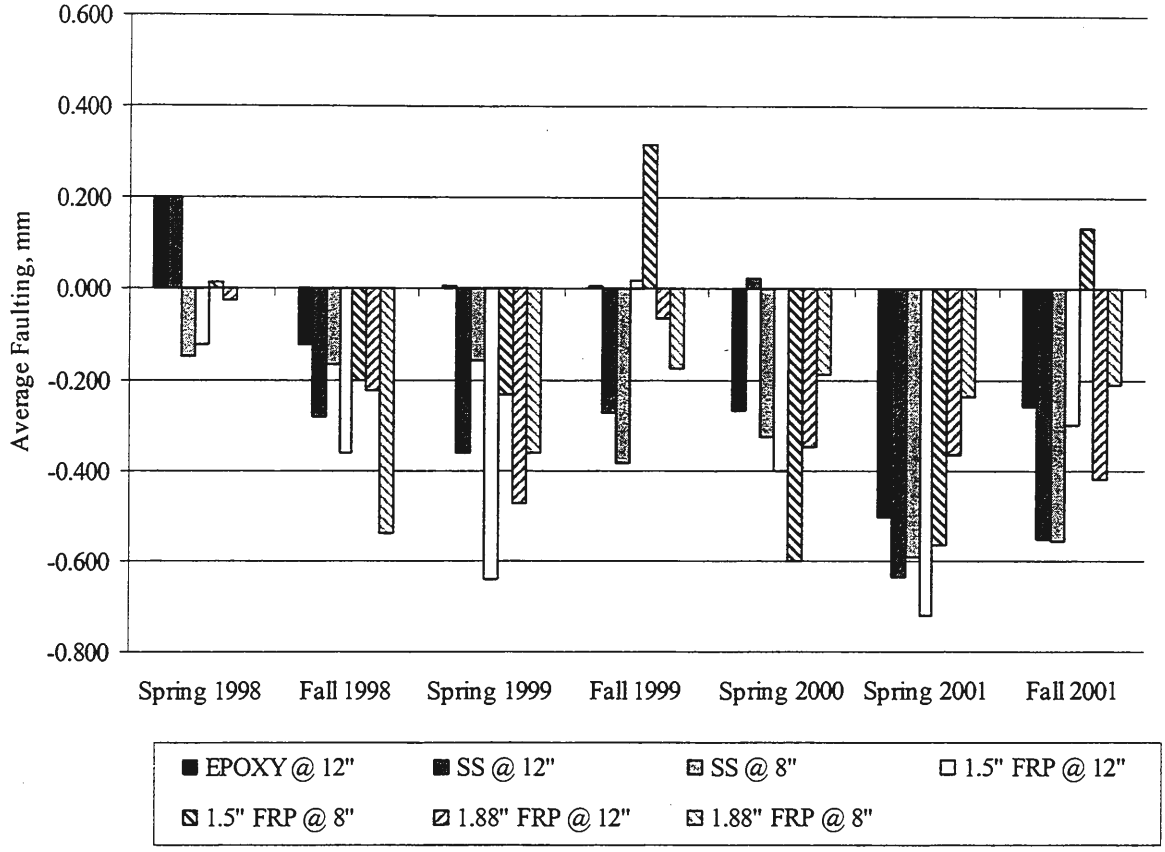

Figure 16E. Seasonal variation in average joint faulting in the inside wheel path.

APPENDIX F – STATISTICAL ANALYSIS

Table 1F. Load transfer efficiency statistical analysis of the driving lane.

	Std. Epoxy[a]	SS @ 12[a]	SS @ 8[a]	1.5" FRP @ 12[a]	1.5" FRP @ 8[a]	1.88" FRP @ 12[a]	1.88" FRP @ 8[a]
Std. Epoxy[b]		5.5968*	-0.8512	12.0857*	5.1676*	14.3761*	14.3761*
SS @ 12[b]	0.032		-6.4480*	6.4889*	-0.4291	8.7793*	6.6472*
SS @ 8[b]		0.006		12.9369*	6.0188*	15.2273*	13.0952*
1.5" FRP @ 12[b]	0.000	0.005	0.000		-6.9180*	2.2904	0.1583
1.5" FRP @ 8[b]			0.011	0.001		9.2084*	7.0764*
1.88" FRP @ 12[b]	0.000	0.000	0.000		0.000		-2.1321
1.88" FRP @ 8[b]	0.000	0.004	0.000		0.001		

Note: Upper right values are the mean differences, with the lower left values indicating significance level if difference found to be significant.

Mean difference = b - a

* = Significance found.

Table 2F. Load transfer efficiency statistical analysis of the passing lane.

	Std. Epoxy[a]	SS @ 12[a]	SS @ 8[a]	1.5" FRP @ 12[a]	1.5" FRP @ 8[a]	1.88" FRP @ 12[a]	1.88" FRP @ 8[a]
Std. Epoxy[b]		3.533	-2.5726	10.9507*	2.9198	10.2954*	10.2237*
SS @ 12[b]			-6.10586*	7.4177*	-0.61532	6.7624*	6.6907*
SS @ 8[b]		0.000		13.58233*	5.4924*	12.868*	12.7963*
1.5" FRP @ 12[b]	0.000	0.000	0.000		-8.0309*	-0.6553	-0.727
1.5" FRP @ 8[b]			0.001	0.000		-7.3756*	7.3039*
1.88" FRP @ 12[b]	0.000	0.000	0.000		0.000		-0.0717
1.88" FRP @ 8[b]	0.000	0.000	0.000		0.000		

Note: Upper right values are the mean differences, with the lower left values indicating significance level if difference found to be significant.

Mean difference = b - a

* = Significance found.

Table 3F. Maximum joint deflection statistical analysis of the driving lane.

	Std. Epoxy	SS @ 12	SS @ 8	1.5" FRP @ 12	1.5" FRP @ 8	1.88" FRP @ 12	1.88" FRP @ 8
Std. Epoxy		-0.9493*	1.2676*	0.0090	0.3098	-0.2191	0.4354
SS @ 12	0.001		2.2171*	0.9583*	1.2591*	0.7302*	1.3848*
SS @ 8	0.000	0.000		-1.2588*	-0.9580*	-1.4869*	-0.8323*
1.5" FRP @ 12		0.001	0.000		0.3007	-0.2281	0.4264
1.5" FRP @ 8		0.000	0.000			-0.5289	0.1257
1.88" FRP @ 12		0.033	0.000				0.6546
1.88" FRP @ 8		0.000	0.005				

Note: Upper right values are the mean differences, with the lower left values indicating significance level if difference found to be significant.

Mean difference = b - a

* = Significance found.

Table 4F. Maximum joint deflection statistical analysis of the passing lane.

	Std. Epoxy	SS @ 12	SS @ 8	1.5" FRP @ 12	1.5" FRP @ 8	1.88" FRP @ 12	1.88" FRP @ 8
Std. Epoxy		-0.3075	0.2126	0.1069	0.2123	-0.0846	1.6836*
SS @ 12			0.5201	0.2006	0.5199	0.2230	1.9911*
SS @ 8				-0.3195	-0.0002	-0.2972	1.4710*
1.5" FRP @ 12					0.3193	0.0224	1.7905*
1.5" FRP @ 8						-0.2969	1.4712*
1.88" FRP @ 12							1.7681*
1.88" FRP @ 8	0.000	0.000	0.000	0.000	0.000	0.000	

Note: Upper right values are the mean differences, with the lower left values indicating significance level if difference found to be significant.
Mean difference = b - a
* = Significance found.

Table 5F. Modulus of subgrade reaction statistical analysis of the driving lane.

	Std. Epoxy[a]	SS @ 12[a]	SS @ 8[a]	1.5" FRP @ 12[a]	1.5" FRP @ 8[a]	1.88" FRP @ 12[a]	1.88" FRP @ 8[a]
Std. Epoxy[b]		-33.8795*	-36.1315*	-56.6781*	-38.1119*	-14.0663	-68.239*
SS @ 12[b]	0.000		-2.2520	-22.7985*	-4.2324	19.8132	-34.3594*
SS @ 8[b]	0.000			-20.5464	-1.9803	22.0652*	-32.1074*
1.5" FRP @ 12[b]	0.000	0.039			18.5662	42.6118*	-11.5609
1.5" FRP @ 8[b]	0.000					24.0456*	-30.12714*
1.88" FRP @ 12[b]			0.049	0.000	0.020		-54.1727*
1.88" FRP @ 8[b]	0.000	0.000	0.000		0.001	0.000	

Note: Upper right values are the mean differences, with the lower left values indicating significance level if difference found to be significant.

Mean difference = b - a

* = Significance found.

Table 6F. Modulus of subgrade reaction statistical analysis of the passing lane.

	Std. Epoxy[a]	SS @ 12[a]	SS @ 8[a]	1.5" FRP @ 12[a]	1.5" FRP @ 8[a]	1.88" FRP @ 12[a]	1.88" FRP @ 8[a]
Std. Epoxy[b]		-21.1332*	23.8647*	-18.0374*	-7.4789	-5.5348	-50.9200*
SS @ 12[b]	0.002		44.9978*	3.0958	13.6542	15.5983	-29.7869*
SS @ 8[b]	0.000	0.000		-41.9021*	-31.3436*	-29.3995	-74.7847*
1.5" FRP @ 12[b]	0.021		0.000		10.5584	12.5026	-32.8826*
1.5" FRP @ 8[b]			0.000			1.9441	-43.4411*
1.88" FRP @ 12[b]			0.000				-45.3852*
1.88" FRP @ 8[b]	0.000	0.000	0.000	0.000	0.000	0.000	

Note: Upper right values are the mean differences, with the lower left values indicating significance level if difference found to be significant.
Mean difference = b - a
* = Significance found.

Table 7F. Concrete modulus of elasticity statistical analysis of the driving lane.

	Std. Epoxy[a]	SS @ 12[a]	SS @ 8[a]	1.5" FRP @ 12[a]	1.5" FRP @ 8[a]	1.88" FRP @ 12[a]	1.88" FRP @ 8[a]
Std. Epoxy[b]		1.74E+06*	1.27E+06*	3.72E+06*	2.67E+06*	2.35E+06*	2.62E+06*
SS @ 12[b]	0.000		-4.66E+05	1.98E+06*	9.29E+05	6.11E+05	8.78E+05
SS @ 8[b]	0.004			2.44E+06*	1.39E+06*	1.08E+06*	1.34E+06*
1.5" FRP @ 12[b]	0.000	0.000	0.000		1.05E+06*	1.37E+06*	1.10E+06*
1.5" FRP @ 8[b]	0.000		0.001	0.041		-3.18E+05	-5.05E+04
1.88" FRP @ 12[b]	0.000		0.032	0.001			2.67E+05
1.88" FRP @ 8[b]	0.000		0.002	0.026			

Note: Upper right values are the mean differences, with the lower left values indicating significance level if difference found to be significant.

Mean difference = b - a

* = Significance found.

Table 8F. Concrete modulus of elasticity statistical analysis of the passing lane.

	Std. Epoxy[a]	SS @ 12[a]	SS @ 8[a]	1.5" FRP @ 12[a]	1.5" FRP @ 8[a]	1.88" FRP @ 12[a]	1.88" FRP @ 8[a]
Std. Epoxy[b]		1.44E+05	6.36E+05	1.56E+06*	7.41E+05	3.70E+05	-1.06E+06*
SS @ 12[b]			4.92E+05	1.42E+06*	5.97E+05	2.26E+05	-1.21E+06*
SS @ 8[b]				9.27E+05	1.05E+05	-2.65E+05	-1.70E+06*
1.5" FRP @ 12[b]	0.000	0.000			-8.21E+05	-1.19E+06*	-2.62E+06*
1.5" FRP @ 8[b]						-3.70E+05	-1.80E+06*
1.88" FRP @ 12[b]				0.005			-1.43E+06*
1.88" FRP @ 8[b]	0.022	0.004	0.000	0.000	0.000	0.000	

Note: Upper right values are the mean differences, with the lower left values indicating significance level if difference found to be significant.
Mean difference = b - a
* = Significance found.

Table 9F. Standard epoxy coated steel statistical analysis between testing periods.

		S98 - F97	F98 - S98	S99 - F98	F99 - S99	S00 - F99	F00 - S00	S01 - F00	F01 - S01
Driving Lane	**Load Transfer**	-4.3822	-2.1101	-0.07951	3.9696	-7.8318*	2.1509	3.9403	11.6670*
	Significance	0.449	0.984	1.000	0.592	0.004	0.982	0.602	0.000
	Area	-1.1316	0.7585	-0.7697	4.2117*	-3.9906*	0.3489	1.2073	1.7091
	Significance	0.860	0.986	0.985	0.000	0.000	1.000	0.810	0.364
	Concrete Modulus of Elasticity	8.63E+05	9.25E+05	-2.66E+06	3.46E+06*	-2.19E+06	-7.70E+05	-4.92E+05	5.09E+06*
	Significance	0.997	0.995	0.246	0.034	0.526	0.999	1.000	0.000
	Modulus of Subgrade Reaction	49.5449*	-12.9174	-18.8263	-69.2266*	87.2865*	-23.0245	-39.1200*	6.7634
	Significance	0.002	0.981	0.842	0.000	0.000	0.630	0.035	1.000
	Max Joint Deflection	-0.7344	0.6456	0.7644	3.6267*	-3.4933*	0.2889	0.1500	0.6822
	Significance	0.492	0.670	0.433	0.000	0.000	0.997	1.000	0.598
		S98 - F97	**F98 - S98**	**S99 - F98**	**F99 - S99**	**S00 - F99**	**F00 - S00**	**S01 - F00**	**F01 - S01**
Passing Lane	**Load Transfer**	-1.0127	-0.6605	-6.1097*	4.3000*	-5.1398*	0.9761	0.2839	13.7721*
	Significance	0.997	1.000	0.000	0.015	0.001	0.997	1.000	0.000
	Area	-0.9665	1.6809	-1.852	1.211	-1.1742	0.2945	-0.3027	1.9751
	Significance	0.964	0.515	0.372	0.873	0.891	1.000	1.000	0.282
	Concrete Modulus of Elasticity	-8.21E+05	-7.75E+05	-3.86E+05	49357	3.14E+06*	-1.19E+06	-1.11E+06	3.46E+06*
	Significance	0.968	0.977	1.000	1.000	0.000	0.833	0.833	0.000
	Modulus of Subgrade Reaction	9.1825	-42.5767*	26.3291	-19.7682	71.9953*	-28.3697*	-9.7559	1.5279
	Significance	0.981	0.000	0.059	0.358	0.000	0.029	0.973	1.000
	Max Joint Deflection	0.6622	2.9211*	-1.2300	1.4533*	-3.8467*	2.1600*	-0.8300	0.6233
	Significance	0.838	0.000	0.093	0.019	0.000	0.000	0.591	0.880

Table 10F. Stainless steel, 12 inch on center spacing, statistical analysis between testing periods.

		S98 - F97	F98 - S98	S99 - F98	F99 - S99	S00 - F99	F00 - S00	S01 - F00	F01 - S01
Driving Lane	**Load Transfer**	-14.5577*	10.8402*	-18.9340*	22.2787*	-18.6072	5.6369	3.7867	13.0228*
	Significance	0	0.006	0.000	0	0	0.591	0.934	0.000
	Area	-3.8326	1.3821	-0.3536	3.7415*	-4.8865*	0.6653	-0.09924	2.2459
	Significance	0.001	0.868	1.000	0.010	0.000	0.999	1.000	0.278
	Concrete Modulus of Elasticity	-1.15E+06	1.80E+06	-3.11E+06*	3.13E+06*	2.69E+06*	2.58E+04	-1.09E+06	3.46E+06*
	Significance	0.876	0.351	0.012	0.011	0.018	1.000	0.908	0.000
	Modulus of Subgrade Reaction	107.6379*	-14.0104	-51.6385	-54.5415	108.7753*	-24.7403	-21.3969	-7.5696
	Significance	0.000	0.999	0.341	0.163	0.000	0.952	0.980	1.000
	Max Joint Deflection	-2.6589*	0.5100	0.5356	2.8667*	-2.8800*	0.5189	0.1822	0.3100
	Significance	0.000	0.810	0.961	0.000	0.000	0.795	1.000	0.989
		S98 - F97	**F98 - S98**	**S99 - F98**	**F99 - S99**	**S00 - F99**	**F00 - S00**	**S01 - F00**	**F01 - S01**
Passing Lane	**Load Transfer**	-0.6707	3.0322	-5.5705	3.5047	-3.8124	1.3921	6.4204	3.8234
	Significance	1	0.909	0.213	0.813	0.73	0.999	0.081	0.727
	Area	-0.2473	0.9046	-0.4837	2.5293*	-3.8689*	1.0755	0.7646	1.1781
	Significance	1.000	0.959	0.999	0.021	0.000	0.891	0.985	0.829
	Concrete Modulus of Elasticity	-1.62E+06*	-1.03E+06	7.30E+04	1.93E+06*	-4.73E+05	-3.75E+04	-7.52E+05	3.48E+06*
	Significance	0.014	0.414	1.000	0.001	0.986	1.000	0.809	0.000
	Modulus of Subgrade Reaction	-25.5236	-41.9025	12.9894	-19.8337	88.3077*	-34.4746	-32.0589	25.7291
	Significance	0.673	0.067	0.992	0.896	0.000	0.250	0.349	0.663
	Max Joint Deflection	0.6444	1.9000*	-1.2567*	1.9011*	-4.4178*	2.4911*	-0.8133	0.7500
	Significance	0.465	0.000	0.001	0.000	0.000	0.000	0.156	0.249

Table 11F. Stainless steel, 8 inch on center spacing, statistical analysis between testing periods.

		S98 - F97	F98 - S98	S99 - F98	F99 - S99	S00 - F99	F00 - S00	S01 - F00	F01 - S01
Driving Lane	Load Transfer	-2.1178	-0.4557	1.6882	1.8198	-4.1427	-7.1808*	10.8698*	4.4221
	Significance	0.863	1	0.960	0.939	0.08	0	0	0.045
	Area	-3.4807*	2.2604*	-1.9387	4.4130*	-4.4501*	-0.9205	1.6341	0.1784
	Significance	0.000	0.028	0.110	0.000	0.000	0.925	0.302	1.000
	Concrete Modulus of Elasticity	9.57E+05	1.79E+05	-2.03E+06	4.55E+06*	-3.49E+06*	-9.30E+05	-1.87E+04	2.86E+06*
	Significance	0.972	1.000	0.292	0.000	0.001	0.977	1.000	0.000
	Modulus of Subgrade Reaction	-128.8969*	-82.0451	27.0784	-67.4510*	92.4065*	14.9427	-60.7992*	50.3719*
	Significance	0.000	0.000	0.470	0.000	0.000	0.966	0.000	0.003
	Max Joint Deflection	-1.0289	0.7244*	0.4389	1.7900*	-1.7133*	1.1656*	-1.0678	-0.2222
	Significance	0.000	0.005	0.365	0.000	0.000	0.000	0.000	0.969
		S98 - F97	F98 - S98	S99 - F98	F99 - S99	S00 - F99	F00 - S00	S01 - F00	F01 - S01
Passing Lane	Load Transfer	0.4964	1.9384	-0.8526	-1.4387	-0.1564	-8.3617*	9.8405*	-1.3813
	Significance	1	0.985	1.000	0.998	1	0	0.000	0.999
	Area	0.7602	0.4455	0.3838	1.9378	-2.0206	0.02527	0.8192	1.3529
	Significance	0.996	1.000	1.000	0.437	0.376	1.000	0.993	0.858
	Concrete Modulus of Elasticity	-2.31E+06*	-1.48E+06	4.83E+05	1199830	1.83E+06*	1.99E+05	-7.40E+05	3.23E+06*
	Significance	0.000	0.069	0.989	0.276	0.007	1.000	0.866	0.000
	Modulus of Subgrade Reaction	-53.0135*	-30.0010*	4.5503	-10.312	51.3313*	0.271	-23.1979	6.9774
	Significance	0.000	0.006	1.000	0.943	0.000	1.000	0.098	0.995
	Max Joint Deflection	1.5689*	2.7333*	-0.0511	1.2867	-3.9844*	1.6200*	-0.7900	0.2922
	Significance	0.010	0.000	1.000	0.080	0.000	0.007	0.690	0.999

Table 12F. 1.5 inch diameter FRP, 12 inch on center spacing, statistical analysis between testing periods.

		S98 - F97	F98 - S98	S99 - F98	F99 - S99	S00 - F99	F00 - S00	S01 - F00	F01 - S01
Driving Lane	Load Transfer	-4.7482	6.9579	-22.3703*	8.0477	-10.164	-4.0785	17.6252*	2.7493
	Significance	0.963	0.737	0.000	0.551	0.221	0.986	0.000	0.999
	Area	-1.6801	0.1304	-0.5887	1.5303	-0.533	-1.5462	1.5701	0.2385
	Significance	0.201	1.000	0.994	0.322	0.997	0.307	0.286	1.000
	Concrete Modulus of Elasticity	1.13E+06	-5.90E+05	-1.13E+06	1.43E+06	2.59E+05	-1.32E+06	-1.31E+06	2.59E+06*
	Significance	0.529	0.981	0.524	0.200	1.000	0.304	0.311	0.000
	Modulus of Subgrade Reaction	82.4402	-23.6672	-9.3342	-14.4388	24.7581	22.2699	-56.1571*	55.8813*
	Significance	0.000	0.569	0.998	0.959	0.504	0.651	0.000	0.000
	Max Joint Deflection	-1.3211	0.8600	1.1344	1.9311*	-2.1944*	0.9811	-.7100	0.2489
	Significance	0.149	0.720	0.336	0.003	0.000	0.549	0.884	1.000
		S98 - F97	F98 - S98	S99 - F98	F99 - S99	S00 - F99	F00 - S00	S01 - F00	F01 - S01
Passing Lane	Load Transfer	-5.5772	1.9947	-7.9618	-2.0084	4.1098	-8.8863	12.0104	-1.0691
	Significance	0.947	1.000	0.693	1.000	0.992	0.547	0.144	1.000
	Area	-0.1312	1.3339	-1.2563	0.5646	-0.4946	-0.9044	1.8968*	0.7548
	Significance	1.000	0.160	0.228	0.977	0.988	0.686	0.005	0.858
	Concrete Modulus of Elasticity	-1.50E+06*	-6.69E+05	-4.69E+05	1.29E+06*	1.21E+06*	-3.44E+05	-2.36E+04	2.05E+06*
	Significance	0.001	0.634	0.930	0.008	0.017	0.990	1.000	0.000
	Modulus of Subgrade Reaction	-31.3784*	-40.2487*	12.9635	17.2723	38.6708*	16.5112	-49.0499*	18.5873
	Significance	0.000	0.000	0.454	0.102	0.000	0.140	0.000	0.055
	Max Joint Deflection	1.4700	2.9922*	-0.7411	-0.3478	-2.5122*	1.7333	-0.3178	0.2956
	Significance	0.415	0.000	0.975	1.000	0.005	0.192	1.000	1.000

Table 13F. 1.5 inch diameter FRP, 8 inch on center spacing, statistical analysis between testing periods.

		S98 - F97	F98 - S98	S99 - F98	F99 - S99	S00 - F99	F00 - S00	S01 - F00	F01 - S01
Driving Lane	**Load Transfer**	-2.7185	0.2261	-6.6317	3.8424	-4.9823	-2.8314	12.2225*	7.5699
	Significance	0.992	1.000	0.377	0.934	0.760	0.990	0.001	0.201
	Area	-2.1461	-1.2914	0.9395	2.0712	-1.1962	-2.36	2.4127	0.1585
	Significance	-0.641	0.972	0.997	0.686	0.983	0.508	0.476	1.000
	Concrete Modulus of Elasticity	-1.78E+05	-2.27E+06	-1.47E+05	1.72E+06	4.93E+05	-2.28E+06	2.82E+05	2.96E+06
	Significance	1.000	0.482	1.000	0.817	1.000	0.474	1.000	0.134
	Modulus of Subgrade Reaction	70.2247*	-17.414	-24.3897	-28.6256	46.2723	81.6416*	-75.9423*	54.0043*
	Significance	0.001	0.980	0.862	0.715	0.101	0.000	0.000	0.024
	Max Joint Deflection	-1.1567	1.1011	0.7411	1.6411*	-2.1722*	0.7344	0.2422	-0.6244
	Significance	0.377	0.450	0.887	0.037	0.001	0.892	1.000	0.956
		S98 - F97	**F98 - S98**	**S99 - F98**	**F99 - S99**	**S00 - F99**	**F00 - S00**	**S01 - F00**	**F01 - S01**
Passing Lane	**Load Transfer**	-4.101	6.7530	-2.6939	1.2433	-3.3063	-6.2238	6.9858	-0.7281
	Significance	0.971	0.645	0.998	1.000	0.993	0.742	0.600	1.000
	Area	-0.336	-1.0115	1.7187	0.669	-0.7429	-0.8424	1.8662	0.5749
	Significance	1.000	0.986	0.747	0.999	0.998	0.996	0.649	1.000
	Concrete Modulus of Elasticity	-1.90E+06*	-1.57E+06*	1.07E+06	-6.44E+05	2.71E+06*	2.68E+05	-7.88E+05	2.95E+06
	Significance	0.003	0.034	0.408	0.930	0.000	1.000	0.804	0.000
	Modulus of Subgrade Reaction	-27.9591*	-23.9067	1.1564	-21.5224	58.3381*	28.2882*	-60.0081*	27.1163
	Significance	0.045	0.157	1.000	0.282	0.000	0.040	0.000	0.060
	Max Joint Deflection	0.9978	2.3389*	-0.6689	2.1122*	-3.6711*	1.0989	0.6389	-0.7944
	Significance	0.596	0.000	0.936	0.001	0.000	0.457	0.951	0.843

Table 14F. 1.88 inch diameter FRP, 12 inch on center spacing, statistical analysis between testing periods.

		S98 - F97	F98 - S98	S99 - F98	F99 - S99	S00 - F99	F00 - S00	S01 - F00	F01 - S01
Driving Lane	**Load Transfer**	-6.9265	14.1545	-8.3921	-1.7009	-11.1642	-12.5399	24.0447*	-8.2198
	Significance	0.946	0.197	0.849	1.000	0.527	0.356	0.000	0.864
	Area	-1.424	1.1673	-1.2525	3.1514-	-2.4957*	-1.9293	1.842	-2973
	Significance	-0.599	0.821	0.755	0.001	0.020	0.179	0.233	1.000
	Concrete Modulus of Elasticity	5.69E+05	2.08E+05	-2.53E+06	2.95E+06*	-5.70E+05	-2.05E+06	4.33E+05	1.70E+06
	Significance	0.999	1.000	0.090	0.020	0.999	0.319	1.000	0.589
	Modulus of Subgrade Reaction	54.2706*	-35.0640*	-7.792	-38.0396*	60.7126*	23.3228	-49.5162*	43.8649*
	Significance	0.000	0.008	0.997	0.003	0.000	0.280	0.000	0.000
	Max Joint Deflection	-0.1978	0.1978	1.0567	1.8822*	-2.2178*	1.5100*	-0.8467	0.1011
	Significance	1.000	1.000	0.201	0.000	0.000	0.007	0.510	1.000
		S98 - F97	**F98 - S98**	**S99 - F98**	**F99 - S99**	**S00 - F99**	**F00 - S00**	**S01 - F00**	**F01 - S01**
Passing Lane	**Load Transfer**	-12.6665	17.8931*	-8.8405	2.5771	-1.9487	-6.5181	12.8973	-5.6869
	Significance	0.209	0.009	0.704	1.000	1.000	0.932	0.188	0.969
	Area	-0.7491	1.1118	-0.9626	1.7212*	-0.8921	-1.1524	2.1189*	0.6202
	Significance	0.675	0.146	0.320	0.001	0.430	0.113	0.000	0.858
	Concrete Modulus of Elasticity	-1.93E+06*	-1.06E+06	-7.54E+05	2.15E+06*	1.26E+06	-7.83E+05	7.98E+04	1.99E+06*
	Significance	0.000	0.291	0.749	0.000	0.101	0.707	1.000	0.000
	Modulus of Subgrade Reaction	-15.9651	-40.2103*	3.212	3.5309	38.0757*	16.0746	-47.5021*	11.649
	Significance	0.184	0.000	1.000	1.000	0.000	0.177	0.000	0.621
	Max Joint Deflection	1.3600	1.4922	0.4322	-0.1989	-2.4333*	2.1144*	-0.4467	0.3489
	Significance	0.128	0.062	0.995	1.000	0.000	0.001	0.993	0.999

Table 15F. 1.88 inch diameter FRP, 8 inch on center spacing, statistical analysis between testing periods.

		S98 - F97	F98 - S98	S99 - F98	F99 - S99	S00 - F99	F00 - S00	S01 - F00	F01 - S01
Driving Lane	**Load Transfer**	-0.1223	5.6618	-12.9373	0.3859	-12.9489	0.3347	18.7007*	-2.3519
	Significance	1.000	0.979	0.256	1.000	0.255	1.000	0.011	1.000
	Area	-0.9038	-0.0689	-1.0772	0.8594	-0.336	-1.7732	1.8267	0.02741
	Significance	0.952	1.000	0.874	0.964	1.000	0.272	0.233	1.000
	Concrete Modulus of Elasticity	1.01E+05	9.91E+02	-2.84E+06*	9.94E+05	5.44E+05	-1.41E+06	2.42E+05	2.25E+06*
	Significance	1.000	1.000	0.003	0.911	0.998	0.581	1.000	0.045
	Modulus of Subgrade Reaction	37.1394	1.3604	-28.0446	-8.0453	24.5264	36.1939	-63.3146*	55.0402*
	Significance	0.277	1.000	0.673	1.000	0.814	0.312	0.001	0.010
	Max Joint Deflection	-0.4226	0.6411	1.1033	1.2322	-1.4144	0.9178	-0.2589	0.1400
	Significance	0.994	0.930	0.364	0.216	0.085	0.630	1.000	1.000
		S98 - F97	**F98 - S98**	**S99 - F98**	**F99 - S99**	**S00 - F99**	**F00 - S00**	**S01 - F00**	**F01 - S01**
Passing Lane	**Load Transfer**	-0.2989	8.1106	-10.8999	1.9107	-4.783	-5.4136	5.9764	-3.9837
	Significance	1.000	0.749	0.348	1.000	0.986	0.970	0.946	0.996
	Area	-0.6339	0.831	-0.2548	2.0711	0.8007	-3.1701*	2.329	0.0128
	Significance	0.999	0.995	1.000	0.450	0.996	0.028	0.281	1.000
	Concrete Modulus of Elasticity	-2.18E+06	1.26E+05	-7.17E+05	1.58E+06	2.14E+06	-2.50E+06	5.49E+05	3.13E+06
	Significance	0.460	1.000	0.999	0.841	0.488	0.264	1.000	0.057
	Modulus of Subgrade Reaction	-29.8258	-21.2382	-8.8178	-23.13	8.0084	48.6853*	-54.9279*	49.6263*
	Significance	0.219	0.690	0.998	0.578	0.999	0.001	0.000	0.001
	Max Joint Deflection	0.8456	0.8878	0.322	0.3611	-1.2644	1.3689	-0.0278	-0.6344
	Significance	0.815	0.770	1.000	0.999	0.295	0.195	1.000	0.960

REFERENCES

1. Benkelman, A.C., "Tests of Aggregate Interlock at Joints and Cracks," *Engineering News Record*, Vol. III, No. 8, Aug. 1933, pp. 227-232.

2. Nowlen, W.J., "Influence of Aggregate Properties on Effectiveness of Interlock Joints in Concrete Pavements," *Journal of the PCA*, Research and Development Laboratories, Vol. 10, No. 2, May 1968, pp 2-8.

3. Raja, Zafar I. and Snyder, Mark B, "Factors Affecting Deterioration of Transverse Cracks in Jointed Reinforced Concrete Pavements," *Transportation Research Record 1307*, 1991.

4. Sutherland, E.C. and Cahsell, H.D., "Structural Efficiency of Transverse Weakened-Plane Joints," *Public Roads*, Vol. 24, No. 4, April-June 1945.

5. Tayabji, Shiraz D. and Colley, Bert E., "Improved Rigid Pavement Joints," Report No. FHWA/RD-86/040, report prepared for Federal Highway Administration, February 1986.

6. Breemen, W.V. and Finney, E.A., "Design and Construction of Joints in Concrete Pavements," *Journal of the American Concrete Institute*, June 1950.

7. McDaniel, Lisa Lee, "Using Deflection Basins to Estimate Alternative Joint Reinforcement load transfer," *Masters Thesis*, Iowa State University, 1998.

8. Darter, M.I. and Barenberg, Ernest J., "Design of Zero Maintenance Plain Jointed Concrete Pavement, Vol. II – Design Manual," report prepared for Federal Highway Administration, Report No. FHWA-RD-77-112, 1977.

9. American Concrete Pavement Association, "Joint and Crack Sealing and Repair for Concrete Pavments," *Concrete Paving Technology*, Illinois, ACPA, 1993.

10. Davids, William G., "Effect of Dowel Looseness on Response of Jointed Concrete Pavements," *Journal of Transportation Engineering*, Vol. 126, No. 1, January/February, 2000.

11. Fish, Kent "Development Length of Fiber Composite Concrete Reinforcement." *Masters Thesis*, Iowa State University, 1992.

12. Encyclopedia.com, "Composition and Properties of Glass", Date Accessed: July 2002, http://www.encyclopedia.com/html/section/glass_compositionandpropertiesofglass.asp.

13. Proctor, B.A., Oakely, D.R. and Litherland, K.L., "Developments in the Assessment and Performance of GRC over 10 Years", Composites, Volume 13, Number 2, 1982, pg 173-179.

14. Yilmaz, V.T., Lachowske, E.E., And Glasser, F.P., "Chemical and Microstructural Changes at Alkali-Restant Glass Fiber-Cement Interfaces", Journal of the American Ceramic Society, Volume 74, Number 12, 1991, pp 5054-5060.

15. Yilmaz, V.T., and Glasser, F.P, "Reaction of Alkali-Resistant Glass Fibers with Cement", Glass Technology, Volume 32, Number 3, a991, pg 91-98.

16. Porter, M.L, Guinn Jr., R.J., Lundy, A.L, Davis, D.D., and Rohner, J.G., "Investigation of Glass Fiber Composite Dowel Bars for Highway Pavement Slabs", *Final Report HR-408, Submitted to Highway Division of the Iowa Department of Transportation and Iowa Highway Research Board*, Ames, IA, June 2001.

17. Rostasy, F.S. and Budelmann, H., "FRP-Tendons for the Post-tensioning of Concrete Structures", Proceedings of the Specialty Conference - Advanced Composite Materials in Concrete Structures, American Society of Civil Engineers, Flaming Hilton, Las Vegas, NV, January 31 and February 1, 1991, pf. 155-166.

18. Kakihara, R., Kamiyoshi, M., Kumagai, S, and Noritake, K., "A new Aramid Rod for the Reinforcemtn of Concrete Structures", Proceedings of the Specialty Conference – Advanced Composte Materials in Concrete Structures, S.L. Iyer, Ed., American Society of Civil Engineers, Flaming Hilton, Las Vegas, NV, January 31 and February 1, 1991, pg 132 – 142.

19. Gerritse, A., and Werner, J., "ARAPREE, a Non-Metallic Tendon, Performance and Design Redquirements", Proceedings of the Specialty Conference - Advanced Composite Materials in Concrete Structures, American Society of Civil Engineers, Flaming Hilton, Las Vegas, NV, January 31 and February 1, 1991, pg. 143-154.

20. Davis, D.D, "Fatigue Behavior of Glass Fiber Reinforced Polymer Dowels," *Masters Thesis*, Iowa State University, 2001.

21. Specialty Steel Industry of North American, "The Stainless Steel Information Center, Date Accessed: May, 2002, www.ssina.com.

22. Albertson, Michael D., "Fibercomposite and Steel Pavement Dowels," *Masters Thesis*. Iowa State University, 1992.

23. Hughes, Bradley W., "Experimental Evaluation of Non-Metallic Dowel Bars for Highway Pavements," *Masters Thesis*, Iowa State University, 1993.

24. Lorenz, Eric A., "Accelerated Aging of Fiber Composite Bars and Dowels," *Masters Thesis*, Iowa State University, 1993.

25. Mehus, Jacob, "Long Term Durability of Fiber composite Reinforcement for Concrete," *Masters Thesis*, Iowa State University, 1995.

26. American Association of State Highway and Transportation Officials (AASHTO), *AASHTO Guide for Design of Pavement Structures*, Washington D.C., AASHTO, 1993.

27. Highway Innovative Technology Evaluation Center (HITEC), *HITEC Evaluation Plan for Fiber Reinforced Polymer Composite Dowel Bars and Stainless Steel Dowel Bars*, Washington D.C., HITEC, 1998.

28. Applied Pavement Technology Incorporated, "Status of High Performance Concrete Pavements", *Submitted to Federal Highway Administration*, Washington D.C., June 2001.

29. Foinquinos, Rafael, Jose Roesset and Kenneth Stokoe. "Response of Pavement Systems to Dynamic Loads imposed by Nondestructive Tests." *Transportation Research Record 1504,* 1995, pg. 57-67.

30. Sebaaly, Boutros, Davis, Trevor G., and Mamlouk, Michael, S., "Dynamics of Falling Weight Deflectometer," *Journal of Transportation Engineering*, Vol. 111, No. 6, November, 1985, pg. 618-631.

31. Boyd, T. M., "Geophones," Colorado School of Mines, Date Accessed: June 29, 2002, http://www.mines.edu/fs_home/tboyd/GP311/MODULUS/SEIS/NOTES/geophone.html

32. Lev Khazanovich, Shiraz D. Tayabji, and Michael I. Darter, "Backcalculation of Layer Parameters for LTPP Test Sections, Volume I: Slab on Elastic Solid and Slab on Dense-Liquid Foundation Analysis of Rigid Pavements," Report No. FHWA-RD-00-086, report prepared for the Federal Highway Administration, January, 2001.

33. Westergaard, H.M., "Computation of Stresses in Concrete Roads," Proceedings, 5th Annual Meeting of the Highway Research Board, Part I, 1926, pp. 90-112.

34. Westergaard, H.M., "Stresses in Concrete Runways of Airports," Proceedings, 19th Annual Meeting of the Highway Research Board, 1939, pp. 197-202.

35. Ioannides, Anastasios M., "Concrete Pavement Backcalculation Using *ILLI-BACK 3.0*," Nondestructive Testing of Pavements and Backcalculation of Moduli, 2nd Vol., Philadelphia, American Society for Testing and Materials, 1994.

36. Cable, J.K and McDaniel, L.L., "Demonstration and Field Evaluation of Alternative Portland Cement Concrete Pavement Reinforcement Materials," *Construction Report HR-1069, Submitted to Highway Division of the Iowa Department of Transportation and Iowa Highway Research Board*, Ames, IA, August, 1998.

37. Somsky, Sara J., "Number and Location of Dowel Bars in a Low Traffic Volume Concrete Pavement," *Masters Thesis*, Iowa State University, 2002.

38. Strategic Highway Research Program, "Distress Identification Manual for the Long-term Pavement Performance Project," SHRP-P-338, Washington, DC, 1993.

39. Hall, Kathleen T., "Backcalculation Solutions for Concrete Pavements," Long Term Pavement Performance Memo Prepared for SHRP Contract P-020, May 1992.

40. Mindess, Sidney and Young, J. Francis, Concrete, Upper Saddle River, NJ: Prentice-Hall, Inc., 1981.